A CHIRONOMID-BASED PALEOLIMNOLOGICAL ASSESSMENT OF LONG-TERM CUMULATIVE EFFECTS OF MULTIPLE ANTHROPOGENIC STRESSORS ON HYPOLIMNETIC OXYGEN DYNAMICS IN LAKE ERIE

DMITRI PERLOV

A THESIS SUBMITTED TO THE FACULTY OF GRADUATE STUDIES IN PARTIAL FULFILMENT OF THE REQUIREMENTS FOR THE DEGREE OF MASTER OF SCIENCE

GRADUATE PROGRAM IN BIOLOGY
YORK UNIVERSITY,
TORONTO, ONTARIO

MAY 2018

Abstract

The central basin of Lake Erie is annually subjected to hypoxia, which has implications for fish communities and nutrient recycling. As limnological monitoring data for Lake Erie does not extend beyond the 1970s, paleolimnological techniques can be used to reconstruct long-term water quality trends. Chironomidae (Diptera) remains preserved in dated sediment cores from the western, central, and eastern basins in Lake Erie were used to assess the long-term cumulative effects of multiple anthropogenic stressors on hypolimnetic dissolved oxygen. Results from analyses of subfossil chironomid remains indicated that the central basin has exhibited mesotrophic to eutrophic conditions since 1850. However, a transition in chironomid communities further towards anoxic-type taxa between 1930-1950 suggests that the severity and duration of hypolimnetic anoxia has increased in recent decades. Variance partitioning analysis (VPA) indicated that the effects of land use and climate had significant implications in driving changes in chironomid assemblages in the central basin.

Acknowledgments

I would like to thank my supervisor, Dr. Roberto Quinlan, for providing me with this great opportunity, and for providing assistance and guidance during my studies. I was very fortunate for having such a great mentor. Also thank you to my committee member, Dr. Andrew Donini, for helping me stay on track.

Many thanks go to my colleagues at the Quinlan Lab, Ryan Scott and Chris Luszczek, I am forever grateful for your feedback on data analysis, and our many discussions about paleo and beyond. I would also like to thank Dr. Euan Reavie and Kitty Kennedy for proving the sediments, environmental, and geochemical data used in this study, and Dr. Euan Reavie's feedback along the way. Thanks also to Daniel Rucinski for helping me obtain most of my historical environmental data, Dr. Andrew Medeiros and Dr. Gavin Simpson for their assistance with R, and Frank Talarico who assisted with sediment processing and picking of head capsules.

Thank you to my parents, Alexandr and Elena Perlov, my sister, Olga, and Nik for their love and support. A special thank you to Anastasia Korosteliov for her love, support, an inspiration to pursue my university education, and her tolerance during my academic journey.

Table of Contents

List of Tables

Chapter 2

Chapter 3

List of Figures

Chapter 1

Chapter 2

List of Abbreviations

AF	Anoxia factor
avgVWHO	Average volume-weighted hypolimnetic oxygen
CA	Correspondence analysis
CCA	Canonical correspondence analysis
DCA	Detrended correspondence analysis
DCCA	Detrended canonical correspondence analysis
DO	Dissolved oxygen
jack	Leave-one-out jackknifing cross-validation
MTA	Metric tons per annum
P	Phosphorus
PCA	Principal component analysis
RDA	Redundancy analysis
RMSEP	Root mean squared error of prediction
SA	Surface area
TIN	Total inorganic nitrogen
TN	Total nitrogen
TP	Total phosphorus
VPA	Variance partitioning analysis
$\mathbf{Z_{max}}$	Maximum depth
$\mathbf{Z_{mean}}$	Mean depth

CHAPTER 1: Introduction and Literature Review

Introduction

Anthropogenic activities have had a tremendous impact on aquatic ecosystems by dramatically altering the natural fluxes of growth-limiting nutrients. As a result, cultural eutrophication of freshwater and marine environments is the primary issue faced by most aquatic ecosystems today (Smith 2003; Smith and Schindler 2009). Just as fertilization of agricultural fields results in enhanced plant growth, increased nutrient inputs into aquatic ecosystems results in increased phytoplankton and macrophyte growth. However, the environmental consequences of enhanced productivity in aquatic ecosystems result in the degradation of water resources (e.g. cyanophyte blooms, microcystin toxin, and hypolimnetic hypoxia) which lead to socioeconomic (amenities and services) losses that these aquatic resources provide (Postel and Carpenter 1997).

Lake Erie is the southernmost, warmest, and most productive of the Laurentian Great Lakes. Although Lake Erie accounts for only 2% of water (by volume) of all the Great Lakes, its watershed is populated by 12 million people accounting for nearly 30% of the total population in the Great Lakes (Carter and Hites 1992). Consequently, Lake Erie has been experiencing multiple anthropogenic stressors since European settlement, including landscape changes within its catchment, nutrient pollution, climate change, contaminant inputs, and invasive species. Arguably, the effects of phosphorus (P) have been particularly influential at driving lake-wide water quality changes (Ludsin et al. 2001). Rapid population growth, introduction of phosphate detergents, and inadequate water treatment facilities in the early 20th century led to the eutrophication of Lake Erie, resulting in increased phytoplankton biomass, cyanophyte and *Cladophora* blooms, and severe hypolimnetic dissolved oxygen (DO) depletion in the central basin by the 1960s (Beeton 1961; Davis 1964; Hartman 1973; Allinger and Reavie 2013).

While summer oxygen depletion in the hypolimnion of the central basin of Lake Erie may be a natural phenomenon due to the lake's morphometry, hypolimnetic DO depletion rates have been exacerbated by anthropogenic activity since the 1930s (Harris and Vollenweider 1982; Rosa and Burns 1987; Stoermer et al. 1987). Hypolimnetic DO depletion occurs in the summer months due to formation of a strong vertical thermal gradient (i.e. stratification) which greatly reduces water mixing between the thermal water layers and DO flux into the hypolimnion. Bacterial decomposition of settling phytoplankton and other organic matter consumes DO which can often lead to hypoxic and anoxic conditions in the hypolimnion; the Ontario Ministry of the Environment and Climate Change (MOECC) defines hypoxic conditions as DO concentrations > 4 mg L^{-1}, while anoxic conditions are defined as DO concentrations > 1 mg L^{-1}.

These deteriorating water quality conditions in the mid-20th century have led to the development of P abatement programs initiated in the early 1970s as part of the Great Lakes Water Quality Agreement (GLWQA). Lake-wide TP targets (11,000 MTA) were established which included P reductions from point- and nonpoint sources (IJC 1972, 1978, 1983), followed by a period of apparent recovery through the 1980s (De Pinto et al. 1986; Makarewicz and Bertram 1993; Ludsin et al. 2001). However, by the late 1990s, Lake Erie began returning to a more eutrophic state similar to conditions observed in the 1960s, as evidenced by increases in summer cyanophyte blooms (Stumpf et al. 2012; Michalak et al. 2013; Wynne and Stumpf 2015), resurgence of *Cladophora* (Auer et al. 2010; Depew et al. 2011), and increased hypolimnetic hypoxic extent in the central basin (Zhou et al. 2013; Rucinski et al. 2014; Zhou et al. 2015). Although TP loads have not changed significantly since the 2000s (Dove and Chapra 2015; Maccoux et al. 2016), in 2014, the city of Toledo, Ohio had to shut off water to 500,000 residents for two days because their water treatment facilities were overwhelmed by microcystin toxin (Wilson 2014; Carmichael and Boyer 2016). The re-eutrophication of Lake Erie and development of *Microcystis* blooms in the western basin was suggested to be due to agricultural activities in the

Maumee River watershed (Baker et al. 2014; Scavia et al. 2014). Consequently, a 40% reduction from 2008 TP loads to 6,000 MTA was suggested to reduce cyanophyte blooms in the western basin and hypoxia in the central basin (IJC 2015).

Due to unavailability of continuous, long-term monitoring data pre-1950s, paleolimnological data can be used to supplement modeling and monitoring data for the development of effective remediation plans. Sgro and Reavie (2017) conducted a diatom-based paleolimnological study on the same sediment cores analyzed here in order to assess long-term ecological changes and diatom-inferred TP in Lake Erie in response to multiple anthropogenic stressors. This study uses a chironomid-based paleolimnological approach to build on the findings of Sgro and Reavie (2017) in order to qualitatively infer long-term trends in hypolimnetic DO conditions and conducting a quantitative reconstruction of hypolimnetic DO dynamics using a published average volume-weighted hypolimnetic oxygen (avgVWHO) model (Chapter 2).

As the current state of Lake Erie is the result of cumulative effects of multiple anthropogenic stressors, it can be difficult to interpret changes in biological assemblages and identify the relative impact of the different stressors. However, the use of numerical techniques, such as variance partitioning analysis (VPA), permits for the determination of the relative impact of stressors such as water quality, land use, and climate change, on biological communities. This numerical approach has been successfully used to examine the relative impact of various stressors on fossil assemblages (Hall et al. 1999; Paterson et al. 2008) and fish communities (Kelly et al. 2016). In similar fashion, I examined the long-term changes in chironomid assemblages in a sediment core from the central basin of Lake Erie and used VPA to evaluate the relative importance of three groups of environmental stressors (water quality, land use, and climate) on the observed variation in subfossil chironomid compositions (Chapter 3). Examination of VPA results will allow for the identification of environmental factors most important in influencing chironomid communities and inferred hypolimnetic DO, which will provide valuable

information for the development of science-based policies and remediation plans for the restoration of Lake Erie's water quality.

Literature Review

Eutrophication

Eutrophication is a general term used to describe a set of symptoms exhibited by lentic and marine ecosystems in response to nutrient enrichment (Hutchinson 1973). Eutrophication of aquatic ecosystems in North America has steadily increased since the establishment of substantial European settlement (circa 1800-1850), and by the 1960s it was deemed as the leading cause of water quality degradation (Schindler and Vallentyne 2008; Smol 2008). The primary symptoms of eutrophication include excessive growth of macrophytes, phytoplankton, and periphyton. Secondary symptoms include increased risk of harmful algal blooms, impaired water quality, hypolimnetic oxygen depletion, and altered aquatic community compositions (Wetzel 2001).

While eutrophication of aquatic ecosystems can occur naturally, it has become synonymous with cultural eutrophication, which refers to increased nutrient inputs resulting from anthropogenic activities within a lake's catchment (Schindler and Vallentyne 2008). The classic experiment by Schindler (1974) in the Experimental Lakes Area demonstrated that P is the limiting nutrient in aquatic ecosystems and should be addressed in watershed nutrient management to limit primary productivity. However, there has been some debate surrounding whether management of P alone is sufficient in controlling primary productivity and reducing hypolimnetic oxygen depletion in eutrophic systems and suggest that a dual nutrient (P and N) management approach is required to control primary productivity and cyanophyte blooms due to P and N colimitation in such systems (Moon and Carrick 2007; North et al. 2007; Sterner 2008; Paerl et al. 2010) although this has been contested by others (Schindler et al. 2008; Molot 2017).

A survey study of phytoplankton composition in the central and western basins of Lake Erie by Reavie et al. (2015) suggested that winter-spring diatom abundance (by biovolume) were greater than summer algal blooms between 2008 and 2011 and are likely to have a greater contribution to driving hypolimnetic oxygen depletion in the central basin of Lake Erie. However, unlike summer algal blooms in Lake Erie, the production of diatoms has been suggested to be limited by bioavailable silica, with majority of silica inputs from Lake Huron, rather than P or N (Schelske et al. 1986; Schelske et al. 2006; Reavie et al. 2015; Reavie et al. 2017; Sgro and Reavie 2017) as was indicated by silica depletion in the water column by mid-spring (Twiss et al. 2012; Reavie et al. 2014). Consequently, early season diatom biomass may be an important contributor of organic matter and hypolimnetic oxygen depletion via bacterial degradation (Lashaway and Carrick 2010; Reavie et al. 2015). As a result, a watershed nutrient management approach which is focused on reductions of P, N, or both must consider whether these reductions will reduce diatom abundance in addition to summer cyanophyte blooms.

Hypolimnetic oxygen depletion

In aquatic ecosystems, the rates of dissolved oxygen supply from the atmosphere, photosynthetic inputs, and hydrological distribution, are counterbalanced by the consumptive metabolism of biota and abiotic chemical processes. While dissolved oxygen is essential to the metabolism of all aerobic aquatic organisms, it also plays crucial roles in the abiotic processes involved in nutrient and contaminant cycling between sediments and the water column (Wetzel 2001; Dodds 2002). As such, in order to implement successful environmental mitigation strategies to reduce the incidence and extent of anoxic and hypoxic conditions knowledge of the underlying drivers of dissolved oxygen dynamics and long-term trends in aquatic ecosystems is essential.

Seasonal cycles in temperature and sunlight influence water density and mixing. In deep temperate lakes summer thermal stratification occurs when the surface water becomes warm enough

that wind can no longer thoroughly mix the warm and less dense surface water with the cooler, more dense water below. The warm and well-mixed surface layer is called the epilimnion, the zone of rapid temperature transition below the epilimnion is called the thermocline, and the cool bottom layer is called the hypolimnion. The thermocline acts as a barrier between the epilimnion and hypolimnion, resulting in negligible vertical diffusion of heat and DO (Dodds 2002). Since the hypolimnion has a finite DO capacity, metabolic and respiratory processes which require oxygen result in its gradual depletion from the hypolimnion.

Sedimentation of phytoplankton and other organic matter to the bottom of lakes stimulates bacterial decomposition. As a result, most of the biological oxygen demand in the hypolimnion occurs at the sediment-water interface due to bacterial respiration (Charlton 1980a). Thus, phytoplankton productivity is an important factor in hypolimnetic DO depletion (Hutchinson 1973). Generally, in most temperate lakes, phytoplankton productivity is limited by P (Schindler 1974; Schindler 1977; Schindler et al. 2008; Schindler and Vallentyne 2008). Correspondingly, aquatic ecosystems which undergo cultural eutrophication often demonstrate an increase in the magnitude, frequency, and duration of hypolimnetic hypoxia (Hutchinson 1973; Rosa and Burns 1987; Diaz and Rosenberg 2008).

Although the lake's trophic status is an important determinant of hypolimnetic DO depletion, other factors, such as temperature and lake morphometry, also have a substantial role in regulating hypolimnetic hypoxia (Charlton 1980a; Rosa and Burns 1987). Hypolimnetic temperature has both direct and indirect effects on DO depletion rates: as water temperature increases its maximum capacity to carry oxygen decreases (Wetzel 2001; Dodds 2002), at the same time higher temperatures affect chemical reaction kinetics and thereby increase bacterial decomposition rates (Charlton 1980a; Dodds 2002). Due to limited DO diffusion between the hypolimnion and thermocline, hypolimnetic thickness is also an important determinant of end-of-summer hypolimnetic hypoxia, where thin hypolimnia are more likely to be depleted of their oxygen reservoir sooner compared to thick hypolimnia in deep lakes

with comparable primary productivity because of a higher sediment area to hypolimnetic volume ratio (Charlton 1980a). In addition, since most of the biological oxygen demand occurs at the sediment-water interface, sediment surface area is also an important determinant of hypolimnetic DO depletion rates (Molot et al. 1992).

Description of Lake Erie

Lake Erie is the fourth in surface area among the five Laurentian Great Lakes and ranks 11th of the largest lakes in the world. It receives discharge from Lakes Superior and Michigan via Huron through Lake St. Clair through the Detroit River and empties via the Niagara Falls into Lake Ontario which drains through the St. Lawrence River into the Atlantic Ocean. The Great Lakes took their present shape 10,000 years ago, yet their developmental history goes back at least 1,000 million years when the Precambrian rocks of the Canadian Shield were formed, and these rock types still dominate the upper Great Lakes (Hough 1958). While a full review of the geological development of Lake Erie and its watershed is outside the scope of this paper, I will provide an overview of the lake's geography and prominent geological features within its watershed and how climatic forces and human influences have shaped Lake Erie into its present state.

Lake geography, morphometry, and watershed geology

Lake Erie is the southernmost lake of the Great Lakes, with a surface area of 25,500 km^2, and a watershed area of 102,000 km^2; it has a general southwest to northeast orientation with a maximum length of 390 km and an average width of 70 km (Burns 1985). Approximately 95% of the water inflow into Lake Erie comes through the western basin via the Detroit, Maumee, and Sandusky rivers, with inflows from the Detroit River accounting for approximately 90% of total water inflow (Hartman 1973; Burns 1985; Carter and Hites 1992). Lake Erie has the shortest hydraulic retention time of all the

Laurentian Great Lakes, approximately 2.6 years (Scavia et al. 2014), which makes water quality vulnerable to changes from these inflows.

Lake Erie has three distinct basins (Fig. 1.1). The western basin is the shallowest and has an average depth of 7.6 m (maximum depth 19 m), its western edge lies in the inlet of the Maumee River and extends northeast to Point Pelee National Park, Ontario. It covers approximately 13% of the area of Lake Erie and holds roughly 5% of the volume of the lake. The central basin extends east from the western basin to the eastern basin, separated by a sand and gravel moraine from the base of Long Point National Park, Ontario to Erie, Pennsylvania. With an average depth of 18 m (maximum depth 24 m), it is considerably deeper than the western basin. The central basin covers approximately 63% of the area of Lake Erie and contains approximately 63% of the volume. The eastern basin is the deepest, with an average depth of 24.4 m (maximum depth 64m) it constitutes 24% of the lake's surface and 32% of its volume (Hartman 1973).

Most of the Lake Erie watershed is flat with rolling hills, with only the southeast shores having steep-sided hills (Burns 1985). Geologically, the Lake Erie watershed is composed primarily of post-glacial sedimentary rock, including limestone, dolomite, sandstone, and shale. The northern shoreline of Lake Erie consist primarily of erodible banks of glacial till and sand and in many areas this till shoreline consists of steep bluffs, while the southern shoreline is dominated by clay (Hough 1958; Hatcher 1971). As a result of the geology in the Lake Erie watershed, it is prone to high sediment accumulation rates due to weathering and erosion processes. Sly (1976) estimated that over the past 2,000 years Lake Erie has shallowed by up to 3.8 m while its surface area increased by 20%. These erosion and sediment accumulation rates within Lake Erie are strongly influenced by climatic variability and have been exacerbated by anthropogenic land use changes within Lake Erie's catchment.

Climate and thermal cycles

The nature of a lake is as dependent on climate and weather as it is on its bathymetry, watershed geology, and nutrient supply. With a detailed description of the long-term interannual climatic variability is discussed in Chapter 3, here I will only provide details on the prevailing climate within Lake Erie and its watershed in order to provide a general picture of the natural forces influencing its water quality.

The range between mean summer and mean winter air temperatures is approximately 23°C; the mean air temperatures for the summer and winter are 21°C and -2°C, respectively. Approximately 80% of the lake is frozen during most winters, and it is completely frozen during the coldest winters. In contrast, mean surface water temperatures in the summer often reach 23°C. These warm water temperatures make Lake Erie popular for recreation. The average long-term combined annual precipitation of rain and snow in the Lake Erie watershed is approximately 870 mm. Mean long-term annual evaporation is also approximately 870 mm, with highest evaporation rates occurring in August and fall months. However, higher evaporation generally occurs during years with low precipitation, thus the effects of evaporation accentuate rather than moderate the effects of low precipitation. Since wet and dry years generally occur in grouped patterns, large periodic variations in annual average lake level are observed.

Due to the morphometry of Lake Erie, seasonal thermal cycles vary considerably among the three basins. The shallow western basin is the first to freeze in the winter, and water temperature under ice become isothermal at approximately 1°C (Hartman 1973). The ice begins to thaw in early March and surface water temperatures gradually reach 5°C by late April, 15°C by June, and 24-26°C by early August (Hartman 1973; Burns 1985). Generally, in the summer the water in the western basin is kept at near isothermal conditions due to vertical mixing induced by wind stress. Temporary stratification can occur

in the form of an intermittent thermocline, where water in contact with the sediment is 1-2^{o}C cooler than the overlying water, during years which experience hot and calm weather (Burns 1985).

The deeper central basin only freezes over completely during extremely cold winter years and generally remains isothermal at 1^{o}C. Spring warming is slower than the western basin and water temperatures generally lag by about one week (Hartman 1973). Summer stratification forms in June, but due to the depth of the central basin, the thermocline quickly sinks to 18-20 m below the water surface and has a sharp gradient of 10^{o}C m^{-1} (Burns 1985). In the deeper part of the central basin, the average thickness of the epilimnion, thermocline, and hypolimnion is approximately 17 m, 2-3 m, and 3-5 m, respectively (Burns 1985). Consequently, the thin hypolimnion which forms during summer stratification in the central basin is prone to oxygen depletion and due to the relatively flat surface of the central basin the hypoxic extent can be as large as 11,000 km^{2} (Fig. 1.2; Beeton 1963; Zhou et al. 2013; Zhou et al. 2015)

Seasonal thermal cycles in the deep eastern basin more closely resemble cycles in the other Great Lakes. As the ice breaks up in the western and central basins in early spring, ice floes move east and pack over the eastern basin. As a result, surface water warming in the eastern lags behind temperatures observed in the western and central basins (Hartman 1973). Stratification of the eastern basin begins in early June, soon after the water becomes vertically isothermal at 4^{o}C. Generally, summer stratification in the eastern basin is comprised of a 20 m thick epilimnion with a 5-10 m thick thermocline which has a temperature gradient of approximately 1.5^{o}C m^{-1}, and the top of the hypolimnion is generally found at a depth of approximately 28 m (Burns 1985). Since the formation of the thermocline in the eastern basin occurs at relatively the same level as the hypolimnion in the central basin, cool oxygenated water from the eastern basin thermocline mixes to some extent with the hypolimnetic water in the central basin (Burns 1985; Rosa and Burns 1987). By late October all the water in Lake Erie is vertically isothermal, although water in the eastern basin remains warmer than in the

central and western basins. These conditions prevail until December when the surface water in the shallow western basin begins to freeze (Burns 1985). Due to high fall and winter turbulence within Lake Erie, neither the central or eastern basin become stratified in the winter. Instead, the water is nearly isothermal at 1^{o}C (Hartman 1973; Burns 1985).

European settlement in the Lake Erie watershed

Before European colonization, the south shores of the western basin consisted of extensive marsh complexes covering most of the shoreline from Sandusky to Detroit and extended far inland (Burns 1985). The most notable of these complexes was the Black Swamp which was approximately 40 km wide and covered an estimated area of 4,000 km^2 (Mitsch and Gosselink 2015). This vast marsh complex was a network of wetlands, grasslands, and forests. It extended from the mouth of Sandusky River to Toledo, Ohio and southwest along the Maumee River to New Haven, Indiana (Burns 1985). These extensive wetland networks served as an important sediment filtration systems (Mitsch and Gosselink 2015).

Exploration and early settlement around Lake Erie began in the late 1700s and the early 1800s. This was a tremendous period for the Lake Erie watershed in terms of the growth in the number of inhabitants and was accompanied by changes in landscape (Hatcher 1971). By the early 20th century most of the wetlands in the western Lake Erie watershed, including the Black Swamp, were drained, forests were cleared, and prairies burnt to convert most of this region into farmland (Hartman 1973; Burns 1985). Coastal wetlands which provided nutrient and sediment filtration were primarily lost, and now the southwestern Lake Erie shoreline comprises less than 5% of the original wetland habitat (Herdendorf 1987). These changes in vegetation cover and land use led to drastic changes in drainage dynamics, resulting in increased erosion and causing streams and rivers to become turbid (Hartman 1973).

Rapid population growth and the introduction of phosphate detergents and commercial fertilizers (nitrogen) in the 1920s resulted in a dramatic increase in nutrient loads into Lake Erie. Most of the nutrient loads into the lake came from domestic, industrial, and agricultural wastes which were discharged into the western basin via the Detroit and Maumee Rivers (Hartman 1973). For example, in the 1960s the Detroit River received an estimated 6.1 billion liters of domestic and industrial waste per day (Powers and Robertson 1966), resulting in a 5-fold increase in TP and 30% increase in TN between 1948-1962 (Verduin 1969), and an increase in total dissolved solids from 133 to 198 mg L^{-1} between 1960-1968 (Beeton 1965; Chawla 1971). These changes resulted in a rapid decline of Lake Erie's water quality.

Water quality: multiple stressors and cumulative effects

Lake Erie is the shallowest of the Great Lakes primarily for two reasons: first, the lake basins which remained following the last glacial retreat were shallower than the other Laurentian Great Lakes; and its watershed is dominated by erodible shorelines which have filled the lake considerably since its formation (Sly 1976; Kemp et al. 1977; Burns 1985). The central basin shorelines consist of clay bluffs that are continually eroded by fluctuating water levels and waves. However, the highest sedimentation rates occur in the western basin near the inlets from the Detroit and Maumee rivers and the eastern basin off of Long Point (Fig. 1.3; Kemp et al. 1977). Consequently, interannual variation in lake level, precipitation, and wind (i.e. wave stress) are important factors influencing erosion.

However, erosion processes have been exacerbated by anthropogenic landscape alterations such as wetland draining, deforestation, and extensive agricultural developments. For example, sheet erosion within the Lake Erie watershed carries an estimated 6.5 million tons of suspended solids into the lake each year, while erosional loads into Lake Superior and Lake Ontario are 1.4 and 1.6 million tons yr^{-1}. These immense erosional loads are primarily the result of the intense agricultural activity within the

western watershed (Burns 1985). As a result, increased erosion in western Lake Erie results in high water turbidity which leads to loss of aquatic vegetation and fish-spawning areas (Hartman 1973). In addition, there are anthropogenically-induced effects on sediment chemistry composition, which include inputs of heavy metals (e.g. Pb, Cu, Cd, Hg) and other contaminants into Lake Erie (Kemp et al. 1976).

While Lake Erie experienced several anthropogenic stressors since European settlement (e.g. wetland draining, deforestation, modification of catchment, eutrophication, and climate change), TP loadings into the lake have been particularly influential at driving lake-wide ecological change (Ludsin et al. 2001). By the 1960s, increased TP loads into Lake Erie resulted in severe degradation of water quality through changes in phytoplankton composition with pronounced increases in phytoplankton biomass and cyanobacteria blooms in the western basin (Beeton 1961; Beeton 1963; Davis 1964; Beeton 1965; Casper 1965; Britt et al. 1973), and contributed to severe depletion of hypolimnetic DO in the central basin (Burns 1976; Charlton 1980b; Charlton 1987; Rosa and Burns 1987). Reduced oxygen conditions in the central basin eliminated the thermal habitat required by cold-water organisms and contributed to the local extirpation of important benthic macroinvertebrates and declines in several fish species (Carr and Hiltunen 1965; Hartman 1973; Ludsin et al. 2001).

These deteriorating water quality conditions in Lake Erie led to a legislative response with the 1972 Great Lakes Water Quality Agreement (GLWQA), amended in 1978, which established point-source TP abatement programs by removal of P from detergents and limiting TP in industrial and water treatment effluents (IJC 1972; IJC 1978). Lake-wide TP targets of 11,000 metric tons per annum (MTA) were established in 1983 and included TP inputs from nonpoint sources (IJC 1983). Lake Erie appeared to respond to these changes in TP loads relatively quickly, and by the mid-1980s there were reported reductions in water column TP (De Pinto et al. 1986; Ludsin et al. 2001), reduction in summer diatom and cyanophyte biomass (Makarewicz 1991; Bertram 1993; Makarewicz and Bertram 1993), and

decreased hypolimnetic DO depletion rates in the central basin (Charlton 1987; Bertram 1993; Burns et al. 2005).

However, this apparent period of recovery was short-lived and by the late 1990s, Lake Erie was once again beset by severe cyanophyte blooms in the western basin and extensive hypoxia in the central basin (Millie et al. 2009; Michalak et al. 2013). Zhou et al. (2013) showed that while there was substantial interannual variability in summer hypoxic extent, there appeared to be cyclical trends, with the largest hypoxic extents in the late 1980s and early 2000s with minimal hypoxia in the mid-1990s. These trends were consistent with hypolimnetic DO depletion trends estimated using hydrodynamic models (Burns et al. 2005; Rucinski et al. 2010). As a result, hypolimnetic hypoxia continues to negatively influence biological and physical processes in the central basin of Lake Erie.

Hypolimnetic hypoxia influences several ecological processes which result in negative impacts on individual fish growth, survival, reproduction, and ultimately population growth (Rao et al. 2014; Kraus et al. 2015). While rapid changes in hypolimnetic oxygen concentrations may trap fish in hypoxic waters and lead to direct mortality, a more common immediate fish response to hypolimnetic hypoxia is avoidance of deep waters (Hartman 1973; Ludsin et al. 2001). Such behavioral response can lead to shifts away from preferred diets, increase in total metabolic costs, potential negative reproductive impacts, and increased susceptibility to disease (Pihl 1994; Craig et al. 2001). The impacts of hypolimnetic hypoxia in Lake Erie on fish species mobility within the water column appear to vary between species. For example, rainbow smelt entirely avoid hypoxic water by moving just above the hypoxic zone (Roberts et al. 2012). In contrast, white and yellow perch appear to be more tolerant of hypoxic hypolimnia by undertaking short feeding times in hypoxic zones (Roberts et al. 2009; Roberts et al. 2012).

The effects of hypolimnetic hypoxia were also evident in predator-prey interactions, where owing to species-specific responses, hypoxia may reduce the overlap of predator and prey. For example in Lake Erie, cold-water rainbow smelt showed strong selection for Chironomidae larvae during periods of oxygenated hypolimnion, but changed diet almost entirely to zooplankton during hypoxic conditions (Pothoven et al. 2009). In contrast, the diet of the emerald shiner, a warm-water epilimnetic zooplanktivore was unaffected by change in hypolimnetic oxygen, in fact, their foraging rates increased as zooplankton was forced into the epilimnion (Pothoven et al. 2009). White and yellow perch also alter their diets to consume more zooplankton in response to hypolimnetic hypoxia, but these changes are not as dramatic as seen in rainbow smelt (Roberts et al. 2009; 2012).

Lake sediments can act as a sink and source of P and other contaminants depending on the redox conditions at the sediment-water interface. Under oxic conditions, lake sediments act as P sinks, where P forms complexes with iron (III) under oxidizing conditions. However, when oxygen is depleted at the sediment-water interface, reducing conditions dominate, causing iron to change from solid ferric form to highly soluble ferrous form, releasing bound P into the water column (Mortimer 1942; Boström et al. 1988). Since Lake Erie experiences hypoxic conditions within the central basin annually, its sediments are an important internal source of P (Matisoff et al. 2016; Paytan et al. 2016).

Thus, understanding of the dominant forces governing hypolimnetic DO depletion is crucial for developing effective remedial and legislative action. However, parsing out the dominant driving forces of hypolimnetic hypoxia within the central basin is difficult due to multiple stressors that the lake experiences. For example, Rucinski et al. (2010) demonstrated that changes in hypolimnetic DO depletion were driven by TP loads rather than climate; similarly, Burns et al. (2005) demonstrated that DO depletion rates were related to the previous year's TP loads. While Reavie et al. (2015) suggested that winter-spring diatom blooms and soluble silica may be important drivers of summer hypoxia in the central basin. Although there has been considerable, though unsystematic, monitoring of water quality

(Burns 1976; Rosa and Burns 1987; Burns et al. 2005) and phytoplankton composition (Allinger and Reavie 2013) in Lake Erie over the past century, there remains a substantial lack of information about the long-term (pre-20th century) trends in central basin hypolimnetic DO dynamics and a consensus of the dominant driving forces influencing DO depletion rates. As a result, there is a need for a proxy method, such as paleolimnology, to understand historical environmental trends preceding monitoring.

Paleolimnology and paleolimnological reconstructions

Paleolimnology is a multidisciplinary science that uses physical, chemical, and biological information preserved in sediment profiles to reconstruct past environmental conditions in lakes and their catchments (Smol 2008). It addresses a very broad range of issues relating to former ecosystem composition and development, lake ontology, climate change, water quality trends, and the variability of catchment and land use processes.

Lake sediments are derived from both external and internal sources – allochthonous matter is transported by water movement from its surrounding drainage basin (e.g. eroding soils, weathering materials, nutrients, etc.) or by air as particulates (e.g. pollen, ash, and airborne industrial pollutants), while autochthonous matter is produced within the lake (e.g. remains from algae and invertebrates, and chemical precipitates such as carbonate) (Smol 2008). As a result, the paleolimnological method uses these proxy data archived in lake sediments in order to determine baseline or pre-disturbance conditions when long-term monitoring data is not available.

Paleolimnology assumes two key principles, the law of *superposition* and *sediment focusing*. The law of superposition states that undisturbed sedimentary sequences possess a depth-time profile, such that younger material overlays older deposited material (Smol 2008). Sediment focusing is a process by which matter is deposited to the deepest point in the lake and is a function of the lake's bathymetry, catchment topography, river inputs, and internal water movement (Smol 2008). As a result, sediment

cores are collected from the deepest part of the basin where the stratigraphic profile contains archived information about the watershed ontology and anthropogenic activity.

While direct quantification of historical water quality conditions from sediments, such as water P or hypolimnetic oxygen concentrations, can be problematic due to the dual nature of lake sediments which are able to act as P sinks or sources depending on the redox conditions, pH, and iron concentrations (Jensen et al. 1992; Eckert et al. 1997; Søndergaard et al. 2003), it is possible to use an indirect proxy method coupled with inference model techniques to reconstruct long-term historical water quality trends. Paleolimnological inference models estimate historical watershed changes by using statistical methods to link modern species assemblage data and indicator species environmental optima and tolerances to limnological data from a group of lakes in a particular geographical region which are chosen to reflect a gradient of the parameter of interest (calibration set). Based on modern species-environment relationships observed in the calibration set, a transfer function can be generated and applied to stratigraphic sediment intervals of a sediment core extracted from a lake of interest in order to infer historic environmental conditions. The resulting inferences can be used to infer trends in natural variability, changes in lake trophic status, and effects of anthropogenic activity (Smol 2008). This approach has been facilitated by statistical advances in linear and unimodal response gradient analysis (Birks 1995; Birks 1998; Birks et al. 2012; Legendre and Birks 2012) Several methods for quantitative reconstruction have been described by ter Braak (1995), Birks (1995), and Birks (2014) for dealing with unimodal species responses to environmental gradients. However, the accuracy and reliability of the reconstruction depends on the size, coverage, and quality of the calibration set. Furthermore, taxonomic consistency, both within the calibration set and between the calibration set and study core fossil material is critical (Birks 1995).

It is also important to note that quantitative reconstructions have five major undelying assumptions (Birks 1995): (1) taxa used in the calibration set are systematically related to the

environment in which they live; (2) the environmental variable to be reconstructed is an ecologically important determinant of the ecosystem under study; (3) taxa in the calibration set are the same entities in the fossil data under study and their ecological responses to environmental variables have not changed significantly over time; (4) statistical methods used in the transfer function adequately model the biological responses to environmental variables with sufficient predictive power to allow for accurate and unbiased environmental reconstructions; and (5) other environmental variables have negligible influence, or their joint distribution with the environmental variable of interest in the studied core is the same as in the calibration set.

Following environmental reconstruction, it may be necessary to assess the relative importance of different sets of environmental variables (e.g. climate, water quality, land use) on changes in fossil assemblages (Smol 2008; Birks et al. 2012). Variance partitioning analysis uses direct gradient analysis or canonical ordination to estimate which fraction of the total variation in assemblage composition can be explained by specific categories of measured environmental variables (Borcard et al. 1992; Šmilauer and Lepš 2003). However, it has been shown that the coefficient of determination (R^2) is a biased estimator of the proportion of explained variation. Peres-Neto et al. (2012) have shown that the adjusted coefficient of determination (R_{adj}^2) is a more suitable estimator of the proportion of variation explained as it is unbiased.

Paleolimnological studies in Lake Erie

To date, there have been three paleolimnological studies which examined the effects of anthropogenic stressors on Lake Erie's water quality using chemical and diatom proxies. Kemp et al. (1976) examined the chemical composition of sediment cores collected from the Great Lakes in order to estimate the influence of anthropogenic activities within the Great Lakes watershed on lake sediment geochemistry. Using *Ambrosia* pollen as the dating method, Kemp et al. (1976) concluded that in Lake

Erie since the 1850s there have been dramatic increases in several heavy metals (e.g. Pb, Cu, Cd, Hg) and sediment accumulation rates.

However, most paleolimnological studies in Lake Erie concentrated on examining microfloral fossils in sediment cores in order to infer long-term trends in phytoplankton ecology and the effects of anthropogenic TP loads on Lake Erie's water quality. A comprehensive account of pelagic phytoplankton research is provided by Allinger and Reavie (2013) which details a chronological summary of major events, environmental conditions and determinants that affected algal productivity, abundance and species composition in the three Lake Erie basins. As a result, here I will only provide a brief overview of the major findings from diatom-paleolimnological studies.

The first diatom-based paleolimnological study was conducted by Harris and Vollenweider (1982) and used a qualitative approach to examine a sediment core from the central basin dated by pollen (*Ambrosia*). Harris and Vollenweider (1982) concluded that anthropogenic P inputs, primarily due to deforestation and expansion of agricultural lands in the 19th century, were the primary drivers of changing phytoplankton assemblages and suggest that signs of eutrophication appeared as early as the 1850s. Stoermer et al. (1987) followed the study conducted by Harris and Vollenweider (1982) by collecting a sediment core from the same location in the central basin but used newer chronological methods (^{210}Pb dating). While Stoermer et al. (1987) confirmed the trends observed by Harris and Vollenweider (1982) that European settlement in the Lake Erie watershed had a substantial impact on the lakes trophic status and ecology. Early signs of eutrophication occurred between 1860-1900 with more disruptive changes occurring by the 1920s, and rapid eutrophication in the 1930s-1970s.

Since the work by Harris and Vollenweider (1982) and Stoermer et al. (1987), Lake Erie has undergone substantial ecological changes. Following a period of hypereutrophic conditions between the 1960s-1970s which was characterized by severe cyanophyte and *Cladophora* blooms, increased

phytoplankton biomass, and extensive anoxia in the central basin (Beeton 1961; Davis 1964), legislative action to limit TP inputs into Lake Erie took place in the 1970s and 1980s (IJC 1972; IJC 1978; IJC 1987). These TP load reductions lead to a temporary recovery by the 1980s (Makarewicz and Bertram 1993; Ludsin et al. 2001). However, by the late 1990s, the lake has once again been subjected to severe nuisance algal blooms and extensive hypoxia in the central basin (Michalak et al. 2013).

Sgro and Reavie (2017) collected sediment cores from the western and central basins of Lake Erie in 2011 to evaluate the ecological history of Lake Erie from diatom assemblages and geochemical markers. The central basin core was collected from a location corresponding to precisely collected sediment cores by Harris and Vollenweider (1982) and Stoermer et al. (1987), while the western basin core was collected from an area that is likely to have high sedimentation rates (Sgro and Reavie 2017).

Chironomidae as hypolimnetic oxygen proxies

The chironomids (Class: Insecta; Order: Diptera; Family: Chironomidae), commonly referred to as non-biting midges, are frequently the most abundant insects found in freshwater ecosystems (Hofmann 1988; Armitage et al. 2012). Although they are most conspicuous as swarms of adults at many lakeshores, the majority of their lifecycle occurs in the aquatic larval stages (Oliver 1971; Armitage et al. 2012). In addition, chironomids occupy a wide range of environmental conditions due to the ability of individual species to tolerate different gradients in lake depth, salinity, pH, temperature, productivity, and dissolved oxygen (Brundin 1951; Sæther 1979; Wiederholm 1980; Walker 1987, 1995, 2001; Armitage et al. 2012).

Numerous studies have examined the relationship between hypolimnetic oxygen levels and chironomid DO tolerances and spatial distribution (e.g. Brundin 1951; Heinis and Crommentuijn 1992; Heinis et al. 1994; Panis et al. 1996; Quinlan and Smol 2001; Brodersen et al. 2004). Some members of the chironomid family developed morphological (e.g. body size) and physiological (e.g. hemoglobin)

adaptations in order to survive under low hypolimnetic DO conditions (Weber 1980; Heinis et al. 1994; Panis et al. 1996; Armitage et al. 2012), while other taxa use behavioural adaptations such as migration (Bazzanti et al. 1998), or tube ventilation (Brodersen and Quinlan 2006) to deal with low hypolimnetic DO conditions often associated with highly eutrophic lakes. For example, members of the *Chironomus* spp. (especially *C. anthracinu*s and *C. plumosus*), have a large body size coupled with high content of hemoglobin permitting them to tolerate long periods of anoxic conditions (Weber 1980; Panis et al. 1996; Quinlan and Smol 2001a); similarly, *Procladius* have a large body size but low levels of hemoglobin which allow members of this genus to tolerate short periods of hypoxic conditions (Panis et al. 1996; Quinlan and Smol 2001a); while taxa such as *Heterotrissocladius* and *Micropsectra* have high oxygen optima and are unable to tolerate low hypolimnetic DO conditions (Quinlan and Smol 2001a; Brodersen and Quinlan 2006).

Since hypolimnetic DO conditions are influenced by the interaction of multiple stressors, such as inputs from catchments, eutrophication, and thermal stability induced by climate change, changes in the distribution and abundance of chironomid taxa are often indicative of changes in hypolimnetic DO and water quality resulting from the cumulative effects of multiple stressors (Brodersen and Quinlan 2006). Moreover, the chitinous head capsules from molted exuviae are well preserved in sediments permitting taxonomic identification of their remains (Hofmann 1988). Consequently, chironomid species-specific tolerances to environmental gradients and their head capsule preservation properties make them good paleoindicators, such that paleolimnological assessment of subfossil chironomid remains preserved in sediments could potentially allow for quantitative reconstruction of past hypolimnetic DO conditions (Walker 1987; Hofmann 1988; Smol 2008).

While early use of chironomids as indicators was restricted to qualitative trophic state models (Sæther 1979; Lindegaard 1995), more recent research focused on generating semi-quantitative and quantitative models, and the scope of paleoreconstructions has been extended to include temperature

and hypolimnetic DO conditions (e.g. Quinlan and Smol 2001; Brodersen and Anderson 2002; Walker and Cwynar 2006; Eggermont and Heiri 2012). In deep temperate lakes that stratify during the summer months, such as Lake Erie, hypolimnetic DO is generally more limiting than food availability; thus changes in chironomid assemblages primarily reflect changing DO conditions (Langdon et al. 2006). Based on these characteristics Quinlan et al. (1998) developed a transfer function that related subfossil chironomid assemblages to hypolimnetic DO conditions expressed through anoxia factor (AF), which represents the number of days per season a sediment area equal to the lake's surface area is overlaid by anoxic water (Nürnberg 1995). However, because the chironomid-based AF transfer function relies on predictive equations to calculate historic physical (Z_{mean}, SA) and chemical (TP) data, it may not represent accurate DO conditions downcore (Birks 1998). In addition, the chironomid assemblage predicted AF is most robust in a limited geographical area in which the model was developed (Little and Smol 2001).

Thus, Quinlan and Smol (2001) further explored the relationship between hypolimnetic DO condition and subfossil chironomids by relating chironomid assemblages to avgVWHO. These relationships were used to develop a series of species optima curves and enabled generation of inferred avgVWHO values downcore; this transfer function (R^2_{jack} = 0.56, RMSEP = 2.15 mg O_2 L^{-1}) was based on 54 lakes located in south-central Ontario and used 44 chironomid taxa. Several studies used this transfer function for quantitative reconstruction of hypolimnetic DO conditions in Lake Simcoe and Lake of the Woods (Rodé 2009; Summers et al. 2012).

Paleolimnology as a tool for lake-wide management plans

Effective management of aquatic resources requires long-term data in order to understand how various variables influence these resources. However, because long-term monitoring data which span beyond the point of impact are rarely available, indirect proxy methods can be used to generate this missing data. Due to the major advances in paleolimnological quantitative techniques in recent decades

(Borcard et al. 1992; Birks 1998; Smol 2008; Peres-Neto et al. 2012), the paleolimnological approach can be directly integrated into cost-effective assessments of aquatic ecosystem health (Smol 1992).

As there are a multitude of factors which influenced water quality in Lake Erie and predate monitoring data, it is impossible to accurately assess how anthropogenic stressors have impacted water quality and the effectiveness of remedial actions undertaken since the 1970s. Thus the purpose of this study is to (1) examine the long-term (1850-2011) hypolimnetic DO trends in the central basin of Lake Erie using a chironomid assemblage inferences (Chapter 2); (2) quantitatively reconstruct the historic hypolimnetic DO dynamics using a published avgVWHO inference transfer function (Quinlan and Smol 2001a) (Chapter 2); and (3) determine the key drivers of change in chironomid assemblage compositions and inferred avgVWHO (Chapter 3). Findings from this study are aimed to supplement historical data generated by diatom-based paleolimnological studies (Harris and Vollenweider 1982; Stoermer et al. 1987; Sgro and Reavie 2017) in order to provide policy makers and lake managers with crucial long-term data and assist in the development of effective remedial strategies.

References

Allinger LE, Reavie ED. 2013. The ecological history of Lake Erie as recorded by the phytoplankton community. J Great Lakes Res. 39:365–382.

Armitage PD, Pinder LC, Cranston P. 2012. The Chironomidae: biology and ecology of non-biting midges. Springer Science & Business Media.

Auer MT, Tomlinson LM, Higgins SN, Malkin SY, Howell ET, Bootsma HA. 2010. Great Lakes Cladophora in the 21st century: same algae-different ecosystem. J Great Lakes Res. 36:248–255.

Baker DB, Confesor R, Ewing DE, Johnson LT, Kramer JW, Merryfield BJ. 2014. Phosphorus loading to Lake Erie from the Maumee, Sandusky and Cuyahoga rivers: The importance of bioavailability. J Great Lakes Res. 40:502–517.

Bazzanti M, Seminara M, Baldoni S. 1998. Assessing hypolimnetic stress in a monomictic, eutrophic lake using profundal sediment and macrobenthic characteristics. J Freshw Ecol. 13:405–412.

Beeton AM. 1961. Environmental changes in Lake Erie. Trans Am Fish Soc. 90:153–159.

Beeton AM. 1963. Limnological survey of Lake Erie 1959 and 1960. Great Lakes Fishery Commission.

Beeton AM. 1965. Eutrophication of the St. Lawrence great lakes. Limnol Oceanogr. 10:240–254.

Bertram PE. 1993. Total Phosphorus and Dissolved Oxygen Trends in the Central Basin of Lake Erie, 1970–1991. J Great Lakes Res. 19:224–236.

Birks HJB. 1995. Quantitative paleoenvironmental reconstructions. In: Statistical modeling of Quaternary science data. Quaternary Research Association. p. 161–254.

Birks HJB. 1998. DG Frey and ES Deevey Review 1: Numerical tools in palaeolimnology–Progress, potentialities, and problems. J Paleolimnol. 20:307–332.

Birks HJB, Lotter AF, Juggins S, Smol JP. 2012. Tracking Environmental Change Using Lake Sediments: Data Handling and Numerical Techniques. Springer Science & Business Media.

Birks HJB. 2014. Quantitative palaeoenvironmental reconstructions from Holocene biological data. In: Mackay A, Battarbee R, Oldfield F, editors. Global change in the Holocene. Routledge. p. 123–139.

Borcard D, Legendre P, Drapeau P. 1992. Partialling out the Spatial Component of Ecological Variation. Ecology. 73:1045–1055.

Boström B, Andersen JM, Fleischer S, Jansson M. 1988. Exchange of phosphorus across the sediment-water interface. Hydrobiologia. 170:229–244.

ter Braak CJF. 1995. Non-linear methods for multivariate statistical calibration and their use in palaeoecology: a comparison of inverse (k-nearest neighbours, partial least squares and weighted averaging partial least squares) and classical approaches. Chemom Intell Lab Syst. 28:165–180.

Britt NW, Addis JT, Engel R. 1973. Limnological studies of the island area of western Lake Erie. Bull Ohio Biol Surv 4 p 1-85, 1973.

Brodersen KP, Anderson NJ. 2002. Distribution of chironomids (Diptera) in low arctic West Greenland lakes: Trophic conditions, temperature and environmental reconstruction. Freshw Biol. 47:1137–1157.

Brodersen KP, Pedersen O, Lindegaard C, Hamburger K. 2004. Chironomids (Diptera) and oxy-regulatory capacity: An experimental approach to paleolimnological interpretation. Limnol Oceanogr. 49:1549–1559.

Brodersen KP, Quinlan R. 2006. Midges as palaeoindicators of lake productivity, eutrophication and hypolimnetic oxygen. Quat Sci Rev. 25:1995–2012.

Brundin L. 1951. The relation of O2-microstratification at the mud surface to the ecology of the profundal bottom fauna. Rep Inst Freshwat Res Drottningholm. 32:32–42.

Burns NM. 1976. Temperature, Oxygen, and Nutrient Distribution Patterns in Lake Erie, 1970. J Fish Res Board Canada. 33:485-511.

Burns NM. 1985. Erie: The Lake That Survived. Rowman & Allanheld.

Burns NM, Rockwell DC, Bertram PE, Dolan DM, Ciborowski JJH. 2005. Trends in temperature, Secchi depth, and dissolved oxygen depletion rates in the central basin of Lake Erie, 1983–2002. J Great Lakes Res. 31:35–49.

Carmichael WW, Boyer GL. 2016. Health impacts from cyanobacteria harmful algae blooms: Implications for the North American Great Lakes. Harmful Algae. 54:194–212.

Carr JF, Hiltunen JK. 1965. Changes in the Bottom Fauna of Western Lake Erie from 1930 to 1961. Limnol Oceanogr. 10:551–569.

Carter DS, Hites RA. 1992. Fate and transport of Detroit River derived pollutants throughout Lake Erie. Environ Sci Technol. 26:1333–1341.

Casper VL. 1965. A phytoplankton bloom in western Lake Erie.

Charlton MN. 1980a. Hypolimnion oxygen consumption in lakes: discussion of productivity and morphometry effects. Can J Fish Aquat Sci. 37:1531–1539.

Charlton MN. 1980b. Oxygen depletion in Lake Erie: has there been any change? Can J Fish Aquat Sci. 37:72–80.

Charlton MN. 1987. Lake Erie oxygen revisited. J Great Lakes Res. 13:697–708.

Chawla VK. 1971. Changes in the water chemistry of Lakes Erie and Ontario. In: Changes in the chemistry of Lakes Erie and Ontario. Bull. Buffalo Soc. of Natural Sci. Vol. 25. p. 31–65.

Craig JK, Crowder LB, Gray CD, Carrie J, Henwood T a, Hanifen JG. 2001. Ecological Effects of Hypoxia on Fish, Sea Turtles, and Marine Mammals in the Northwestern Gulf. Coast Estuar Stud.:269–292.

Davis CC. 1964. Evidence for the eutrophication of Lake Erie from phytoplankton records. Limnol Oceanogr. 9:275–283.

Depew DC, Houben AJ, Guildford SJ, Hecky RE. 2011. Distribution of nuisance Cladophora in the lower Great Lakes: patterns with land use, near shore water quality and dreissenid abundance. J Great Lakes Res. 37:656–671.

Diaz RJ, Rosenberg R. 2008. Spreading dead zones and consequences for marine ecosystems. Science 321:926–929.

Dodds WK. 2002. Freshwater ecology: concepts and environmental applications. Academic Press.

Eckert W, Nishri A, Parparova R. 1997. Factors regulating the flux of phosphate at the sediment-water interface of a subtropical calcareous lake: A simulation study with intact sediment cores. Water Air Soil Pollut. 99:401–409.

Eggermont H, Heiri O. 2012. The chironomid-temperature relationship: Expression in nature and palaeoenvironmental implications. Biol Rev. 87:430–456.

Hall RI, Leavitt PR, Quinlan R, Dixit AS, Smol JP. 1999. Effects of agriculture, urbanization, and climate on water quality in the northern Great Plains. Limnol Oceanogr. 44:739–756.

Harris GP, Vollenweider RA. 1982. Paleolimnological evidence of early eutrophication in Lake Erie. Can J Fish Aquat Sci. 39:618–626.

Hartman WL. 1973. Effects of exploitation, environmental changes, and new species on the fish habitats and resources of Lake Erie. Great Lakes Fishery Commission. Technical report.

Hatcher HH. 1971. Lake Erie. Greenwood Press.

Heinis F, Crommentuijn T. 1992. Behavioral Responses to Changing Oxygen Concentrations of Deposit Feeding Chironomid Larvae(Diptera) of Littoral and Profundal Habitats. Arch für Hydrobiol AHYBA 4, 124.

Heinis F, Sweerts J-P, Loopik E. 1994. Micro-environment of chironomid larvae in the littoral and profundal zones of Lake Maarsseveen I, The Netherlands. Arch für Hydrobiol. 130:53–67.

Herdendorf CE. 1987. The ecology of the coastal marshes of western Lake Erie: a community profile. Ohio State Univ Columbus.

Hofmann W. 1988. The significance of chironomid analysis (Insecta: Diptera) for paleolimnological research. Palaeogeogr Palaeoclimatol Palaeoecol. 62:501–509.

Hough JL. 1958. Geology of the Great Lakes. University of Illinois Press.

Hutchinson GE. 1973. Eutrophication: The scientific background of a contemporary practical problem. Am Sci. 61:269–279.

International Joint Commission (IJC). 1972. Great Lakes Water Quality Agreement with Annexes and Texts and Terms of Reference between the United States and Canada Signed at Ottawa, April 15, 1972. International Joint Commission, Windsor, Ontario, Canada.

International Joint Commission (IJC). 1978. Great Lakes Water Quality Agreement of 1978 with Annexes and Terms of Reference between the United States and Canada Signed at Ottawa, November 22, 1978.

International Joint Commission (IJC). 1983. Great Lakes Water Quality Agreement of 1978. Phosphorus Load Reduction Supplement of 1983.

International Joint Commission (IJC). 1987. Report on the Great Lakes Water Quality. Report of the Great Lakes Water Quality Board.

International Joint Commission (IJC). 2015. Recommended Phosphorus Loading Targets for Lake Erie. Annex 4 Objectives and Targets Task Team Final Report to the Nutrients Annex Subcommittee (2015).

Jensen HS, Kristensen P, Jeppesen E, Skytthe A. 1992. Iron: phosphorus ratio in surface sediment as an indicator of phosphate release from aerobic sediments in shallow lakes. In: Sediment/Water Interactions. Springer. p. 731–743.

Kelly NE, O'Connor EM, Wilson RF, Young JD, Winter JG, Molot LA. 2016. Multiple stressor effects on stream health in the Lake Simcoe Watershed. J Great Lakes Res. 42:953–964.

Kemp ALW, MacInnis GA, Harper NS. 1977. Sedimentation Rates and a Revised Sediment Budget for Lake Erie. J Great Lakes Res. 3:221–233.

Kemp ALW, Thomas RL, Dell CI, Jaquet J-M. 1976. Cultural Impact on the Geochemistry of Sediments in Lake Erie. J Fish Res Board Canada. 33:440–462.

Kraus RT, Knight CT, Farmer TM, Gorman AM, Collingsworth PD, Warren GJ, Kocovsky PM, Conroy JD. 2015. Dynamic hypoxic zones in Lake Erie compress fish habitat, altering vulnerability to fishing gears. Can J Fish Aquat Sci. 72:1–10.

Langdon PG, Ruiz Z, Brodersen KP, Foster IDL. 2006. Assessing lake eutrophication using chironomids: Understanding the nature of community response in different lake types. Freshw Biol. 51:562–577.

Lashaway AR, Carrick HJ. 2010. Effects of light, temperature and habitat quality on meroplanktonic diatom rejuvenation in Lake Erie: Implications for seasonal hypoxia. J Plankton Res. 32:479–490.

Legendre P, Birks HJB. 2012. From classical to canonical ordination. In: Tracking environmental change using lake sediments. Springer. p. 201–248.

Lindegaard C. 1995. Classification of water-bodies and pollution. In: The Chironomidae. Springer. p. 385–404.

Little JL, Smol JP. 2001. A chironomid-based model for inferring late-summer hypolimnetic oxygen in southeastern Ontario lakes. J Paleolimnol. 26:259–270.

Ludsin SA, Kershner MW, Blocksom KA, Knight RL, Stein RA. 2001. Life After Death in Lake Erie: Nutrient Controls Drive Fish Species Richness, Rehabilitation. Ecol Appl. 11:731–746.

Makarewicz JC. 1991. Phytoplankton and Zooplankton Composition, Abundance and Distribution and Trophic Interactions: Offshore Region of Lakes Erie, Lake Huron and Lake Michigan, 1985. US Environmental Protection Agency, Great Lakes National Program Office.

Makarewicz JC, Bertram PE. 1993. Evidence for the Restoration of the Lake Erie Ecosystem. J Great Lakes Res. 19:197.

Matisoff G, Kaltenberg EM, Steely RL, Hummel SK, Seo J, Gibbons KJ, Bridgeman TB, Seo Y, Behbahani M, James WF, et al. 2016. Internal loading of phosphorus in western Lake Erie. J Great Lakes Res. 42:775–788.

Michalak AM, Anderson EJ, Beletsky D, Boland S, Bosch NS, Bridgeman TB, Chaffin JD, Cho K, Confesor R, Daloglu I, et al. 2013. Record-setting algal bloom in Lake Erie caused by agricultural and meteorological trends consistent with expected future conditions. Proc Natl Acad Sci. 110:6448–6452.

Millie DF, Fahnenstiel GL, Bressie JD, Pigg RJ, Rediske RR, Klarer DM, Tester PA, Litaker RW. 2009. Late-summer phytoplankton in western Lake Erie (Laurentian Great Lakes): bloom distributions, toxicity, and environmental influences. Aquat Ecol. 43:915–934.

Mitsch WJ, Gosselink JG. 2015. Wetlands. Wiley.

Molot LA, Dillon PJ, Clark BJ, Neary BP. 1992. Predicting End-of-Summer Oxygen Profiles in Stratified Lakes. Can J Fish Aquat Sci. 49:2363–2372.

Moon JB, Carrick HJ. 2007. Seasonal variation of phytoplankton nutrient limitation in Lake Erie. Aquat Microb Ecol. 48:61–71.

Mortimer C. 1942. The exchange of dissolved substances between mud and water in lakes. J Ecol. 30:147–201.

North RL, Guildford SJ, Smith REH, Havens SM, Twiss MR. 2007. Evidence for phosphorus, nitrogen, and iron colimitation of phytoplankton communities in Lake Erie. Limnol Oceanogr. 52:315–328.

Nürnberg GK. 1995. Quantifying anoxia in lakes. Limnol Oceanogr. 40:1100–1111.

Oliver DR. 1971. Life history of the Chironomidae. Annu Rev Entomol. 16:211–230.

Paerl HW, Xu H, Mccarthy MJ, Zhu G, Qin B, Li Y, Gardner WS. 2010. Controlling harmful cyanobacterial blooms in a hyper-eutrophic lake (Lake Taihu, China): The need for a dual nutrient (N & P) management strategy. Water Res. 45:1973–1983.

Panis LI, Goddeeris B, Verheyen R. 1996. On the relationship between vertical microdistribution and adaptations to oxygen stress in littoral Chironomidae (Diptera). Hydrobiologia. 318:61–67.

Paterson AM, Winter JG, Nicholls KH, Clark BJ, Ramcharan CW, Yan ND, Somers KM. 2008. Long-term changes in phytoplankton composition in seven Canadian Shield lakes in response to multiple anthropogenic stressors. Can J Fish Aquat Sci. 65:846–861.

Paytan A, Roberts K, Watson S, Peek S, Chuang P-C, Defforey D, Kendall C. 2016. Internal loading of phosphate in Lake Erie Central Basin. Sci Total Environ. (In press):1356–1365.

Peres-Neto PR, Legendre P, Dray S, Borcard D. 2012. Variation Partitioning of Species Data Matrices: Estimation and Comparison of Fractions. Ecology. 59:2614–2625.

Pihl L. 1994. Changes in the Diet of Demersal Fish due to Eutrophication-induced Hypoxia in the Kattegat, Sweden. Can J Fish Aquat Sci. 51:321–336.

De Pinto J V, Young TC, McIlroy LM. 1986. Great Lakes water quality improvement. Environ Sci Technol. 20:752–759.

Postel S, Carpenter S. 1997. Freshwater ecosystem services. In: Nature's services: Societal dependence on natural ecosystems. Island Press, Washington, DC. p. 195–214.

Pothoven SA, Vanderploeg HA, Ludsin SA, Höök TO, Brandt SB. 2009. Feeding ecology of emerald shiners and rainbow smelt in central Lake Erie. J Great Lakes Res. 35:190–198.

Powers CF, Robertson A. 1966. The aging Great Lakes. Sci Am. 215:94–106.

Quinlan R, Smol JP. 2001. Chironomid-based inference models for estimating end-of-summer hypolimnetic oxygen from south-central Ontario shield lakes. Freshw Biol. 46:1529–1551.

Quinlan R, Smol JP, Hall RI. 1998. Quantitative inferences of past hypolimnetic anoxia in south-central Ontario lakes using fossil midges (Diptera: Chironomidae). Can J Fish Aquat Sci. 55:587–596.

Rao YR, Howell T, Watson SB, Abernethy S. 2014. On hypoxia and fish kills along the north shore of Lake Erie. J Great Lakes Res. 40:187–191.

Reavie ED, Cai M, Twiss MR, Carrick HJ, Davis TW, Johengen TH, Gossiaux D, Smith DE, Palladino D, Burtner A, et al. 2015. Winter-spring diatom production in Lake Erie is an important driver of summer hypoxia. J Great Lakes Res. 42:608–618.

Reavie ED, Heathcote AJ, Shaw Chraïbi VL. 2014. Laurentian Great Lakes phytoplankton and their water quality characteristics, including a diatom-based model for paleoreconstruction of phosphorus. PLoS One. 9.

Reavie ED, Sgro G V., Estepp LR, Bramburger AJ, Shaw Chraïbi VL, Pillsbury RW, Cai M, Stow CA, Dove A. 2017. Climate warming and changes in Cyclotella sensu lato in the Laurentian Great Lakes. Limnol Oceanogr. 62:768–783.

Roberts JJ, Grecay P a., Ludsin S a., Pothoven S a., Vanderploeg H a., Höök TO. 2012. Evidence of hypoxic foraging forays by yellow perch (Perca flavescens) and potential consequences for prey consumption. Freshw Biol. 57:922–937.

Roberts JJ, Höök TO, Ludsin S a., Pothoven S a., Vanderploeg H a., Brandt SB. 2009. Effects of hypolimnetic hypoxia on foraging and distributions of Lake Erie yellow perch. J Exp Mar Bio Ecol. 381: 132–142.

Rodé DL. 2009. A paleolimnological assessment of coldwater fish habitat quality in Lake Simcoe, Ontario. York University.

Rosa F, Burns NM. 1987. Lake Erie central basin oxygen depletion changes from 1929–1980. J Great Lakes Res. 13:684–696.

Rucinski DK, Beletsky D, DePinto J V, Schwab DJ, Scavia D. 2010. A simple 1-dimensional, climate-based dissolved oxygen model for the central basin of Lake Erie. J Great Lakes Res. 36:465–476.

Rucinski DK, Depinto J V, Scavia D, Beletsky D. 2014. Modeling Lake Erie's hypoxia response to nutrient loads and physical variability. J Great Lakes Res. 40:151–161.

Sæther O a. 1979. Chironomid communities as water quality indicators. Holarct Ecol. 2:65–74.

Scavia D, David Allan J, Arend KK, Bartell S, Beletsky D, Bosch NS, Brandt SB, Briland RD, Daloğlu I, DePinto J V., et al. 2014. Assessing and addressing the re-eutrophication of Lake Erie: Central basin hypoxia. J Great Lakes Res. 40:226–246.

Schelske CL, Conley DJ, Stoermer EF, Newberry TL, Campbell CD. 1986. Biogenic silica and phosphorus accumulation in sediments as indices of eutrophication in the Laurentian Great Lakes. Hydrobiologia. 143:79–86.

Schelske CL, Stoermer EF, Kenney WF. 2006. Historic low-level phosphorus enrichment in the Great Lakes inferred from biogenic silica accumulation in sediments. Limnol Oceanogr. 51:728–748.

Schindler DW. 1974. Eutrophication and recovery in experimental lakes: implications for lake management. Science 184:897–899.

Schindler DW. 1977. Evolution of Phosphorus Limitation in Lakes. Science. 195:260–262.

Schindler DW, Hecky RE, Findlay DL, Stainton MP, Parker BR, Paterson MJ, Beaty KG, Lyng M, Kasian SEM. 2008. Eutrophication of lakes cannot be controlled by reducing nitrogen input: Results of a 37-year whole-ecosystem experiment. Proc Natl Acad Sci. 105:11254–11258.

Schindler DW, Vallentyne JR. 2008. The Algal Bowl: over-fertilization of the world's freshwaters and estuaries. Edmonton: University of Alberta Press.

Sgro G V, Reavie ED. 2017. Lake Erie's ecological history reconstructed from the sedimentary record. J Great Lakes Res. 44:54-69

Sly PG. 1976. Lake Erie and its Basin. J Fish Res Bd Can. 33:355–370.

Šmilauer P, Lepš J. 2003. Multivariate Analysis of Ecological Data using CANOCO. Cambridge University Press.

Smith VH. 2003. Eutrophication of freshwater and coastal marine ecosystems a global problem. Environ Sci Pollut Res. 10:126–139.

Smith VH, Schindler DW. 2009. Eutrophication science: where do we go from here? Trends Ecol Evol. 24:201–207.

Smol JP. 1992. Paleolimnology: an important tool for effective ecosystem management. J Aquat Ecosyst Heal. 1:49–58.

Smol JP. 2008. Pollution of lakes and rivers: a paleoenvironmental perspective. John Wiley & Sons.

Søndergaard M, Jensen JP, Jeppesen E. 2003. Role of sediment and internal loading of phosphorus in shallow lakes. Hydrobiologia. 506–509:135–145.

Sterner RW. 2008. On the phosphorus limitation paradigm for lakes. Int Rev Hydrobiol. 93:433–445.

Stoermer EF, Kociolek JP, Schelske CL, Conley DJ. 1987. Quantitative analysis of siliceous microfossils in the sediments of Lake Erie's central basin. Diatom Res. 2:113–134.

Stumpf RP, Wynne TT, Baker DB, Fahnenstiel GL. 2012. Interannual variability of cyanobacterial blooms in Lake Erie. PLoS One. 7:e42444.

Summers JC, Rühland KM, Kurek J, Quinlan R, Paterson AM, Smol JP. 2012. Multiple stressor effects on water quality in Poplar Bay, Lake of the Woods, Canada: A midge-based assessment of hypolimnetic oxygen conditions over the last two centuries. J Limnol. 71:34–44.

Twiss MR, McKay RML, Bourbonniere RA, Bullerjahn GS, Carrick HJ, Smith REH, Winter JG, D'souza NA, Furey PC, Lashaway AR, et al. 2012. Diatoms abound in ice-covered Lake Erie: An investigation of

offshore winter limnology in Lake Erie over the period 2007 to 2010. J Great Lakes Res. 38:18–30.

Verduin J. 1969. Man's influence on Lake Erie. Ohio J Sci. 69:65–70.

Walker I. 1995. Chironomids as indicators of past environmental change. In: The Chironomidae. Springer. p. 405–422.

Walker IR. 1987. Chironomidae (Diptera) in paleoecology. Quat Sci Rev. 6:29–40.

Walker IR. 2001. Midges: Chironomidae and related Diptera. In: Tracking environmental change using lake sediments. Springer. p. 43–66.

Walker IR, Cwynar LC. 2006. Midges and palaeotemperature reconstruction—the North American experience. Quat Sci Rev. 25:1911–1925.

Weber RE. 1980. Functions of invertebrate hemoglobins with special reference to adaptations to environmental hypoxia. Am Zool. 20:79–101.

Wetzel RG. 2001. Limnology: Lake and River Ecosystems. In: Nature. 3rd ed. Gulf Professional Publishing. p. 1006.

Wiederholm T. 1980. Use of benthos in lake monitoring. Water Pollut Control Fed. 52:537–547.

Wilson EK. 2014. Danger from microcystins in Toledo water unclear. Chem Eng News. 92:9.

Wynne TT, Stumpf RP. 2015. Spatial and temporal patterns in the seasonal distribution of toxic cyanobacteria in western Lake Erie from 2002–2014. Toxins (Basel). 7:1649–1663.

Zhou Y, Michalak AM, Beletsky D, Rao YR, Richards RP. 2015. Record-breaking Lake Erie hypoxia during 2012 drought. Environ Sci Technol. 49:800–807.

Zhou Y, Obenour DR, Scavia D, Johengen TH, Michalak AM. 2013. Spatial and Temporal Trends in Lake Erie Hypoxia, 1987 − 2007. Environ Sci Technol. 47:899–905.

Figures and Tables

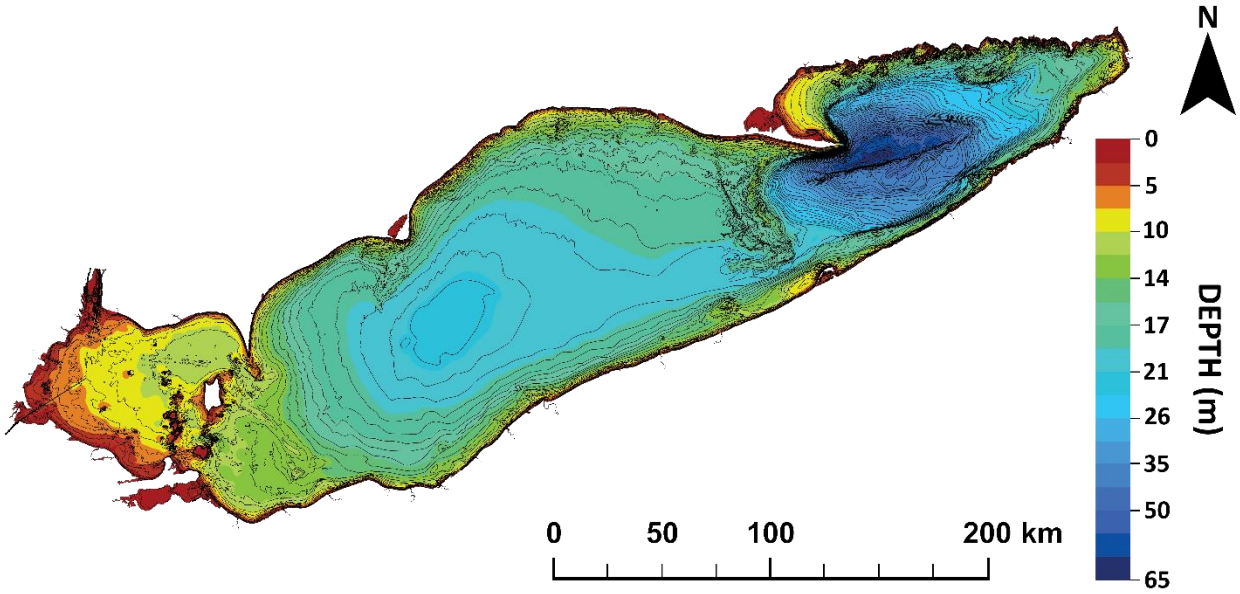

Figure 1.1: Lake Erie bathymetry. Bathymetry map was compiled using bathymetry data obtained from National Oceanic and Atmospheric Administration (NOAA).

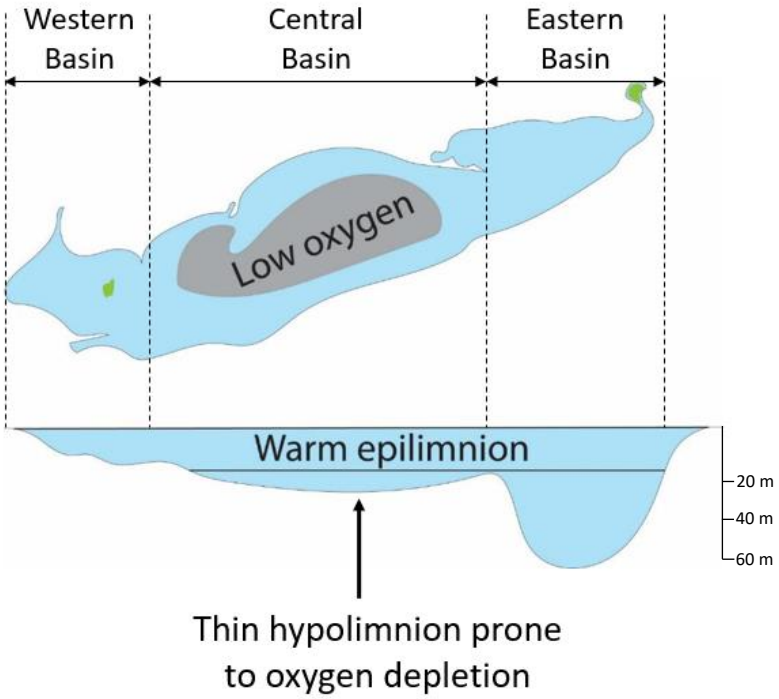

Figure 1.2: Conceptual diagram of the Lake Erie basins and their depths. The area prone to oxygen depletion is highlighted in grey ("low oxygen").

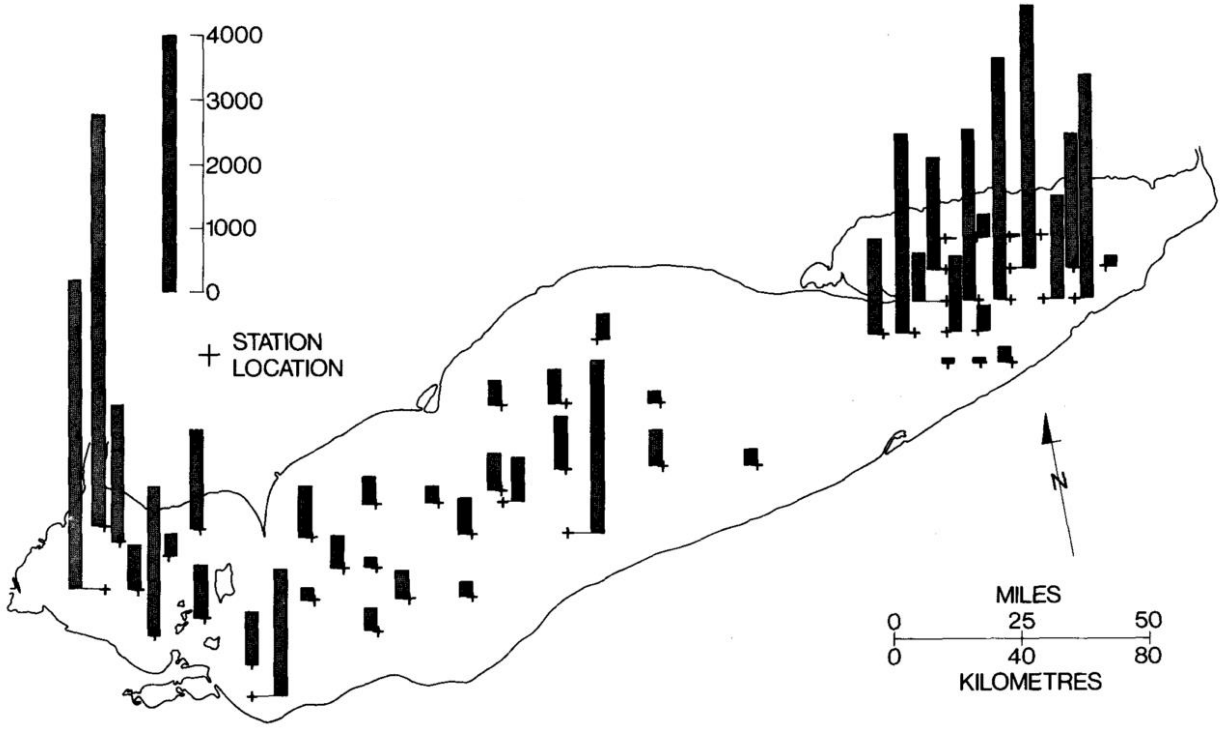

Figure 1.3: Distribution of sedimentation rates in (g m^{-2} yr^{-1}) in the 1970s, adapted from Kemp et al. (1977).

Chapter 2: Qualitative and quantitative inferences of long-term hypolimnetic oxygen dynamics in the central basin of Lake Erie as determined by chironomid-based paleolimnological analysis

Introduction

Since European settlement, the Lake Erie watershed has undergone a dramatic change due to multiple anthropogenic stressors, including wetland draining, deforestation, increases in population and agricultural land cover, cultural eutrophication, climate change, contaminants, and the effects of invasive species (Harris and Vollenweider 1982; Burns 1985; Nicholls et al. 2001; Zhang et al. 2011; Allinger and Reavie 2013). The effects of nutrient inputs have been particularly influential and have had severe implications for the lake's metabolic status and hypolimnetic dissolved oxygen (DO) conditions in the central basin (Burns 1976; Harris and Vollenweider 1982; Stoermer et al. 1987; Bertram 1993; Makarewicz and Bertram 1993; Burns et al. 2005). Several diatom-based paleolimnological studies have indicated that Lake Erie began to show first signs of eutrophication as early as the 1850s (Harris and Vollenweider 1982; Stoermer et al. 1987). This influx of nutrients, in turn, led to nuisance algal (cyanophyte and *Cladophora*) blooms, increased total phytoplankton biomass, and extensive anoxia in the central basin by the 1960s (Beeton 1961; Davis 1964; Burns 1976). The deteriorating water conditions prompted a legislative response which lead to the bi-national Great Lakes Water Quality Agreement (GLWQA) of 1972 (IJC 1972) and amended in 1978 to include phosphorus (P) abatement programs and point-source P limits (IJC 1978). In 1983, lake-wide total phosphorus (TP) loading targets were set to include limits on P inputs from non-point sources (IJC 1983).

Lake Erie appeared to respond to these TP reductions, and by the 1980s water clarity has been improved; numerous studies indicated declines in phytoplankton biomass as a result of these TP loading

reductions (Munawar and Munawar 1976; Rathke 1982; Makarewicz 1987; Makarewicz 1991; Makarewicz and Bertram 1993). However, these improvements did not translate to improvements in hypolimnetic DO conditions in the central basin, as end-of-summer anoxic conditions persisted and only anoxic extent showing interannual variability (Burns et al. 2005; Zhou et al. 2013). However, due to the depth of the central basin which is naturally prone to oxygen depletion (Chapter 1), the required long-term hypolimnetic DO data does not exist to understand how hypolimnetic DO dynamics have changed since European settlement.

Changes in nutrient loading to lakes, whether natural or anthropogenic, have strong influences on benthic community composition, including non-biting midges (Diptera: Chironomidae), which have been used as a key indicator for short- and long-term environmental changes (Brundin 1951; Sæther 1979; Smol 2008). The distribution of profundal chironomids is especially indicative of changing hypolimnetic DO as they are one of the few aquatic groups whose species possess a wide range of tolerances to oxygen conditions typical of profundal environments (Brodersen and Quinlan 2006; Armitage et al. 2012). In addition, advances in statistical analyses allow for quantitative average volume-weighted hypolimnetic oxygen (avgVWHO) reconstructions (Quinlan and Smol 2001a; Paterson et al. 2009; Summers et al. 2012). The aim of this chapter is to infer, both qualitatively and quantitatively, the long-term trends in hypolimnetic oxygen dynamics within the central basin of Lake Erie in order to better understand the effects of cumulative multiple anthropogenic stressors on central basin hypolimnetic DO dynamics.

Methods

Field and laboratory methods

A sediment core was collected from each of the three basins in Lake Erie. The central basin core (41.998733° N, -81.650054° W) and western basin core (41.892335° N, -82.716719° W) were collected on

July 2011, the eastern basin core (42.516667° N, -79.805638° W) was collected on July 2016 (Table 2.1, Fig. 2.1). Cores were collected using an Oceanic Instruments Model MC-400 multicorer. The central basin core site was selected to correspond to cores previously collected for paleolimnological studies by Harris and Vollenweider (1982) and Stoermer et al. (1987), while the western basin and eastern basin cores served as controls.

The central basin has a mean depth of 18 m (Z_{max} = 24 m); the western basin has a mean depth of 7.4 m (Z_{max} = 19 m) and generally remains unstratified during the summer months due to wind-induced mixing; the eastern basin has an average depth of approximately 24 m (Z_{max} = 64 m) such that when thermal stratification occurred in the summer, it formed a thick hypolimnion (Burns 1985). As a result, the western core provides a littoral "control" for interpreting changes in central basin assemblages, as the western core should not contain any profundal oxic-type taxa, such as *Micropsectra* and *Heterotrissocladius,* indicative of cool and oxygenated hypolimnia.

All cores were sectioned at 0.5 cm intervals between 0-10 cm, with 1 cm sections from 10 cm to the end of the core. The central, western, and eastern cores were 49 cm, 21 cm, and 41 cm long, respectively. Chironomid head capsules were prepared for microscope identification using methods similar to Medeiros and Quinlan (2011), with some modifications to deal with semi-dry sediment and permit isolation of cladoceran remains for possible future analysis. Approximately 10-21g of sediment (wet weight) per interval was examined for subfossil chironomid remains. Sediment samples were freeze-dried (-40°C at 0.120 mbar) for 48 hours (Appendix A). Freeze dried sediments were deflocculated in 10% KOH solution at 70°C for 30 min under constant mixing using a self-designed and built overhead stirrer (Appendix B).

Following KOH deflocculation, each interval was washed though 212 and 106 µm mesh sieves, flow-through was collected and washed in 36 µm sieves in order to collect cladoceran remains for future

analysis. All retained residues were then washed with and stored in 95% ethanol. The 212 and 106 µm residues were sifted using a Nikon SMZ1500 stereomicroscope at 30-40x magnification; chironomid head capsules were extracted with the use of fine forceps. Specimens were permanently mounted on glass slides in Entellan mounting medium. While efforts have been made to extract a minimum of 50 chironomid head capsules per interval (Quinlan and Smol 2001b), many intervals had < 50 head capsules. As a result, adjacent intervals were combined when examining stratigraphic results as % relative abundances (Appendix D). Identification of specimens was carried out under a compound light microscope with 400-1,000x magnification based on taxonomic information provided by Brooks et al. (2007).

Chronology and sedimentation rates of the sediment cores were determined by Sgro and Reavie (2017). Chronology of the central basin core was conducted using constant rate of supply (CRS) model of ^{210}Pb accumulation (Appleby and Oldfield 1978). However, the western and eastern basin cores did not contain supported background concentrations of ^{210}Pb at maximum core depth, as a result, gamma spectroscopy was used to measure ^{137}Cs in the core (McHenry et al. 1973; Ritchie and McHenry 1990). Organic carbon and carbonate content (expressed as % of dry sediment) were determined for the central and western basin cores for each interval by measuring the weight loss following sequential burns of the dried sediment at 550^{o}C (4h) and 1000 ^{o}C (2h) (Heiri et al. 2001).

Numerical Analysis

All numerical analyses of chironomid assemblages were based on Hellinger transformed species data (Birks et al. 2012). An exploratory detrended correspondence analysis (DCA; detrending by segments and non-linear rescaling) was performed, which indicated that linear-based techniques (<2 SD) would be appropriate (Šmilauer and Lepš 2003; Birks et al. 2012). Consequently, temporal patterns of chironomid community change (ca. 1853-2011) were explored using principal component analysis (PCA;

covariance matrix) in CANOCO version 4.5 (ter Braak and Smilauer 2002), with rare taxa removed (≥2% relative abundance in at least two samples; Quinlan and Smol 2001b), resulting in a total of nine taxa retained.

Chironomid assemblage zones were defined by stratigraphically constrained cluster analysis with incremental sum some of squares partitioning (CONISS) and a squared chord-distance dissimilarity coefficient (Gordon and Birks 1974; Grimm 1987) using the "rioja" package (Juggins 2017) in R 3.4.3 (R Core Team 2014). Statistical significance of the zones was assessed by comparing the hierarchical classification to that obtained from the broken stick model (Bennett 1996).

Downcore avgVWHO reconstruction was performed using an inference model published by Quinlan and Smol (2001a) in C2 version 1.5 (Juggins 2007) using the weighted-average (WA) regression model with leave-one-out cross-validation (jackknifing), tolerance down-weighting, and inverse deshrinking (r^2_{jack} = 0.56, RMSEP = 2.15 mg O_2 L^{-1}). The calibration set consisted of 44 chironomid taxa from 54 lakes located in the south-central Ontario (Muskoka-Haliburton) region. Lake characteristics ranged from shallow to very deep (Z_{max} > 80m), ultraoligotrophic to mesotrophic, and end-of-summer hypolimnetic DO which ranged from nearly saturated to anoxic.

Evaluation of the avgVWHO inference model followed similar methods to Reavie et al. (2014). The reliability of the inferred avgVWHO model was assessed using a goodness-of-fit approach by passively projecting the Lake Erie central basin core chironomid assemblages onto an RDA containing training set chironomid data constrained to the training set avgVWHO. The sample squared residual lengths of the first RDA axis were examined to determine whether the central basin chironomid assemblages lie within the 95% confidence interval (95% CI) of the inference model samples (Birks et al. 2012; Birks 2014). In addition, a correlation coefficient (r) for inferred avgVWHO against corresponding axis 1 sample scores from unconstrained PCA of the central basin chironomid assemblages was

calculated. Then, the fraction of the variance explained by the inferred avgVWHO model was examined by calculating the ratio of the variance in central basin chironomid assemblage captured by the first RDA axis constrained to inferred avgVWHO (λ_{RDA}) and the variance explained by the first axis of an unconstrained PCA of the central basin chironomid data (λ_{PCA}). Such that, the $\lambda_{RDA}/ \lambda_{RDA}$ ratio expressed the proportion of the variance in central basin chironomid assemblage explained by the avgVWHO inference model as a fraction of the maximum explainable variance of chironomid assemblage data in the central basin core. Thus, if the central basin chironomid assemblages were strongly related to changes in inferred avgVWHO, it would be expected that r and $\lambda_{RDA}/ \lambda_{RDA}$ would be close to 1.

Results

Core chronology

Chronology for the central, western, and eastern sediment cores were established using a constant rate of ^{210}Pb supply model with basal dates of approximately 1853, 1930, and 1964, respectively (Fig. 2.2). The CRS model of ^{210}Pb accumulation in the central basin core produced reliable results with little noise (supported background ^{210}Pb activity 1.55 ± 0.03 pCi g^{-1}; oldest reliable date 1866 ± 22). However, both western and eastern cores were too short to reach background ^{210}Pb levels due to high sediment accumulation rates. This problem was resolved in the western core by supplementing with a secondary dating marker from ^{137}Cs. Initially modeled dates at 23-24 cm by CRS did not match the 1963 ^{137}Cs peak; thus dates were fitted to match the 1963 ^{137}Cs peak, resulting in reliable dating from 1963-2011 and decreasing dating reliability thereafter (Sgro and Reavie 2017; Supplementary Data). Due to the short time scales covered by the western and eastern cores and low head capsule counts (discussed below), these cores are unable to provide meaningful information about pre-disturbance conditions.

Chironomids assemblage and geochemistry trends

Eastern basin – only 12 intervals were analyzed due to very low chironomid head capsule counts (mean ± SD = 1.9 ± 1.7, range of 0-6), as a result, stratigraphic visualization was based on presence/absence (Fig. 2.3). As a result of low head capsule counts compounded by short lengths of the eastern basin core, no statistical analysis on this core was performed. Sediment accumulation rates ranged from 0.22-0.37 g cm^{-2} yr^{-1}.

Western basin - a total of 18 taxa were identified from the 18 sedimentary intervals which were examined; this core was also relatively short with low head capsule counts (mean ± SD 30.8 ± 21, range of 12-80). Since the minimum suggested head capsule counts for statistical analysis is 40-50 per interval (Quinlan and Smol 2001b), adjacent intervals with low head capsule abundances (< 40) were combined resulting in 12 intervals (mean ± SD 53.7 ± 14, range of 40-80). While *Chironomus* spp dominated the stratigraphy, there was a noticeable shift from *C. plumosus* to *C. anthracinus.* In addition, high relative abundances of *Procladius* were observed throughout the stratigraphy (Fig 2.4). The broken stick model did not identify any significant cluster zones in the western basin core, as a result, no dendrogram is provided. Sediment accumulation rates and % carbonate in the western basin showed an increasing trend. However, stratigraphic analysis of PCA axes and organic C content did not indicate any trends in the western basin core (Fig. 2.5).

Central basin - a total of 49 sediment intervals were analyzed, resulting in 1,229 chironomid remains enumerated comprising a total of 15 taxa, 11 individuals were unidentifiable and were omitted from numerical analysis. However, similar to the western basin, total head capsule counts per interval were low (mean ± SD of 25 ± 17, range of 2-77). As in the western basin core, adjacent intervals with low abundances were pooled, resulting in 28 intervals (mean ± SD of 43.9 ± 13.2, range of 24-77). Overall abundance and diversity of fossil assemblages were low compared to the surface assemblages in most

calibration set lakes (Quinlan and Smol 2001a). Cluster analysis of chironomid assemblages indicated two statistically significant zones within the core (Fig. 2.6).

Zone 1 (pre-1950s; 24-49 cm) was characterized by the presence of oxic-type taxa such as *Micropsectra insignilobus* and *Heterotrissocladius* grp with relative abundances that ranged from 2-16% and 2-6%, respectively. However, hypoxic- and anoxic-type taxa (*Procladius* and *Chironomus*, respectively) were also present in this zone at relative abundance greater than that of *Micropsectra insignilobus* and *Heterotrissocladius* grp. In addition, low relative abundances of *Harnischia/Paracladopelma* and *Paratanytarsus* were found sporadically (Fig. 2.6).

Zone 2 (post-1950; 21.5-0 cm) reflected the period from ~1950 to 2011 AD. This period was marked by the disappearance of oxic-type taxa (*Micropsectra insignilobus* and *Heterotrissocladius* grp), the decline of hypoxia-tolerant *Procladius*. In contrast, Chironomini larvula, which were not present in the sediments prior to 1995 AD, increased in abundance to ~ 3% of the total chironomid community in recent decades (Fig. 2.6). However, in both stratigraphic zones, the genus *Tanytarsus lugens* dominated the biostratigraphy, representing between 30-90% of the chironomid assemblage. *Chironomus* (comprised primarily from *Chironomus anthracinus* and *Chironomus plumosus*) and was the second most abundant taxon throughout the stratigraphy (Fig. 2.6).

Indirect gradient analysis using PCA revealed a unimodal trend in temporal variability of chironomid assemblages where PCA axis 1 and 2 explained 48.4% and 20.8% of the observed variation, respectively (Fig. 2.8). When PCA axis 1 scores are plotted over the stratigraphy, a long-term trend in compositional change of chironomid assemblages is observed (Fig. 2.7). Generally, the top section of the central basin sediment core appears within, or near, the second quadrant, which is closely associated with the *Chironomus* spp and Chironomini larvula, while the bottom section of the core is found within the first and forth quadrants and closely associated with *Micropsectra*, *Procladius*, *Paratanytarsus*, and

Heterotrissocladius grp. While *T. lugens* is associated with intervals that correspond to the 1990s and 2011, it is not closely associated with any other taxa (Fig. 2.8).

Sediment accumulation rates have remained relatively stable early in the record, at approximately 0.08 g cm^{-2} yr^{-1}, until approximately the mid-1970s and have been increasing thereafter, with nearly a 2-fold increase in the recent decade (Fig. 2.7). Percent organic carbon content showed a relatively stable trend until the 1930s, with an abrupt increase by approximately 68% and remained high until the end of the record despite P abatement programs enacted in the early 1970s (GLWQA 1972). However, trends in % carbonate were more sporadic, with relatively low levels early in the record, followed by an increase in the 20th century (Fig. 2.7).

Quantitative paleoreconstruction of avgVWHO in the central basin of Lake Erie

Changes in end-of-summer avgVWHO in the central basin of Lake Erie were quantified through the application of a chironomid-based avgVWHO inference model (Quinlan and Smol 2001a). During the 1850s, inferred avgVWHO levels were relatively low at 3.3 mg O_2 L^{-1}, but increased by the 1880s and remained relatively stable between 4-5 mg O_2 L^{-1} until the 1950s. Inferred avgVWHO for the 1960s-1980s was similar to conditions observed during the early 1850s. However, a rebound in inferred avgVWHO levels was observed in 1985, reaching 5 mg O_2 L^{-1}, following the GLWQA 1972. However, by the 1990s inferred VWHO began to return to the same state as seen in the 1960s, with a historic low of 2.4 mg O_2 L^{-1} in 2006. Although, since that period to 2011, inferred avgVWHO appears to be returning to approximately 4 mg O_2 L^{-1} (Fig 2.7).

However, some caution must be taken when interpreting inferred avgVWHO from the central basin core, as these inferences were made based on a training set from relatively small lakes in the south-central Ontario (Muskoka-Haliburton) region. For example, *T. lugens* comprised the greatest % abundance within the central basin core, making up ≥30% in many sedimentary intervals, while of the 54

lakes in the training set only two lakes had *T. lugens* abundances of ≥30%. Additionally, while *Chironomus* spp was the second most dominant taxon in the central basin core, only three lakes in the training set contained *Chironomus* spp with abundance ≥10%.

Inferred avgVWHO model diagnostic showed that the training set and central basin core chironomid assemblage squared residual lengths (mean ± 95% CI) along the first RDA axis were 0.846 ± 0.0674 and 2.37 ± 0.126, respectively, such that all downcore chironomid assemblages are > 95% CI of the squared residual lengths of the training set samples constrained to the training set avgVWHO (Table D7). There was a relatively low correlation ($r = 0.420$, $p = 0.026$) between inferred avgVWHO and the main gradient (PCA axis 1) in the Lake Erie central basin sedimentary chironomid data (Fig. 2.9). The fraction of variance explained by inferred avgVWHO, represented as the fraction of maximum explainable variance, was also relatively low ($\lambda_{RDA}/\lambda_{PCA} = 0.535$).

Discussion

Chironomid assemblage trends

The eastern basin core has the presence of some key indicator taxa, such as *Chironomus*, *Procladius*, and *Micropsectra* (Fig. 2.3). However, without relative abundance data compounded with the short time scale covered by this core, little information can be drawn about the temporal changes in chironomid assemblages. While head capsule counts were also low in the western basin core, intervals with low counts were combined to allow for assemblage interpretation. However, similar to the eastern basin core, the western core was short and unable to provide information about the long-term changes that occurred in this basin. However, since the GLWQA 1972, there has been no indication of improving water quality as *Chironomus spp* and *Procladius* dominate the stratigraphy (Fig 2.4) indicating highly eutrophic conditions (Sæther 1979; Walker and Mathewes 1987). It is important to note that chironomid assemblage data for pre-1970s is not available.

Although the central basin core, much like the western basin core, had low chironomid head capsule abundances, the central basin core was long enough to provide meaningful long-term trends in chironomid assemblages that can be used to infer trends in water quality since about the 1850s (Fig. 2.6, 2.7). The presence of anoxia tolerant *Chironomus* spp throughout the core suggests that Lake Erie has been mesotrophic or eutrophic throughout the duration of the record, with periods where end-of-summer conditions had low hypolimnetic DO. These inferences are supported by paleolimnological diatom analyses which indicate that Lake Erie became more productive as early as the 1850s (Harris and Vollenweider 1982; Stoermer et al. 1987; Stoermer et al. 1996; Allinger and Reavie 2013). However, the presence of chironomid taxa indicative of oxic conditions, *Micropsectra* and *Heterotrisocladius*, early in the record (1850-1930) indicate that hypoxic conditions were not prevalent throughout the hypolimnion or appreciable in duration.

The disappearance of these oxic-type taxa between 1930s-1950s, along with declines in hypoxia-tolerant *Procladius* and increases in anoxia-tolerant *Chironomus* spp (specifically, *C. anthracinus*) indicate that hypolimnetic DO conditions in the central basin have been deteriorating. These results are in agreement with recent diatom-based paleolimnological analysis, which suggested the 1930s as the first major transition point in Lake Erie's water quality (Sgro and Reavie 2017). In addition, there have been indications of increased preservation in recent decades likely due to decreased decomposition rates as a result of anoxic conditions. For example, there has been a recent increase in Chironomini larvula (Fig. 2.6) which generally do not preserve well due to their thin chitin layer (Brodersen and Quinlan 2006).

Since P abatement programs were set in effect in the 1972 GLWQA, numerous phytoplankton studies indicated a decline in phytoplankton biomass between the 1970s-1980s across all basins (Munawar and Munawar 1976; Rathke 1982; Makarewicz 1987; Makarewicz 1991; Kane et al. 2014). Moreover, Makarewicz and Bertram (1993) noted 40% and 22% declines in phytoplankton biomass

between 1970-1979 in the western and central basins, respectively. However, there has been no observed decline in % organic C in the central basin core since its abrupt increase in the 1950s (Figure 2.7), suggesting that if rates of organic matter influx into bottom sediments has recently declined, then this may not be expressed in sediment core analyses due to a reduction in sediment C decomposition rates as a result of increased hypoxic-anoxic conditions. Alternatively, the constant level of % organic C may also be due to a shift from summer to winter-spring productivity (Twiss et al. 2012; Reavie et al. 2015; Beall et al. 2016).

The dreissenid mussel invasion in Lake Erie was detected in 1988 and they became established in the 1990s (Hebert et al. 1989; Griffiths et al. 1991). The nearshore shunt hypothesis proposed by Hecky et al. (2004) suggests that dreissenid mussel filtration and excretion processes, which occur in the littoral nearshore zones, would result in the shift of primary and secondary production from pelagic to littoral zones. Analysis of dreissenid mussels collected from the St. Lawrence River by Ricciardi (1994) found that *Paratanytarsus* sp larvae were living within the mantle cavity around the gills and siphon which were likely feeding on filtered material by the mussels as no damage to tissue was observed. However, none of the cores examined displayed an increase in abundance of *Paratanytarsus* sp or other littoral taxa following dreissenid invasion in Lake Erie to suggest a shift in chironomid communities towards the littoral zones (Fig. 2.4; 2.6; Table D1; Table D3). Similarly, diatom-based paleolimnological analyses of western and central cores revealed no shifts in dominant diatom species from pelagic to nearshore zones (Sgro and Reavie 2017). However, changes in nutrient cycling caused by dreissenids since the 1990s (Hecky et al. 2004) have been implicated in the increase in cyanophyte blooms (Conroy et al. 2005) which may have contributed to the shift in diatom compositions in the western basin of Lake Erie by 2008 (Sgro and Reavie 2017).

Low total head capsule counts in sedimentary cores from all basins may be attributed, in part, to its high sediment accumulation rates in Lake Erie. For example, the eastern basin had the highest

sediment accumulation rates of the three basins while having the least number of chironomid head capsules though a similar volume of sediment (wet weight per interval) was analyzed in all three basins. There are several lines of evidence that support this hypothesis. The majority of Lake Erie's shorelines consist of 'soft' till which are continually eroded by changing water levels and waves/water currents, which can be quite substantive in a very large lake (Burns 1985). Sly (1976) estimated that over the past 2000 years Lake Erie has become shallower by 30-35%, while the surface area has increased by 15-20%, due to basin infilling. Kemp et al. (1977) suggested that while annual sediment accumulation is relatively high in all three basins, the eastern basin receives the most sediment due to shoreline erosion from Long Point and the general eastward flows which bring sediment from the western and central basins. In addition, sediment accumulation data suggests that accumulation rates have recently been increasing in the western and central basins (Figure 2.5, 2.7), a trend that can be assumed for the eastern basin as well.

In addition, low head capsule counts in the eastern and central basin core may also be explained by the depth at which sediment cores were collected. In the deeper eastern basin, lower quality organic material will be deposited into the profundal zone due to its decomposition while descending through the water column, which may result in food limitation causing lower chironomid densities (Brodersen and Quinlan 2006). The depth in the central basin results in the formation of a relatively thin hypolimnion that is prone to oxygen depletion during periods of thermal stratification, such that during extended periods of anoxia only anoxia-tolerant taxa, such as *Chironomus spp*., will be present while less tolerant taxa may migrate to shallower, more oxygenated, zones (Bazzanti et al. 1998). As a result, the paleorecord from the central basin may reflect the deposition of chironomid remains from shallower profundal zones.

Quantitative paleo-inference of hypolimnetic DO in the central basin of Lake Erie

Low inferred avgVWHO for the 1850s may be attributed to increased settlement and human activities in the Lake Erie watershed at that time, which included anthropogenic stressors such as deforestation, wetland draining, increased farmland cover and population (Hatcher 1971; Burns 1985; Chapter 3). Fossil diatom records indicate that during this time period there were higher nutrient levels, as there was a shift towards more eutrophic diatom taxa, such as *Stephanodiscus* and *Fragilaria* (Harris and Vollenweider 1982; Stoermer et al. 1987; Stoermer et al. 1996; Allinger and Reavie 2013). However, while nutrient inputs and the associated shifts towards more eutrophic diatom continued between 1850s-1860s, there was an increase in inferred avgVWHO, a decline in anoxic-type *Chironomus* spp, and appearance of oxic-type *Heterotrissocladius* suggesting that hypolimnetic DO had returned to more oxic conditions. However, it is important to note that the central basin core did not extend to pre-disturbance condition (i.e. pre-European settlement) and that these changes may be an indication of sediments acting as nutrient sinks early in the record.

According to the chironomid assemblage and inferred avgVWHO, hypolimnetic DO conditions in the central basin remained relatively stable during the 1870s-1930s (Fig 2.6, 2.7). However, post-1930 hypolimnetic DO conditions began to deteriorate as indicated by the disappearance of oxic-type taxa *Heterotrissocladius* by the 1930s, *Micropsectra* by the mid-1950s (Fig 2.6), and the associated decline in inferred avgVWHO in the mid-1950s (Fig 2.7). In addition, during the post-1950 period there was a decline in hypoxia-tolerant *Procladius* and increases in anoxia tolerant *Chironomus spp* (Fig 2.6). These assemblage changes are consistent with results obtained from cluster analysis which identified the mid-1950s as a significant transition point in chironomid community change, all of which suggest that post-1950s the extent and duration of anoxic conditions in the central basin have been increasing, and despite P abatement programs in the 1970s no improvements in hypolimnetic DO conditions have been observed.

Inferred increases in avgVWHO since the late-1970s (Fig. 2.7) are primarily driven by increases in *T. lugens* which has an optimal avgVWHO of approximately 4 mg O_2 L^{-1} (Table 2.3; Quinlan and Smol 2001a). Furthermore, when relative abundance of chironomid taxa between the central basin core and the calibration were compared, there were several indications that there may be an analog problem : (1) the relative abundance of *T. lugens* far exceeded the highest abundance in the calibration set; (2) relative abundance of *Chironomus spp* was also much greater in the central basin core when compared to the calibration set; (3) central basin chironomid assemblage squared residual lengths along RDA axis 1 are outside of the active chironomid assemblage 95% CI; (4) there was a weak correlation between PCA axis 1 and inferred avgVHWO; and (5) the fraction of the variance explained by inferred avgVWHO, as a function of maximum explainable variance ($\lambda_{RDA}/\lambda_{PCA}$), was also relatively low. Thus, while inferred avgVWHO may indicate a general trend in hypolimnetic DO dynamics within the central basin, direct interpretation of avgVWHO inferences should proceed with caution as these inferences may be unreliable.

Conclusion

While the presence of *Chironomus spp* throughout the stratigraphy indicated that the central basin of Lake Erie has historically experienced periods of anoxia, there are strong indications that the extent and/or duration of anoxic conditions has increased since approximately the 1930s-1950s, which has been demonstrated by changes in the chironomid assemblage (i.e. disappearance of the oxic-type taxa *Micropsectra* and *Heterotrissocladius*). The possible drivers for these shifts are explored in Chapter 3. In addition, the presence of Chironomini larvula since the mid-1990s (Fig 2.6) may correspond to enhanced preservation due to anoxic conditions, as early chironomid instars have thin chitin that generally does not preserve well under normal conditions (Brodersen and Quinlan 2006).

While a quantitative reconstruction of hypolimnetic DO in the central basin was conducted and expressed as avgVWHO, given the geography and morphometry (e.g. lake size) which likely resulted in highly different chironomid community compositions from the training set assemblages, these compositional differences between the training set and study site resulted in unreliable hypolimnetic DO reconstructions.

References

Allinger LE, Reavie ED. 2013. The ecological history of Lake Erie as recorded by the phytoplankton community. J Great Lakes Res. 39:365–382.

Appleby PG, Oldfield F. 1978. The calculation of lead-210 dates assuming a constant rate of supply of unsupported 210Pb to the sediment. Catena. 5:1–8.

Armitage PD, Pinder LC, Cranston P. 2012. The Chironomidae: biology and ecology of non-biting midges. Springer Science & Business Media.

Bazzanti M, Seminara M, Baldoni S. 1998. Assessing hypolimnetic stress in a monomictic, eutrophic lake using profundal sediment and macrobenthic characteristics. J Freshw Ecol. 13:405–412.

Beall BFN, Twiss MR, Smith DE, Oyserman BO, Rozmarynowycz MJ, Binding CE, Bourbonniere RA, Bullerjahn GS, Palmer ME, Reavie ED, et al. 2016. Ice cover extent drives phytoplankton and bacterial community structure in a large north-temperate lake: implications for a warming climate. Environ Microbiol. 18:1704–1719.

Beeton AM. 1961. Environmental changes in Lake Erie. Trans Am Fish Soc. 90:153–159.

Bennett KD. 1996. Determination of the number of zones in a biostratigraphic sequence. New Phytol. 132:155–170.

Bertram PE. 1993. Total Phosphorus and Dissolved Oxygen Trends in the Central Basin of Lake Erie, 1970–1991. J Great Lakes Res. 19:224–236.

Birks HJB, Lotter AF, Juggins S, Smol JP. 2012. Tracking Environmental Change Using Lake Sediments: Data Handling and Numerical Techniques. Vol. 5. Springer Science & Business Media.

Birks HJB. 2014. Quantitative palaeoenvironmental reconstructions from Holocene biological data. In: Mackay A, Battarbee R, Oldfield F, editors. Global change in the Holocene. Routledge. p. 123–139.

ter Braak CJF, Smilauer P. 2002. Canoco for Windows version 4.5. Biometrics, Plant Research International. Wageningen, Netherland.

Brodersen KP, Quinlan R. 2006. Midges as palaeoindicators of lake productivity, eutrophication and hypolimnetic oxygen. Quat Sci Rev. 25:1995–2012.

Brooks SJ, Langdon PG, Heiri O. 2007. The Identification and Use of Palaearctic Chironomidae Larvae in Palaeoecology. Quaternary Research Association (Technical guide).

Brundin L. 1951. The relation of O2-microstratification at the mud surface to the ecology of the profundal bottom fauna. Rep Inst Freshwat Res Drottningholm. 32:32–42.

Burns NM. 1976. Temperature, Oxygen, and Nutrient Distribution Patterns in Lake Erie, 1970. J Fish Res Board Canada. 33:485-511.

Burns NM. 1985. Erie: The Lake That Survived. Rowman & Allanheld.

Burns NM, Rockwell DC, Bertram PE, Dolan DM, Ciborowski JJH. 2005. Trends in temperature, Secchi depth, and dissolved oxygen depletion rates in the central basin of Lake Erie, 1983–2002. J Great Lakes Res. 31:35–49.

Conroy JD, Kane DD, Dolan DM, Edwards WJ, Charlton MN, Culver DA. 2005. Temporal trends in Lake Erie plankton biomass: roles of external phosphorus loading and dreissenid mussels. J Great Lakes Res. 31:89–110.

Davis CC. 1964. Evidence for the eutrophication of Lake Erie from phytoplankton records. Limnol Oceanogr. 9:275–283.

Gordon AD, Birks HJB. 1974. Numerical Methods in Quaternary. New Phytol. 73:221–249.

Griffiths RW, Schloesser DW, Leach JH, Kovalak WP. 1991. Distribution and dispersal of the zebra mussel (Dreissena polymorpha) in the Great Lakes region. Can J Fish Aquat Sci. 48:1381–1388.

Grimm EC. 1987. Constrained Cluster Analysis by the Method of Incremental Sum of Squares. Comput Geosci. 13:13–35.

Harris GP, Vollenweider RA. 1982. Paleolimnological evidence of early eutrophication in Lake Erie. Can J Fish Aquat Sci. 39:618–626.

Hatcher HH. 1971. Lake Erie. Greenwood Press.

Hebert PDN, Muncaster BW, Mackie GL. 1989. Ecological and genetic studies on Dreissena polymorpha (Pallas): a new mollusc in the Great Lakes. Can J Fish Aquat Sci. 46:1587–1591.

Hecky RE, Smith REH, Barton DR, Guildford SJ, Taylor WD, Charlton MN, Howell T. 2004. The nearshore phosphorus shunt: a consequence of ecosystem engineering by dreissenids in the Laurentian Great Lakes. Can J Fish Aquat Sci. 61:1285–1293.

Heiri O, Lotter AF, Lemcke G. 2001. Loss on ignition as a method for estimating organic and carbonate content in sediments: Reproducibility and comparability of results. J Paleolimnol. 25:101–110.

International Joint Commission (IJC). 1972. Great Lakes Water Quality Agreement with Annexes and Texts and Terms of Reference between the United States and Canada Signed at Ottawa, April 15, 1972. International Joint Commission, Windsor, Ontario, Canada.

International Joint Commission (IJC). 1978. Great Lakes Water Quality Agreement of 1978 with Annexes and Terms of Reference between the United States and Canada Signed at Ottawa, November 22, 1978.

International Joint Commission (IJC). 1983. Great Lakes Water Quality Agreement of 1978. Phosphorus Load Reduction Supplement of 1983.

Juggins S. 2007. C2 user guide: Software for ecological and palaeoecological data analysis and visualization. Univ Newcastle, Newcastle upon Tyne, UK.:1–73.

Juggins S. 2017. Package 'rioja.' Analysis of Quaternary Science Data, The Comprehensive R Archive Network.

Kane DD, Conroy JD, Peter Richards R, Baker DB, Culver D a. 2014. Re-eutrophication of Lake Erie: Correlations between tributary nutrient loads and phytoplankton biomass. J Great Lakes Res. 40:496–501.

Kemp ALW, MacInnis GA, Harper NS. 1977. Sedimentation Rates and a Revised Sediment Budget for Lake Erie. J Great Lakes Res. 3:221–233.

Makarewicz JC. 1987. Phytoplankton and Zooplankton in Lakes Erie, Huron and Michigan: 1984. United States Environmental Protection Agency. Technical report.

Makarewicz JC. 1991. Phytoplankton and Zooplankton Composition, Abundance and Distribution and Trophic Interactions: Offshore Region of Lakes Erie, Lake Huron and Lake Michigan, 1985. US Environmental Protection Agency, Great Lakes National Program Office.

Makarewicz JC, Bertram PE. 1993. Evidence for the Restoration of the Lake Erie Ecosystem. J Great Lakes Res. 19:197.

McHenry JR, Ritchie JC, Gill AC. 1973. Accumulation of fallout cesium 137 in soils and sediments in selected watersheds. Water Resour Res. 9:676–686.

Medeiros AS, Quinlan R. 2011. The distribution of the Chironomidae (Insecta: Diptera) along multiple environmental gradients in lakes and ponds of the eastern Canadian Arctic. Can J Fish Aquat Sci. 68:1511–1527.

Munawar M, Munawar IF. 1976. A Lakewide Study of Phytoplankton Biomass and its Species Composition in Lake Erie, April–December 1970. J Fish Res Board Canada. 33:581–600.

Nicholls KH, Hopkins GJ, Standke SJ, Nakamoto L. 2001. Trends in Total Phosphorus in Canadian Near–Shore Waters of the Laurentian Great Lakes: 1976–1999. J Great Lakes Res. 27:402–422.

Paterson AM, Quinlan R, Clark BJ, Smol JP. 2009. Assessing hypolimnetic oxygen concentrations in Canadian Shield lakes: Deriving management benchmarks using two methods. Lake Reserv Manag. 25:313–322.

Quinlan R, Smol JP. 2001a. Chironomid-based inference models for estimating end-of-summer hypolimnetic oxygen from south-central Ontario shield lakes. Freshw Biol. 46:1529–1551.

Quinlan R, Smol JP. 2001b. Setting minimum head capsule abundance and taxa deletion criteria in chironomid-based inference models. J Paleolimnol. 26:327–342.

Rathke DE. 1982. Lake Erie intensive study 1978-1979. United States Environmental Protection Agency, Great Lakes National Program Office. Technical report.

Reavie ED, Cai M, Twiss MR, Carrick HJ, Davis TW, Johengen TH, Gossiaux D, Smith DE, Palladino D, Burtner A, et al. 2015. Winter-spring diatom production in Lake Erie is an important driver of summer hypoxia. J Great Lakes Res. 42:608–618.

Reavie ED, Heathcote AJ, Shaw Chraïbi VL. 2014. Laurentian Great Lakes phytoplankton and their water quality characteristics, including a diatom-based model for paleoreconstruction of phosphorus. PLoS One. 9(8):e104705.

Ricciardi A. 1994. Occurrence of chironomid larvae (Paratanytarsus sp.) as commensals of dreissenid mussels (Dreissena polymorpha and D. bugensis). Can J Zool. 72:1159–1162.

Ritchie JC, McHenry JR. 1990. Application of radioactive fallout cesium-137 for measuring soil erosion and sediment accumulation rates and patterns: a review. J Environ Qual. 19:215–233.

Sæther O a. 1979. Chironomid communities as water quality indicators. Holarct Ecol. 2:65–74.

Sgro G V, Reavie ED. 2017. Lake Erie's ecological history reconstructed from the sedimentary record. J Great Lakes Res. 44:54-69

Sly PG. 1976. Lake Erie and its Basin. J Fish Res Bd Can. 33:355–370.

Šmilauer P, Lepš J. 2003. Multivariate Analysis of Ecological Data using CANOCO. Cambridge University Press.

Smol JP. 2008. Pollution of lakes and rivers: a paleoenvironmental perspective. John Wiley & Sons.

Stoermer EF, Emmert G, Julius ML, Schelske CL. 1996. Paleolimnologic evidence of rapid recent change in Lake Erie's trophic status. Can J Fish Aquat Sci. 53:1451–1458.

Stoermer EF, Kociolek JP, Schelske CL, Conley DJ. 1987. Quantitative analysis of siliceous microfossils in the sediments of Lake Erie's central basin. Diatom Res. 2:113–134.

Summers JC, Rühland KM, Kurek J, Quinlan R, Paterson AM, Smol JP. 2012. Multiple stressor effects on water quality in Poplar Bay, Lake of the Woods, Canada: A midge-based assessment of hypolimnetic oxygen conditions over the last two centuries. J Limnol. 71:34–44.

Team RC. 2014. R: A language and environment for statistical computing. Vienna, Austria: R Foundation for Statistical Computing; 2014.

Twiss MR, McKay RML, Bourbonniere RA, Bullerjahn GS, Carrick HJ, Smith REH, Winter JG, D'souza NA, Furey PC, Lashaway AR, et al. 2012. Diatoms abound in ice-covered Lake Erie: An investigation of offshore winter limnology in Lake Erie over the period 2007 to 2010. J Great Lakes Res. 38:18–30.

Walker I, Mathewes R. 1987. Chironomids, lake trophic status, and climate. Quat Res. 437:431–437.

Zhang H, Culver DA, Boegman L. 2011. Dreissenids in Lake Erie: an algal filter or a fertilizer? Aquat Invasions. 6:175–194.

Zhou Y, Obenour DR, Scavia D, Johengen TH, Michalak AM. 2013. Spatial and Temporal Trends in Lake Erie Hypoxia, 1987 − 2007. Environ Sci Technol. 47:899–905.

Figures and Tables

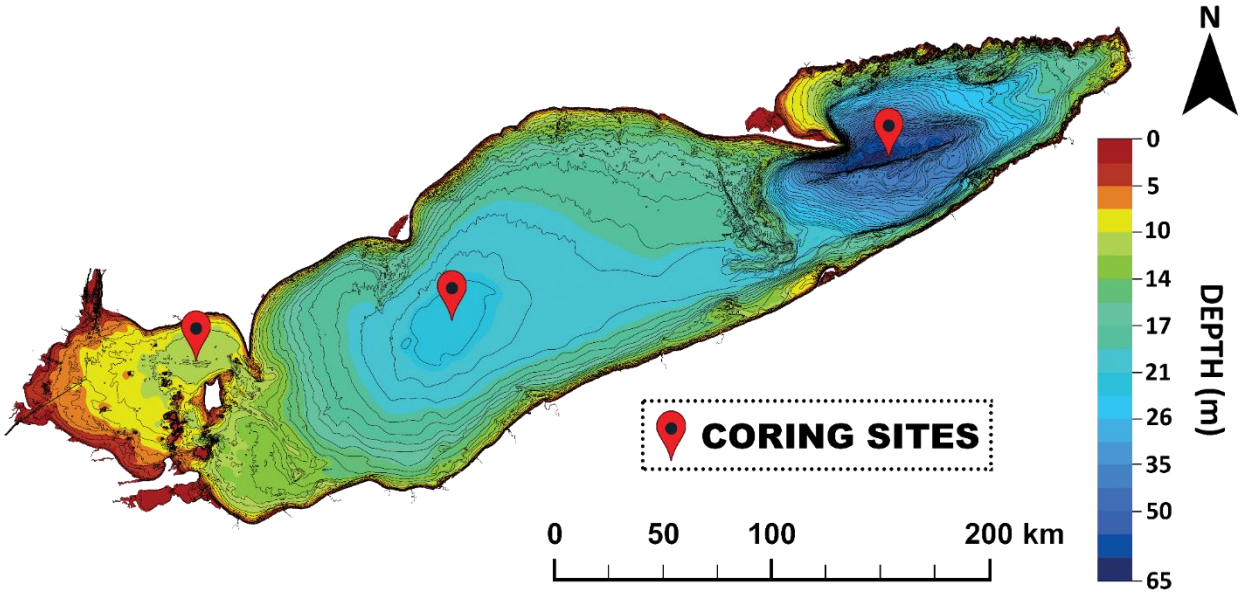

Figure 2.1: Lake Erie bathymetry and core locations. Bathymetry map was compiled using bathymetry data obtained from National Oceanic and Atmospheric Administration (NOAA). Coring site coordinates and depths are shown in Table 2.1.

Table 2.1: Coring locations and depths of each core analyzed. CB – central basin; WB – western basin; and EB – eastern basin

	Latitude	Longitude	Z_{max}	Core length
CB	41.998733	-81.650054	19 m	49.5 cm
WB	41.892335	-82.716719	24 m	32 cm
EB	42.516667	-79.805638	64 m	41 cm

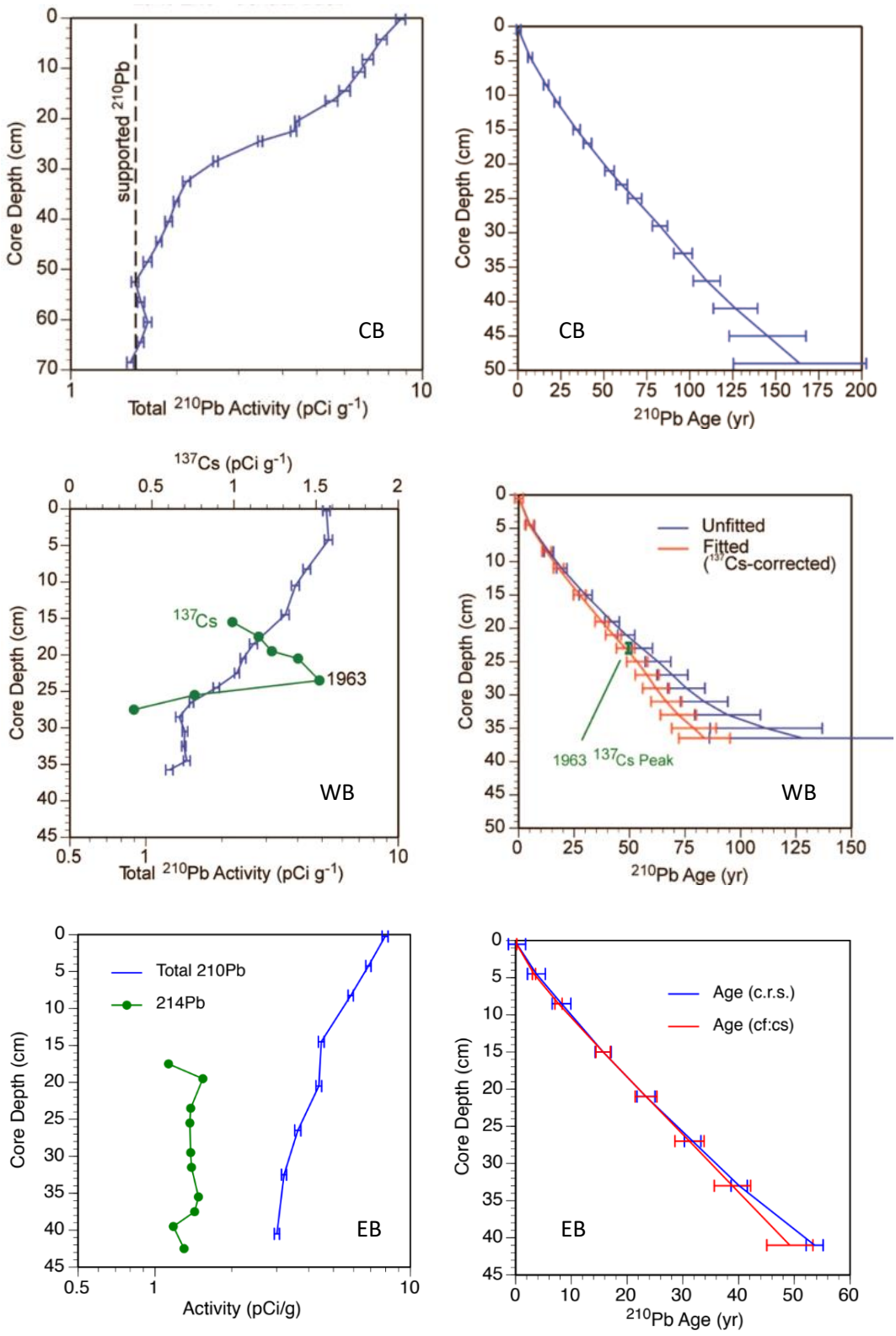

Figure 2.2: The ^{210}Pb activity decay (pCi g^{-1}) versus core depth. Background supported ^{210}Pb is indicated by the dashed line. CB – central basin; WB – western basin; and EB – eastern basin.

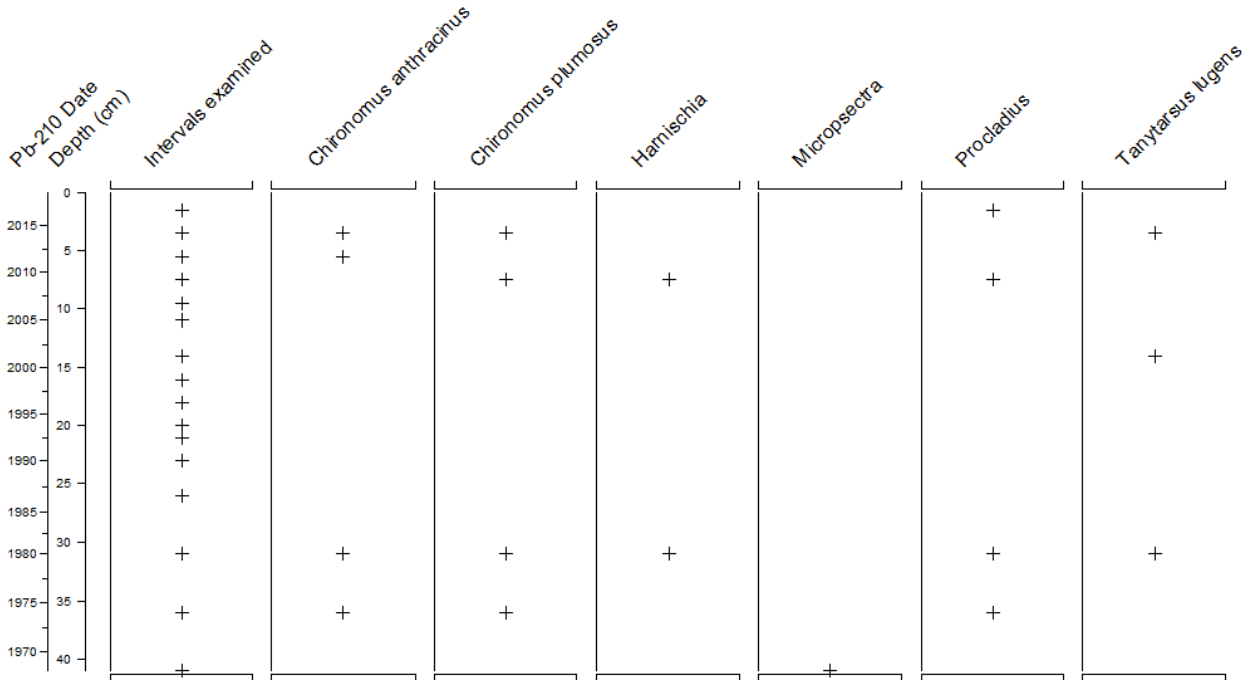

Figure 2.3: Presence/absence chironomid assemblage data for the eastern basin core. Presence of chironomid taxa in a core interval indicated by an +. Taxa arranged alphabetically.

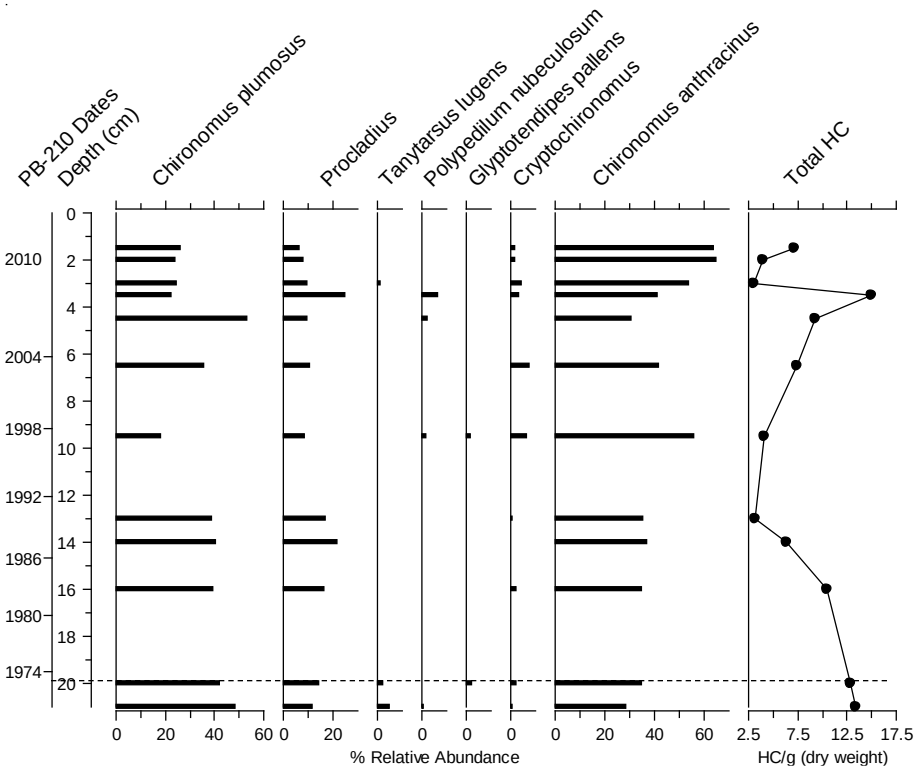

Figure 2.4: Relative percent abundance of selected chironomid taxa from the western basin core. Taxa are arranged according to their PCA axis 1 scores. HC – head capsules. Dashed line represents the 1972 Great Lakes Water Quality Agreement (GLWQA).

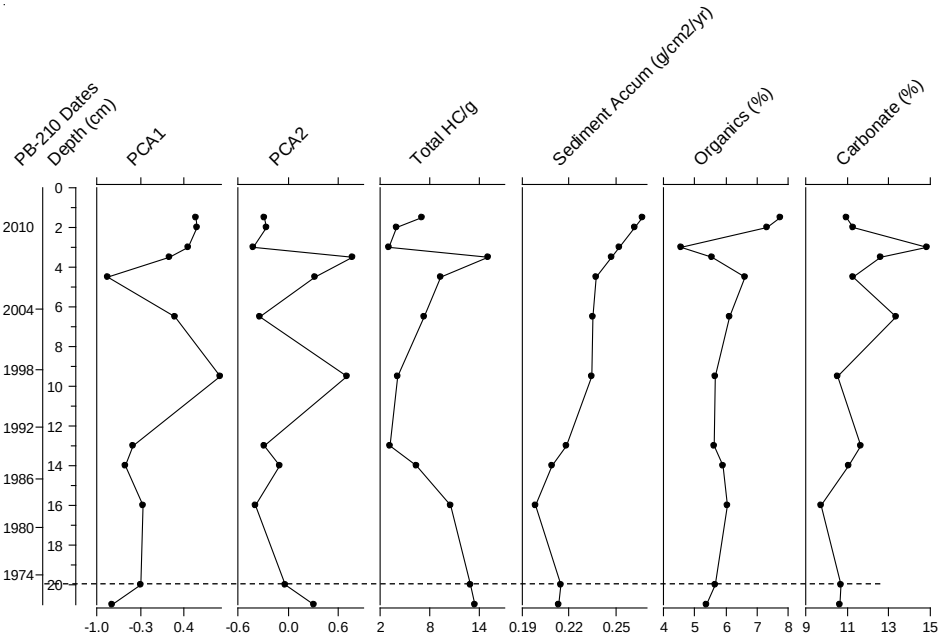

Figure 2.5: Summary diagram of the western basin core showing principal component analysis (PCA) axis scores, total head capsules (HC g^{-1} dry weight), sediment accumulation rates (g cm^{-2} yr^{-1}), percent organic carbon content, and percent carbonate content. Dashed line represents the 1972 Great Lakes Water Quality Agreement (GLWQA).

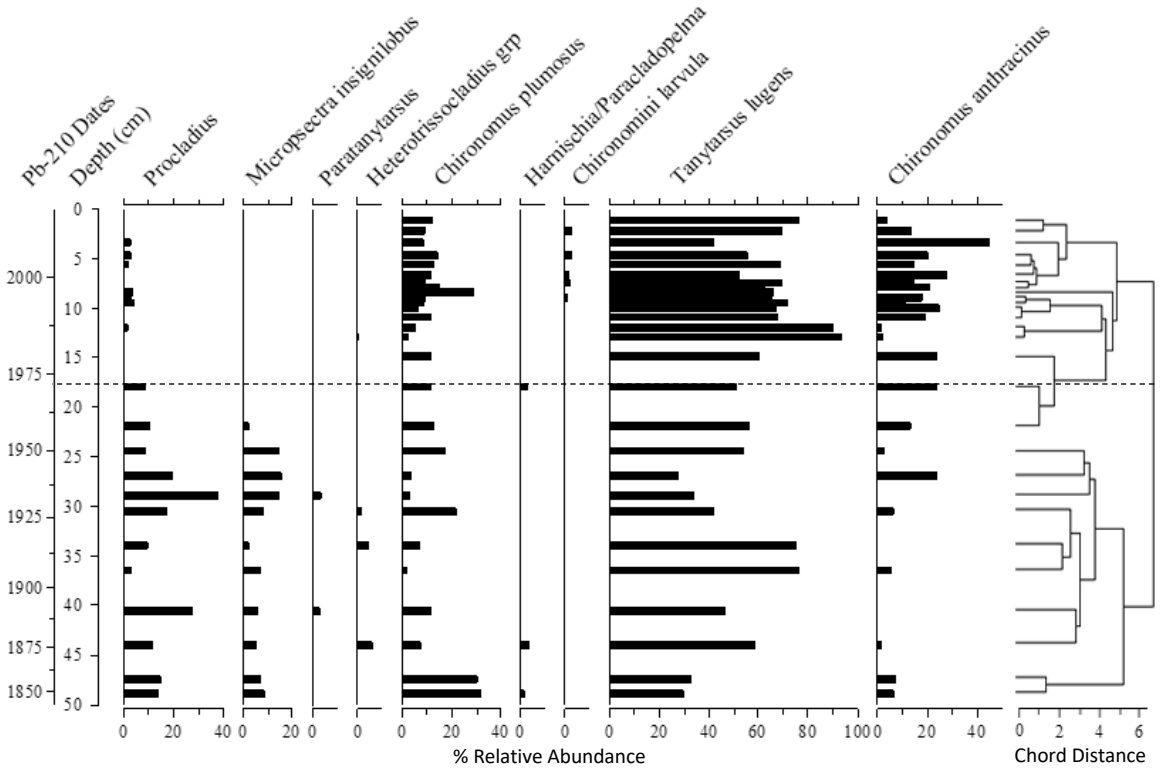

Figure 2.6: Relative percent abundance of selected chironomid taxa from the central basin core. Taxa are arranged according to their principal component analysis (PCA) axis 1 scores. Stratigraphically constrained cluster analysis (CONISS) dendrogram shown on the right. Dashed line represents the1972 Great Lakes Water Quality Agreement (GLWQA).

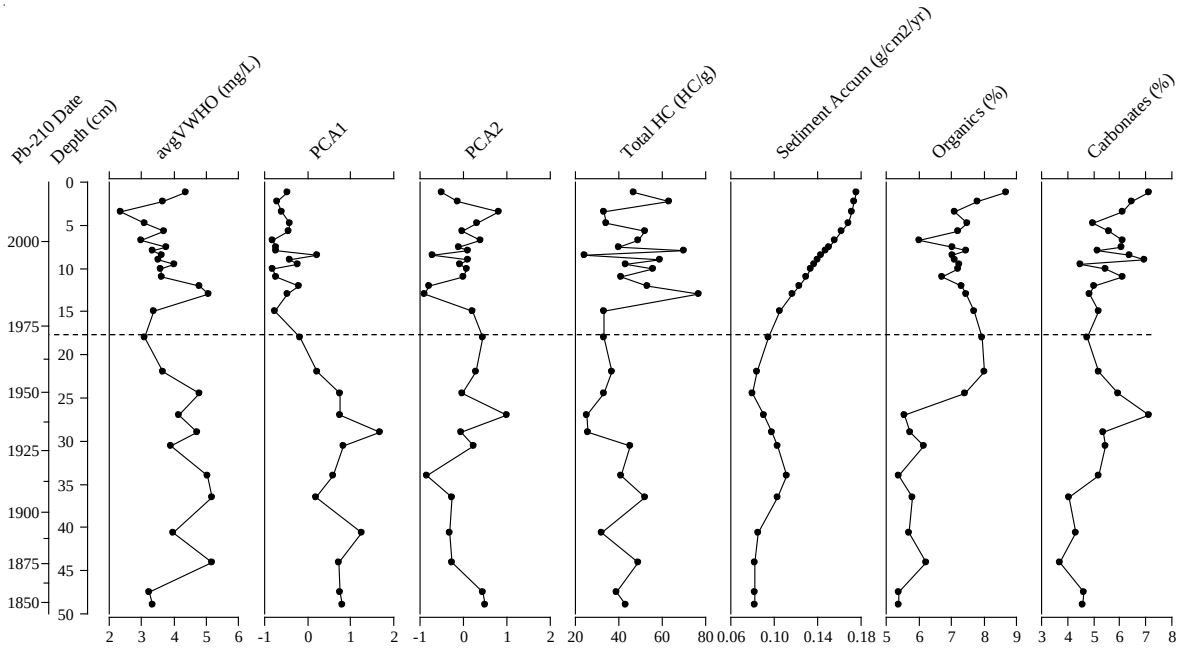

Figure 2.7: Summary diagram of the central basin core showing PCA axis scores, total head capsules (HC g^{-1} dry weight), sediment accumulation rates (g cm^{-2} yr^{-1}), percent organic carbon content, and percent carbonate content. Solid line indicates transitional point; Dashed line represents the 1972 Great Lakes Water Quality Agreement (GLWQA).

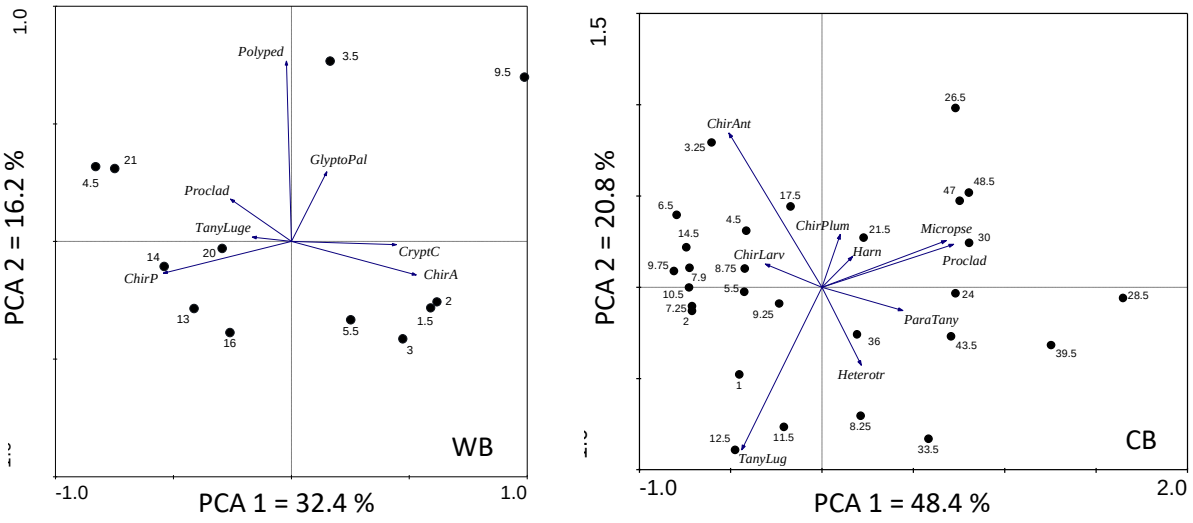

Figure 2.8: Principal component analysis (PCA; covariance matrix) of selected taxa. WB – western basin; CB – central basin. See Table 2.2 for taxa abbreviations.

Table 2.2: List of chironomid taxa from the central and western basins after removal of rare taxa (≥2% relative abundance in at least two samples)

	Taxon	**Code**
1	*Chironomini Larvula*	ChirLarv
2	*Chironomus anthracinus*	ChirAnt
3	*Chironomus plumosus*	ChirPlum
4	*Cryptochironomus*	CryptC
5	*Glyptotendipes pallens*	GlyptoPal
6	*Harnischia/Paracladopelma*	Harn
7	*Heterotrissocladius grp*	Heterotr
8	*Micropsectra insignilobus*	Micropse
9	*Paratanytarus*	ParaTany
10	*Polypedilum*	Polyped
11	*Procladius*	Proclad
12	*Tanytarsus lugens*	TanyLug

Table 2.3: Habitat and oxygen optima of key taxa from principal component analysis (PCA). Based on data from Sæther (1979), Quinlan and Smol (2001a), and Brodersen and Quinlan (2006)

	Taxon	Habitat	avgVWHO optima (mg O_2 L^{-1})
1	*Chironomini Larvula*	Profundal	3.2
2	*Chironomus anthracinus*	Profundal	3.3
3	*Chironomus plumosus*	Profundal	3.3
4	*Cryptochironomus*	Profundal	4.7
5	*Glyptotendipes pallens*	Littoral/Macrophyte	3.3
6	*Harnischia/Paracladopelma*	Profundal	5.1
7	*Heterotrissocladius grp*	Profundal	7.0
8	*Micropsectra insignilobus*	Profundal	6.1
9	*Paratanytarsus*	Littoral/Macrophyte	
10	*Polypedilum*	Littoral	4.3
11	*Procladius*	Profundal	3.7
12	*Tanytarsus lugens*	Profundal	4.1

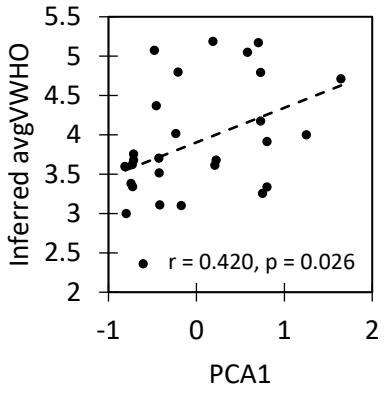

Figure 2.9: Correlation between inferred avgVWHO and principal component analysis (PCA) axis 1.

Chapter 3: Using sediments to track the effects of multiple stressors and cumulative effects in the central basin of Lake Erie using subfossil Chironomidae

Introduction

While Lake Erie is the smallest and shallowest of the Great Lakes it has one of the most densely populated and most intensively farmed watersheds of the Great Lakes, which is primarily due to its arable and fertile soil (Burns 1985). Consequently, Lake Erie experienced multiple anthropogenic stressors since European settlement, including deforestation, draining of wetland, cultural eutrophication, modification of catchment, contaminants, and climate change. Arguably, phosphorus (P) loadings have been particularly influential at driving lake-wide water quality changes and hypolimnetic dissolved oxygen (DO) depletion in the central basin (Burns 1976; Harris and Vollenweider 1982; Stoermer et al. 1987; Bertram 1993; Ludsin et al. 2001). Population growth and an increase in urban sprawl, along with the expansion of agricultural lands have marked the acceleration of nutrient inputs into Lake Erie (Burns 1985). Early settlement in the western Lake Erie watershed has resulted in signs of eutrophication appearing as early as the 1850s (Harris and Vollenweider 1982; Allinger and Reavie 2013). By the 1960s, high levels of P inputs into Lake Erie led to severe blooms of nuisance and cyanobacteria blooms in the western basin and severe hypolimnetic DO depletion in the central basin (Rosa and Burns 1987; Bertram 1993; Burns et al. 2005; Allinger and Reavie 2013).

The 1972 Canada-US Great Lakes Water Quality Agreement (GLWQA) was designed to eliminate algal blooms and restore hypolimnetic DO levels by limiting total phosphorus (TP) loads into the Great Lakes (De Pinto et al. 1986). In the case of Lake Erie, it was suggested that TP loadings of 11,000 tons per year should reflect an average concentration of 10 μg L^{-1} TP in the central basin (Chapra 1977; IJC 1983). These P targets were achieved by limiting point source P inputs through restriction of phosphorus in household detergents and the upgrading of existing water treatment facilities (Burns 1985). Lake Erie

responded relatively quickly to these TP load reductions, and by the 1980s water clarity had improved (Rathke 1982; Makarewicz 1987; Makarewicz 1991; Bertram 1993; Makarewicz and Bertram 1993). However, since the 1990s, Lake Erie has been returning to a more eutrophic state, which is evident by the reappearance of cyanobacteria blooms (Stumpf et al. 2012; Michalak et al. 2013; Wynne and Stumpf 2015), resurgence of benthic algae growth (Auer et al. 2010; Depew et al. 2011), and the return of extensive hypoxia in the central basin (Zhou et al. 2013; Rucinski et al. 2014; Scavia et al. 2014; Zhou et al. 2015) although TP concentrations remained relatively stable. As a result, there were recommendations made to reduce TP loads into Lake Erie by 46% (4,300 MTA from the current 11,000 MTA targets) from observed TP load average between 2003-2011 (IJC 2015).

Numerous independent limnological studies have examined the hypolimnetic DO dynamics in the central basin of Lake Erie (e.g. Rosa and Burns 1987; Burns et al. 2005; Zhou et al. 2013; Zhou et al. 2015). Studies by Burns et al. (2005) and Zhou et al. (2013) which examined the hypoxic extent in the central basin of Lake Erie between 1987-2002 indicated a cyclical trend where nearly the entire central basin was overlaid by an anoxic hypolimnion between 1987-1988 and 1998-2001, with a relatively small area of anoxic hypolimnion observed between 1995-1996. However, since these studies were limited to the previous two decades, it was not possible to assess long-term (i.e. decadal- or centennial-scale) changes in hypolimnetic DO in Lake Erie as a result of multiple anthropogenic stressors. Paleolimnological studies may generate centuries of data, providing baseline environmental data which can be used to better understand Lake Erie's ecosystem dynamics. While there have been numerous paleolimnological studies which examined diatom and biogenic silica assemblages (Harris and Vollenweider 1982; Schelske et al. 1986; Stoermer et al. 1987; Schelske et al. 2006; Sgro and Reavie 2017), these studies investigated trophic status, productivity, and trends in TP inputs, but were unable to provide information on hypolimnetic DO dynamics. An overview of historical changes with respect to Lake Erie's trophic status and associated phytoplankton trends was described in Chapter 1, while an in-

depth literature review of the ecological history of Lake Erie recorded by phytoplankton assemblages is presented in Allinger and Reavie (2013).

Chironomidae (Diptera) are frequently the most abundant insects found in freshwater ecosystems (Hofmann 1988; Armitage et al. 2012), they are good indicators of water quality in lakes (Sæther 1979), and hypolimnetic DO can be a major factor influencing the distribution of profundal chironomids (Brundin 1951). Some members of the Chironomidae, such as *Chironomus* spp., possess hemoglobin (Armitage et al. 2012), while other taxa use migration strategies (Bazzanti et al. 1998), or tube ventilation (Brodersen and Quinlan 2006) to deal with low hypolimnetic DO conditions that are often associated with highly eutrophic lakes. Due to the distribution and abundance of chironomid taxa reflecting a range of DO optima and tolerances, assemblage changes are often used as indicators of changes in hypolimnetic DO and water quality (Brundin 1951; Quinlan and Smol 2001a; Brodersen and Quinlan 2006). As a result, paleolimnological assessment of subfossil chironomid remains preserved in sediments could potentially allow for the reconstruction of past hypolimnetic DO conditions (Walker 1987; Hofmann 1988).

Qualitative and quantitative inference of hypolimnetic DO dynamics have been presented in Chapter 2. The aim of this chapter is to determine which environmental factors have had a significant influence on chironomid community compositions and hypolimnetic DO within the central basin. Results from this work will benefit lake managers and policymakers by providing the necessary information to make effective decisions for improving water quality in Lake Erie, in particular, hypolimnetic DO within the central basin.

Methods

Field and laboratory methods

The central basin core (41.998733° N, -81.650054° W) was collected on July 2011 (Fig. 3.1) using an Oceanic Instruments Model MC-400 multicorer. The central basin core site was selected to correspond to cores previously collected for paleolimnological studies by Harris and Vollenweider (1982) and Stoermer et al. (1987). The core was sectioned at 0.5 cm intervals between 0-10 cm, with 1 cm sections from 10-49 cm.

Chironomid head capsules were prepared for microscope identification using methods similar to Hall et al. (1999) (which are based on methods described by Warwick (1980) and Walker (1987)). Approximately 10-14g of sediment (wet weight) per interval was examined for subfossil chironomid remains. Each interval was deflocculated in 10% KOH solution at 70°C for 30 min then washed through 212 and 106 µm mesh sieves. The flow-through was collected and washed in 36 µm sieves in order to collect cladoceran remain for future analysis. All retained residues were then washed with and stored in 95% ethanol.

Residues were sifted using a Nikon SMZ1500 stereomicroscope at 30-40x magnification, and chironomid head capsules were extracted with the use of fine forceps. Specimens were permanently mounted on glass slides in Entellan mounting medium. While efforts have been made to extract a minimum of 50 chironomid head capsules per interval (Quinlan and Smol 2001b), many intervals had < 50 head capsules, and as a result adjacent intervals were combined (Chapter 2).

Historical data

Continuous annual data for 169 environmental variables within the Lake Erie watershed were collected to determine the impacts of environmental change on water quality and chironomid

compositions between 1850-2011; variables were assigned to either water quality, climate or land use categories (Table 3.1). All seasonal data for winter, spring, summer, and fall was calculated based on data for Dec-Feb, Mar-May, Jun-Aug, and Sep-Nov, respectively. All historical data values were averaged to represent the corresponding interval year range (Appendix C).

Complete records of maximum, mean, and minimum monthly and annual air temperatures (^{o}C; 1948-2011), mean surface water temperature (^{o}C; 1948-2011), precipitation over lake (mm, 1900-2015), precipitation over land (mm, 1882-2015), gross evaporation (mm, 1950-2015), runoff (mm, 1914-2015), and net basin supply (m^3s^{-1}, NBS = precip over lake – evap + runoff, 1950-2015) were obtained from the National Oceanic and Atmospheric Administration - Great Lakes Environmental Research Laboratory (NOAA-GLERL). Historical records of percent ice cover were obtained from the US Environmental protection Agency (EPA) and are based on data from the Canadian Ice Service (1973-1988) and the US National Ice Center (1989-2017). Lake level anomaly (ft, 1860-2015) was calculated based on the 1981-2010 baseline average referenced to IGLD85; data was obtained from the US EPA based on data from NOAA-GLERL.

Historical water quality data was obtained from the US EPA – Great Lakes Environmental Database (GLENDA), with missing values supplemented by data from Canadian Centre for Inland Waters (CCIW) central basin monitoring stations (Fig 3.1). Hypolimnetic DO measurements (mg O_2 L^{-1}, 1962-2011) were taken at inconsistent dates, as a result all hypolimnetic DO data was standardized to end-of-summer (Sept 1st) by linear extrapolation or interpolation, and final hypolimnetic DO values used in analyses represented DO at 1 m above the sediment-water interface at the monitoring station.

Historic water column TP (µg P L^{-1}, 1970-2014) data was compiled for April and August. Historic water column total inorganic nitrogen (TIN) data was calculated as the sum of nitrate+nitrite and ammonia+ammonium for April and August. However, ammona+ammonium data was sparse with many

years missing, as a result, an average of ammonia+ammonium over the historical record was added to all nitrate+nitrite values. Since ammonia+ammonium generally comprised only a small portion of nitrate+nitrite (< 5%), this was considered as an acceptable estimate to make given limits of the available data. Total nitrogen (TN) estimates were not possible due to a lack of long-term organic N (or TN) data

Historical records of TP loads (MTA, 1967-2013) were obtained from Maccoux et al. (2016), which were calculated as a sum of the loads from point sources, tributaries, atmospheric deposition, and the upstream inputs from Lake Huron and Lake St. Clair. Spatial and temporal land use data in the Lake Erie watershed was obtained from Sgro and Reavie (2017). This land use data included population, agricultural land and forest cover for the western and entire Lake Erie watershed (Table 1).

Numerical analysis

All numerical analyses of chironomid assemblages were based on Hellinger transformed species data (Birks et al. 2012). Temporal patterns of chironomid community change (ca. 1852-2011) were explored using principal component analysis (PCA) in CANOCO version 4.5 (ter Braak and Smilauer 2002), with rare taxa removed (≥2% relative abundance in at least two samples), resulting in a total of nine taxa (Chapter 2). All environmental data was examined for normality using a Shapiro-Wilk test, and variables which significantly deviated from normality were transformed using Box-Cox λ as an estimate of optimal transformation to normality (Sokal and Rohlf 1995; Birks et al. 2012) (Appendix C). Inferred avgVWHO reconstruction was performed using a calibration set published by (Quinlan and Smol 2001a) in C2 version 1.5 (Juggins 2007), but due to poor reliability of the reconstruction (Chapter 2), it was omitted from further analysis.

Variance partitioning analysis was based on the procedure outlined by Hall et al. (1999); all ordination and permutation testing computed in CANOCO Version 4.5 (ter Braak and Smilauer 2002). An

initial exploratory detrended canonical correspondence analysis (DCCA), detrending by segments, non-linear scaling, with sample age as the only external constraint, was used to estimate the gradient length of the chironomid assemblage which suggested linear-based redundancy analysis (RDA) would be most appropriate (<2 SD) (Birks et al. 2012). A series of singly-constrained ordinations (RDA; inter-species correlations and centered by species), were used to determine which variables explained a significant ($p < 0.1$, Monte-Carlo permutations, N= 999, plots permuted using cyclic shifts) (Appendix C). Individual environmental variables found to explain significant variance in the chironomid assemblage were retained in each environmental category; variables with the highest variance inflation factor (VIF) were sequentially removed until all VIFs < 10 (Quinlan et al. 2003). The remaining variables were used in variance partitioning in order to evaluate the relationships between the three explanatory variable categories (water quality, climate, and land use) and changes in chironomid assemblage compositions in the central basin of Lake Erie (ter Braak 1988; Borcard et al. 1992). Since CANOCO produces a biased canonical R^2 (Peres-Neto et al. 2012), R 3.4.3 (R Core Team 2014) and the vegan package (Oksanen et al. 2007) were used to compute the adjusted R^2.

Since few historical variables extended to the pre-1915 period, linear extrapolation was used to extend the historical range of some variables, specifically water quality; then three-way partition was performed independently on the chironomid time-series for, post-1915, post-1950, and post-1970 time periods. This approach permitted the identification of how the relative importance of categorical variables varied with the duration of the study. Finally, the relationships between historical and sedimentary variables such as percent organic C and total head capsules (HC g^{-1} dry weight) explored using a series of Pearson correlation tests.

Results

Historical data

Most climatic variables were highly variable during the last 60 years (Fig. 3.2-3.4). For example, total annual net basin supply ($m^3\ s^{-1}$) into Lake Erie was characterized by high interannual variation. Total annual precipitation and evaporation ($mm\ yr^{-1}$) were also highly variable, with low evaporation rates occurring during the wetter years (e.g. 1973-1982) and high evaporation during drier years (e.g. early 1960s and 1987-2003). Thus, the effect of evaporation accentuates rather than moderates the extreme effects of variation in precipitation. Since wet and dry years do not alternate, but occur in a grouped pattern, large periodic variations in annual average lake level are observed (Fig. 3.3). Despite high interannual variability in mean air temperatures, between 1950 and 2011 there has been an average increase of 0.8°C and 0.3°C in air temperature for spring and winter, respectively. Additionally, since the 1980s there have been more frequent occurrences of mean winter air temperature >0°C, which coincides with increased periods of low percent ice cover over Lake Erie (Fig. 3.4).

The historical record indicated that substantial changes occurred in the land use category variables (Fig. 3.5-3.8). While human population in the Lake Erie watershed has been increasing since the beginning of the record (1850s), dramatic increases in population began to occur in 1910s with the greatest increases occurring in 1935-1970, with highest growth occurring in the western watershed (Fig. 3.5). Since 1850-2011, human population increased by approximately 1400% and 870% in the western and entire Lake Erie watershed. Agricultural activities increased rapidly since the 1850s with peak agricultural land cover occurring between 1890s and 1910, especially within the western watershed, then steadily declined thereafter (Fig. 3.6). Inverse trends were observed in forest cover (acres), with a rapid decline occurring between 1850-1910, with a subsequent gradual increase (Fig. 3.7). Burns (1985) and Hatcher (1971) described the 1850s-1900s as a period of rapid population growth which led to

dramatic ecological alterations, including drainage of wetlands, deforestation, rapid agricultural growth and development.

The total annual TP loads into Lake Erie have been steadily declining since the late 1960s (Fig. 3.8). TP loads were high in 1967-1974 with an average of 22,799 MTA (range 27,437-18,077), but have declined thereafter with the introduction of P abatement programs and a TP load target of 11,000 MTA (GLWQA 1972); an average of 10,516 MTA (range 7,342-14,519 MTA) between 1980-1990, 9,699 MTA (range 5,963-16,333 MTA) between 1991-2000, and 8,902 (range 5,839-11,946) between 2001-2011 (Fig. 3.8). Change-point analysis conducted by Maccoux et al. (2016) suggested that a breakpoint in TP load declines occurred in 1987. Two-segmented piecewise regression with 1987 as the breakpoint showed that prior to this time, TP loads have declined at a significant ($R^2 = 0.814$, $p < 0.001$) rate of 5.3% per year, while after 1987, TP load declined at a non-significant ($R^2 = 0.0003$, $p = 0.78$) rate of 0.1% per year (Fig. 3.8).

According to data from Scavia et al. (2014) and Maccoux et al. (2016), Lake Erie continues to receive the majority (~60%) of the annual TP loads into the western basin via the Detroit River, Maumee River, and other western tributaries. TP inputs into the central and eastern basins account for approximately 28% and 12% of the total TP loads, respectively (Maccoux et al. 2016). Furthermore, Maccoux et al. (2016) noted that nonpoint source TP loading dominated the total annual TP loads, contributing an average of 71% of the TP loads for 2003-2013, while point sources averaged only 5% for the same time period. However, TP loading data suggested an 80% reduction in point source TP loads from 1974-1982, while during the 1980s until the late 2000s, there has been a much slower decline in point source TP loads (Maccoux et al. 2016).

April and August [TP] (μm P L^{-1}) in the central basin also showed high interannual variability, with April [TP] generally greater than August [TP] (Fig. 3.9). Trends in central basin [TP] for April and

August were closely related to total annual TP loads into Lake Erie, which was to be expected. August [TP] showed a decreasing trend between 1970-2011, while April [TP] decreased between the 1970s and early 1990s followed by a slight general increasing trend thereafter. According to Annex 4 of the GLWQA 2012, target [TP] for the central basin were set for 10 µm P L^{-1}. However, in the last decade average April [TP] were 14.3 µm P L^{-1}, and generally, between 1991-2011 April [TP] were >10 µm P L^{-1} (Fig. 3.9). Although, August [TP] in the central basin were <10 µm P L^{-1} between 1984-2011, with an average of 7.1 µm P L^{-1} in the last decade (Fig. 3.9). A relationship between April [TP] and spring net basin supply showed a significant, weak but positive relationship ($r = 0.397$, $p = 0.023$; Fig. 3.10).

April and August [TIN] (µg N L^{-1}) in the central basin varied unpredictably from year to year (Fig. 3.11). Generally, on average August [TP] were lower than April [TP]. The average April and August [TIN] for the last decade were at their lowest on record, 165 µg N L^{-1} and 142 µg N L^{-1}, respectively. While between 1983-1999, April and August [TIN] were 224 µg N L^{-1} and 203 µg N L^{-1}, respectively.

Standardized end-of-summer DO showed very little change since the mid-1960s, and generally, hypoxic (< 4 mg O_2 L^{-1}) to anoxic (< 1 mg O_2 L^{-1}) conditions persisted in the central basin, based on DO measurements 1 m above bottom sediment (Fig. 3.12). Between 1966-2011, this stratum in the central basin was hypoxic 65% of the time, and 65% of these occurrences were anoxic. However, there was a notable increase in hypolimnetic DO in 1995, which is consistent with results from Burns et al. (2005). An analysis of oxygen depletion rates in the central basin of Lake Erie by Rosa and Burns (1987) indicated that hypolimnetic DO depletion rates had increased between 1929-1980. Burns et al. (2005) and Zhou et al. (2013) indicated there were cyclical trends in hypolimnetic anoxic extent between 1983-2002. However, these studies showed that some degree of anoxia has persisted in the central basin since the 1980s, especially in the central basin sediment core location.

Variance partitioning

Some missing values within the TP, TIN and DO time series were interpolated in order to complete the available record and all analyses were performed on explanatory variables that were averaged over the sediment interval time period. Variance partitioning analysis was attempted for the post-1920 time period, however, extrapolation of climatic, water quality and land use variables by 30-50 years from the earliest available record would have underestimated the true historical variance within the explanatory categories and are not presented here or discussed further. Instead, variance partitioning analysis was conducted on post-1915, post-1950, and post-1970 for historical variables which span that time period. This approach permitted the identification of the relative importance of some explanatory variables through time and allowed us to forgo all long-term extrapolations.

A series of singly constrained RDAs revealed that historical changes in some climate and land use explanatory variables explained significant ($p < 0.1$) amounts of variance in the subfossil chironomid assemblage, however, water quality variables did not and, as a result, this entire explanatory variable group was removed from further analysis. In addition, no explanatory variable with the earliest record in the 1970s explained significant amounts of variance in the chironomid assemblage. As a result, only post-1915 and post-1950 data sets will be discussed hereafter.

For the post-1915 record, a series of singly constrained RDAs revealed a total of five land use variables that explained a significant amount of variance in the chironomid assemblage (western watershed population, entire watershed population, western watershed agricultural land cover, entire watershed agricultural land cover, and entire watershed forest cover). However, all five variables had high variance inflation factors (VIF > 10). For the same time record, six climatic variables were shown to significantly explain variance in the chironomid assemblage (precipitation over land in August,

precipitation over land in the summer, runoff in June, runoff in July, runoff in August, and runoff in the summer). In contrast to land use variables, only June and summer runoff had a VIF > 10.

During the post-1950 record, singly constrained RDAs showed the same five land use variables explained significant amounts of variance in chironomid assemblage composition, similarly, all five variables were collinear (VIF > 10). In the same time record, six climatic variables significantly explained variance in chironomid composition (minimum March temperature, average March temperature, April MSWT, March MSWT, June MSWT, and precipitation over land in August), all of which had VIF > 10. Following sequential removal of collinear historical variables (VIF > 10), chironomid assemblages were significantly correlated with only seven and four variables for the post-1915 and post-1950 data sets, respectively. The post-1915 and post-1950 climatic and land use datasets explained 39% and 20% of variation in the chironomid assemblage, respectively (Fig. 3.13); of which, significant amounts of variation have been explained by a very small subset of the original 169 historical variables (Table 3.2).

Land use (L) activities, independent of climate, are generally the most important explanatory category regardless of the duration of the study record, explaining 16.5% and 13.5% of the chironomid variation in the post-1915 and post-1950 records, respectively. While climate (C), independent of land use activities, explained roughly 4% of the variance in the chironomid assemblage in both records. The combined effects of land use activities and climate (CL) explained roughly 18% and 2.5% for the post-1915 and post-1950 records, respectively.

Drivers of change in sedimentary organic carbon and total head capsules

The relationship between historic and some stratigraphic sedimentary core variables that were not examined in variance partitioning analysis, such as percent organic carbon and total head capsules (HC g^{-1} dry weight) were explored using a series of Pearson correlation tests. All correlation tests were conducted using the earliest historic records available.

Percent organic C content of each sedimentary interval was obtained using loss-on-ignition (LOI) analysis (Chapter 2). There was a significant relationship between sedimentary organic C content, April TP and TIN:TP ($r = 0.484$, $p = 0.049$; and $r = -0.598$, $p = 0.011$) (Fig. 3.14 a, b). In addition, there was a strong positive relationship between organic C and spring net basin supply ($r = 0.567$, $p = 0.011$) (Fig. 3.14c). However, there were no statistically significant relationships between organic C and DO ($r = -0.074$, $p = 0.778$).Total head capsules (HC g^{-1} dry weight) had a significant positive relationship with August TIN:TP, maximum June temperature, and water level ($r = 0.655$, $p < 0.001$; $r = 0.440$, $p = 0.019$; and $r = 0.542$, $p = 0.003$) (Fig 3.15).

Discussion

Historical changes in Lake Erie and its watershed

Although Lake Erie has been historically productive (Chapter 2; Harris and Vollenweider 1982; Schelske et al. 1986; Stoermer et al. 1996), a diatom-based paleolimnological analysis by Sgro and Reavie (2017) indicated that Lake Erie was more eutrophic between 1930-1980. This time period was also marked by a substantial increase in oxygen depletion rates and hypoxic extent (Herdendorf 1980; Rosa and Burns 1987). These findings are consistent with changes in the chironomid assemblages from the central basin core, as was indicated by a transition point in the mid-1950s (Chapter 2). However, monitoring DO data do not extend to pre-1950s and the entire hypolimnetic DO record in the central basin (Fig. 3.14) is based on monitoring stations within the deepest part of the basin and measurements approximately 1 m above the sediment surface.

Changes in primary productivity and hypolimnetic DO levels have been attributed largely to increasing human activities in the western Lake Erie watershed since settlement and the associated increase in P loadings. Stoermer et al. 1987 and Sgro and Reavie 2017 indicated that the major turning point for Lake Erie occurred in the 1930s at which point it began to transition to a more eutrophic state,

these observations are consistent with rapid population increase in the Lake Erie watershed (Fig 3.5) and a point in time when agricultural land cover was at its maximum (approximately 15,000,000 acres; Fig. 3.6). These ecosystem changes are consistent with the disappearance of oxic-type *Heterotrissocladius* by the 1930s (Chapter 2).

Following P abatement programs set by the GLWQA 1972, TP loads have steadily declined from an average of 22,799 MTA (range 27,437-18,077 MTA) between 1967-1974 to 8,902 MTA (range 5,839-11,946 MTA) between 2001-2011 (Fig. 3.8) which corresponded to a decrease in water column TP concentrations (Fig 3.9).Makarewicz and Bertram (1993) described a shift in diatom composition from eutrophic to mesotrophic species for the 1970 to mid-1980s time period and attributed these changes to declines in TP. However, diatom-based paleolimnological analysis by Sgro and Reavie (2017) showed that the recovery in water quality during that period was only modest, as eutrophic indicators persisted. Furthermore, the shift to more mesotrophic diatom species, such as *Asterionella formosa* and *Aulacoseira islandica*, observed by Makarewicz and Bertram (1993) may have been due to changes in available silica rather than improvements in water column TP (Teubner and Dokulil 2002; Sgro and Reavie 2017). These observations are consistent with results from the central basin chironomid stratigraphy, as the 1980s period was marked by an increase in anoxia-tolerant *C. anthracinus* taxon with no recovery in oxic-type taxa and organic C content remained relatively the same between 1950s-1980s (Chapter 2). In addition, while there was a slight improvement in hypolimnetic DO in the early 1980s and 1990s, as demonstrated by a decrease in DO depletion rates and hypoxic extent (Burns et al. 2005; Zhou et al. 2013), the end-of-summer hypolimnetic DO levels in the central basin have generally remained hypoxic (< 4 mg O_2 L^{-1}) (Fig. 3.12) and the deepest portion of the central basin continues to experience anoxic conditions (Burns et al. 2005; Zhou et al. 2013; Zhou et al. 2015). Thus, while P abatement programs may have reduced summer algal blooms only until the mid-1990s, as was demonstrated by the sedimentary organic C record and the shift towards anoxia-tolerant *Chironomus*

spp (Chapter 2), their effect on reducing total phytoplankton biomass and restoring central basin hypolimnetic DO have been marginal.

The nature of a lake is as dependent on the prevailing climate and weather as it is on its geology, bathymetry, and nutrient supply. As demonstrated in Figure 3.2 and 3.4, both temperature and hydraulic balance of Lake Erie have shown a considerable amount of interannual variability. While most climatic variables remained relatively the same since the 1950s, there has been an increasing number of years of low maximum ice cover (< 50%) over the last two decades (1990-2011) compared to 1970-1990 time period (Fig. 3.4). These periods of low ice cover generally corresponded to years with mean winter air temperatures of approximately 0^{o}C and warmer average spring air temperatures. Coincidentally, some years with severe end-of-summer DO depletion in the central basin (< 2 mg O_2 L^{-1}) occurred during years with low ice cover years.

Phytoplankton surveys conducted by Twiss et al. (2012) and Reavie et al. (2015) demonstrated that winter-spring phytoplankton greatly exceeded summer phytoplankton by biovolume, which suggests that central basin hypolimnetic DO depletion may be driven by decomposition of these diatom blooms rather than summer algal and cyanophyte blooms. Thus, declines in maximum percent ice cover indicate longer ice-free periods (Reavie et al. 2017) which would lead to changes in the duration and extent of open water, light availability, particulate (and nutrient) resuspension, mixing and duration of stratification (Kleeberg et al. 2013; Beall et al. 2016). Such changes are likely to alter phytoplankton community composition by allowing summer populations to begin earlier and persist longer. Additionally, declines in ice cover in Lake Erie have been shown to result in a shift from filamentous diatoms to smaller sized cells and decreased phytoplankton biovolume (Beall et al. 2016) which might also explain the declines in total phytoplankton observed by Makarewicz and Bertram (1993).

As the hypolimnion in the central basin warms and the lake stratifies in the summer, bacterial decomposition of exported diatom biomass accelerates and depletes hypolimnetic DO. However, a prediction that lower phytoplankton biomass during low ice cover years would lessen the extent and magnitude of hypoxia in the central basin is not supported by the available data (Fig. 3.12). Instead, Zhou et al. (2013) and (2015), demonstrated that extensive late summer hypoxia in the central basin followed 1998, 2002, and 2012 low ice years. While winter diatom production can be an important driver of end-of-summer hypoxia (Wilhelm et al. 2014), other factors such as length of stratification period, hypolimnetic volume, temperature, and hydrology contribute to the formation of hypoxia (Zhou et al. 2015).

Identifying mechanisms that regulate changes in chironomid communities

Variance partitioning results suggest that the analysis was highly sensitive to the length of the historical data. For example, historical variables that explained significant amounts of variance in chironomid assemblages for the post-1915 and post-1950 periods were unable to explain significant amounts of variation in the post-1970 time period. In addition, the post-1915 record explained nearly double the amount of chironomid assemblage variation when compared to the post-1950 record (Fig 3.13). This suggested that the record length of the historical variables was an important factor at explaining variation in chironomid communities. Consequently, due to the relatively short record of water quality parameters, which did not extend to the pre-1930s period where the greatest changes in water quality have occurred (Stoermer et al. 1996; Sgro and Reavie 2017), these environmental variables appeared to be nonsignificant. However, lack of significance of water quality variables does not indicate that changes in water quality parameters had no effect on chironomid communities, instead these parameters have likely failed to explain a significant amount of variation in the chironomid assemblages within the temporal constraints of this data set.

Variance partitioning analysis identified land use as the strongest driver of chironomid composition change in the central basin of Lake Erie (Fig 3.11). Population and agricultural land cover in the western watershed were shown to have a significant influence on subfossil chironomid assemblages for the post-1915 and post-1950 time periods (16.5% and 13.5%, respectively) (Table 3.2; Fig 3.13). These changes are consistent with historical changes in population and agricultural land cover (Fig 3.5, 3.6). In addition, prior to European settlement in the south shores of the western Lake Erie watershed, an extensive wetland complex (called the Great Black Swamp), which covered nearly 4,000 km^2 and extended 160 km inland, covered the Maumee River inlet into Lake Erie (Hatcher 1971). Drainage of this wetland complex began in the 1830s and by the 1900s was completely converted to farmland (Burns 1985). As a result, the nutrient and sediment filtration benefits of this wetland were completely lost.

Climate was also a significant driver of change in chironomid assemblages which explained 3.8% of the variation for both post-1915 and post-1950 time periods. However, the climatic drivers differed for these two time periods (Table 2). While summer precipitation and runoff were shown to have a significant influence on chironomid assemblages in the post-1915 period, there was a shift towards early spring temperatures in the post-1950 period. These results indicate a transition point between nutrient inputs and climate change as the primary drivers of profundal chironomid communities and hypolimnetic hypoxia. Interestingly, the interaction of climate and land use for the post-1915 period had the greatest influence (18.3%) on chironomid communities. These observations likely indicate that increasing population and high agricultural land cover compounded with summer rainfall and runoff led to high nutrient inputs resulting in the observed water quality changes for that period. The shift in climatic variables in the post-1950 period towards earlier spring warming and a decreased interaction between land use and climate variables (2.5%), supports this hypothesis. In addition, this shift occurs during a period where TP loadings into the lake started to decline as a result of P abatement programs (GLWQA 1972).

Although 169 environmental variables were examined, a relatively small proportion of variance was explained by the post-1915, post-1950, and post-1970 partitions of the chironomid assemblage corresponding to 38.6%, 19.7%, and 0%, respectively. This is likely due to (1) low sample size, as many sedimentary intervals had low head capsule counts and adjacent samples were combined (Chapter 2), resulting in 23, 19, and 17 sedimentary intervals representing the post-1950, and post-1970 time periods; (2) sensitivity of variance partitioning analysis to length of environmental record as few historical records extended pre-1915, especially water quality variables with their earliest records in 1970, while oxic-type taxa began to disappear in 1925 (Chapter 2); and (3) fluctuations in chironomid community composition may have been regulated by factors not included in this analysis (e.g. contamination, measured avgVWHO, chlorophyll a, dreissenids, and fish stocks). For example, while establishment of dreissenid mussels in Lake Erie did not appear to have a direct impact on chironomid assemblages via the nearshore shunt (Chapter 2; Hecky et al. 2004), Li et al (2008) has shown that dreissenids in Lake Simcoe have increased VWHO since their establishment in 1996, possibly by sequestering phytoplankton and organic material away from the hypolimnion (Kim et al. 2015).

Drivers of change in sedimentary organic carbon and total head capsules

In order to obtain a better understanding of the environmental variables that were responsible for driving water quality changes observed over the past century, a series of Pearson correlation tests were used to examine the relationship between several stratigraphic sedimentary core variables that were not examined in variance partitioning analysis, percent organic carbon and total head capsules (HC g^{-1} dry weight).

While there was a significant relationship between sedimentary organic C content, April TP, TIN:TP, and spring net basin supply (Fig. 3.14). Which suggests that the observed increase in organic C content in the 1930s (Chapter 2) is the result of increased nutrient inputs and the associated increases in

primary productivity which occurred during that time (Harris and Vollenweider 1982; Stoermer et al. 1996; Allinger and Reavie 2013; Sgro and Reavie 2017). However, while hypolimnetic DO levels did not show significant relationships with sedimentary organic C content, biological decomposition rates would have decreased as a result of anoxic conditions and resulted in increased preservation of organic C. Additionally, lack of statistical significance between organic C and DO is likely due to temporal constraints of the DO record which did not extend to pre-1965 and remained generally ≤ 4 mg O L^{-1} throughout the record (Fig. 3.12). Furthermore, since sedimentary organic C was positively correlated with April TP while having a negative correlation with April TIN:TP, these results provide further evidence that watershed management efforts should focus resources to control of P inputs rather than dual nutrient (P and N) management strategies. However, caution must be taken to consider the effect of P reduction on diatom abundances as they comprise a greater phytoplankton biomass than summer algal blooms (Reavie et al. 2015; Reavie et al. 2017).

Total chironomid head capsule counts (per g dried sediment) had a significant positive relationship with August TIN:TP, maximum June temperature, and water level (Fig 3.15). The observed positive relationship between total head capsule counts and August TIN:TP was an interesting result, as high TN:TP conditions favour non-cyanophyte phytoplankton (Smith 1983; Schindler et al. 2008) which may result in a greater availability of higher quality food sources, thus, supporting a greater chironomid population. While, maximum June temperatures are likely to represent increased primary productivity and hypolimnetic temperature, thus increasing hypolimnetic DO depletion rates. As a result of anoxic conditions in the hypolimnion we expect that there may be an increase in preservation due to decreased decomposition rates.

Frey (1988) suggested that changes in lake level may affect interpretations of chironomid subfossil record through changes in deposition of littoral taxa into deepwater sediments. However, a lack of substantial littoral taxa from the central basin stratigraphy indicates that this is not the case.

Instead, it is more likely that the relationship between total head capsule counts and water level are due to changes in hypolimnetic depth. Such that, increased lake levels would result in a thicker hypolimnion corresponding to a greater amount of hypolimnetic oxygen, consistent with observations by Quinlan and Smol (2002).

Conclusion

It is clear from this investigation that there have been significant changes in chironomid communities in Lake Erie over the last century. Overall, the long-term trends in water quality within the central basin of Lake Erie and their drivers are consistent with results from a diatom-based paleolimnological analysis by Sgro and Reavie (2017). Specifically, land use changes, such as increased population and agricultural land cover, in the western watershed have had the strongest impact at driving changes in chironomid assemblages. Additionally, since the 1950s changes in early spring temperatures have been shown to play an important role at driving changes in chironomid assemblages, possibly through increased period of productivity and duration of thermal stratification resulting in increased hypolimnetic DO depletion and anoxic extent. With current climate trends, it is likely that warming winter and spring temperatures are going to play even more important roles in central basin hypolimnetic DO dynamics in the future.

As indicated in Chapter 2, there were strong qualitative indications that hypolimnetic DO conditions have been deteriorating as early as the 1930s with a statistically significant transition point occurring in the mid-1950s characterized by decline of hypoxic-tolerant *Procladius*, disappearance of oxic-type *Heterotrissocladius* and *Micropsectra*, and the increase of anoxia-tolerant *Chironomus* spp. However, due to possible analogue issue, the training set does not relate well to the central basin core, as was demonstrated by (1) goodness-of-fit test; (2) the weak correlation between inferred avgVWHO and PCA axis 1; and (3) the low fraction of variance explained by inferred avgVWHO, represented as the

fraction of maximum explainable variance ($\lambda_{RDA}/\lambda_{PCA}$) (Chapter 2). As a result, accurate quantitative inferences regarding changes in hypolimnetic DO over the last century were not possible. However, qualitative chironomid-based inference indicated no change in hypolimnetic DO since enactment of the 1972 GLWQA, which are in agreement with diatom-based paleolimnological analyses by Sgro and Reavie (2017) which indicated little change in the lake's trophic status.

While recently recommended reduction in TP load targets for Lake Erie (IJC 2015) are a first step towards good lake management of summer nuisance algae and cyanophyte blooms, it may have little effect on improving hypolimnetic DO conditions. Thus, changes need to be made to socio-economic structures on a watershed-wide scale to restore Lake Erie water quality and hypolimnetic DO in the central basin.

References

Allinger LE, Reavie ED. 2013. The ecological history of Lake Erie as recorded by the phytoplankton community. J Great Lakes Res. 39:365–382.

Armitage PD, Pinder LC, Cranston P. 2012. The Chironomidae: biology and ecology of non-biting midges. Springer Science & Business Media.

Auer MT, Tomlinson LM, Higgins SN, Malkin SY, Howell ET, Bootsma HA. 2010. Great Lakes Cladophora in the 21st century: same algae-different ecosystem. J Great Lakes Res. 36:248–255.

Bazzanti M, Seminara M, Baldoni S. 1998. Assessing hypolimnetic stress in a monomictic, eutrophic lake using profundal sediment and macrobenthic characteristics. J Freshw Ecol. 13:405–412.

Beall BFN, Twiss MR, Smith DE, Oyserman BO, Rozmarynowycz MJ, Binding CE, Bourbonniere RA, Bullerjahn GS, Palmer ME, Reavie ED, et al. 2016. Ice cover extent drives phytoplankton and bacterial community structure in a large north-temperate lake: implications for a warming climate. Environ Microbiol. 18:1704–1719.

Bertram PE. 1993. Total Phosphorus and Dissolved Oxygen Trends in the Central Basin of Lake Erie, 1970–1991. J Great Lakes Res. 19:224–236.

Birks HJB, Lotter AF, Juggins S, Smol JP. 2012. Tracking Environmental Change Using Lake Sediments: Data Handling and Numerical Techniques. Vol 5. Springer Science & Business Media.

Borcard D, Legendre P, Drapeau P. 1992. Partialling out the Spatial Component of Ecological Variation. Ecology. 73:1045–1055.

ter Braak CJF. 1988. Partial canonical correspondence analysis. In: Classification and related methods of data analysis: proceedings of the first conference of the International Federation of Classification Societies (IFCS), Technical University of Aachen, FRG, 29 June-1 July 1987. North-Holland. p. 551–558.

ter Braak CJF, Smilauer P. 2002. Canoco for Windows version 4.5. Biometris–Plant Res Int Wageningen.

Brodersen KP, Quinlan R. 2006. Midges as palaeoindicators of lake productivity, eutrophication and hypolimnetic oxygen. Quat Sci Rev. 25:1995–2012.

Brundin L. 1951. The relation of O2-microstratification at the mud surface to the ecology of the profundal bottom fauna. Rep Inst Freshwat Res Drottningholm. 32:32–42.

Burns NM. 1976. Temperature, Oxygen, and Nutrient Distribution Patterns in Lake Erie, 1970. J Fish Res Board Can. 33:485-511.

Burns NM. 1985. Erie: The Lake That Survived. Rowman & Allanheld.

Burns NM, Rockwell DC, Bertram PE, Dolan DM, Ciborowski JJH. 2005. Trends in temperature, secchi depth, and dissolved oxygen depletion rates in the central basin of Lake Erie, 1983–2002. J Great Lakes Res. 31:35–49.

Chapra SC. 1977. Total phosphorus model for the Great Lakes. J Environ Eng Div. 103:147–161.

Depew DC, Houben AJ, Guildford SJ, Hecky RE. 2011. Distribution of nuisance Cladophora in the lower Great Lakes: patterns with land use, near shore water quality and dreissenid abundance. J Great Lakes Res. 37:656–671.

Frey DG. 1988. Littoral and offshore communities of diatoms, cladocerans and dipterous larvae, and their interpretation in paleolimnology. J Paleolimnol. 1:179–191.

Hall RI, Leavitt PR, Quinlan R, Dixit AS, Smol JP. 1999. Effects of agriculture, urbanization, and climate on water quality in the northern Great Plains. Limnol Oceanogr. 44:739–756.

Harris GP, Vollenweider RA. 1982. Paleolimnological evidence of early eutrophication in Lake Erie. Can J Fish Aquat Sci. 39:618–626.

Hatcher HH. 1971. Lake Erie. Greenwood Press.

Herdendorf CE. 1980. Lake Erie nutrient control program: An assessment of its effectiveness in controlling lake eutrophication. Environmental Research Laboratory--Duluth, Office of Research and Development, US Environmental Protection Agency.

Hofmann W. 1988. The significance of chironomid analysis (Insecta: Diptera) for paleolimnological research. Palaeogeogr Palaeoclimatol Palaeoecol. 62:501–509.

International Joint Commission (IJC). 1983. Great Lakes Water Quality Agreement of 1978. Phosphorus Load Reduction Supplement of 1983.

International Joint Commission (IJC). 2015. Recommended Phosphorus Loading Targets for Lake Erie. Annex 4 Objectives and Targets Task Team Final Report to the Nutrients Annex Subcommittee (2015).

Juggins S. 2007. C2 user guide: Software for ecological and palaeoecological data analysis and visualization. Univ Newcastle, Newcastle upon Tyne, UK.:1–73.

Kim TY, North RL, Guildford SJ, Dillon P, Smith REH. 2015. Phytoplankton productivity and size composition in Lake Simcoe: the nearshore shunt and the importance of autumnal production. J Great Lakes Res. 41:1075–1086.

Kleeberg A, Freidank A, Jöhnk K. 2013. Effects of ice cover on sediment resuspension and phosphorus entrainment in shallow lakes: Combining in situ experiments and wind-wave modeling. Limnol Oceanogr. 58:1819–1833.

Li J, Lewis M, Michelle P, Winter J, Joelle Y, Stainsby E. 2018. Long-term changes in hypolimnetic dissolved oxygen in a large lake: Effects of 2 invasive mussels, eutrophication and climate change on Lake Simcoe, 1980-2012. J Great Lakes Res. (in press).

Ludsin SA, Kershner MW, Blocksom KA, Knight RL, Stein RA. 2001. Life After Death in Lake Erie: Nutrient Controls Drive Fish Species Richness , Rehabilitation. Ecol Appl. 11:731–746.

Maccoux MJ, Dove A, Backus SM, Dolan DM. 2016. Total and soluble reactive phosphorus loadings to Lake Erie: A detailed accounting by year, basin, country, and tributary. J Great Lakes Res. 42:1151–1165.

Makarewicz JC. 1987. Phytoplankton and Zooplankton in Lakes Erie, Huron and Michigan: 1984. United States Environmental Protection Agency. Technical report.

Makarewicz JC. 1991. Phytoplankton and Zooplankton Composition, Abundance and Distribution and Trophic Interactions: Offshore Region of Lakes Erie, Lake Huron and Lake Michigan, 1985. US Environmental Protection Agency, Great Lakes National Program Office.

Makarewicz JC, Bertram PE. 1993. Evidence for the Restoration of the Lake Erie Ecosystem. J Great Lakes Res. 19:197.

Michalak AM, Anderson EJ, Beletsky D, Boland S, Bosch NS, Bridgeman TB, Chaffin JD, Cho K, Confesor R, Daloglu I, et al. 2013. Record-setting algal bloom in Lake Erie caused by agricultural and meteorological trends consistent with expected future conditions. Proc Natl Acad Sci. 110:6448–6452.

Oksanen J, Kindt R, Legendre P, O'Hara B, Stevens MHH, Oksanen MJ, Suggests M. 2007. The vegan package. Community ecology package 10.

Peres-Neto PR, Legendre P, Dray S, Borcard D. 2012. Variation Partitioning of Species Data Matrices: Estimation and Comparison of Fractions. Ecology. 59:2614–2625.

De Pinto J V, Young TC, McIlroy LM. 1986. Great Lakes water quality improvement. Environ Sci Technol. 20:752–759.

Quinlan R, Paterson AM, Hall RI, Dillon PJ, Wilkinson AN, Cumming BF, Douglas MS V, Smol JP. 2003. A landscape approach to examining spatial patterns of limnological variables and long-term environmental change in a southern Canadian lake district. Freshw Biol. 48:1676–1697.

Quinlan R, Smol JP. 2001a. Chironomid-based inference models for estimating end-of-summer hypolimnetic oxygen from south-central Ontario shield lakes. Freshw Biol. 46:1529–1551.

Quinlan R, Smol JP. 2001b. Setting minimum head capsule abundance and taxa deletion criteria in chironomid-based inference models. J Paleolimnol. 26:327–342.

Quinlan R, Smol JP. 2002. Regional assessment of long-term hypolimnetic oxygen changes in Ontario (Canada) shield lakes using subfossil chironomids. J Paleolimnol. 27:249–260.

Rathke DE. 1982. Lake Erie intensive study 1978-1979. United States Environmental Protection Agency, Great Lakes National Program Office. Technical report.

Reavie ED, Cai M, Twiss MR, Carrick HJ, Davis TW, Johengen TH, Gossiaux D, Smith DE, Palladino D, Burtner A, et al. 2015. Winter-spring diatom production in Lake Erie is an important driver of summer hypoxia. J Great Lakes Res. 42:608–618.

Reavie ED, Sgro G V., Estepp LR, Bramburger AJ, Shaw Chraïbi VL, Pillsbury RW, Cai M, Stow CA, Dove A. 2017. Climate warming and changes in Cyclotella sensu lato in the Laurentian Great Lakes. Limnol Oceanogr. 62:768–783.

Rosa F, Burns NM. 1987. Lake Erie central basin oxygen depletion changes from 1929–1980. J Great Lakes Res. 13:684–696.

Rucinski DK, Depinto J V, Scavia D, Beletsky D. 2014. Modeling Lake Erie's hypoxia response to nutrient loads and physical variability. J Great Lakes Res. 40:151–161.

Sæther O a. 1979. Chironomid communities as water quality indicators. Holarct Ecol. 2:65–74.

Scavia D, David Allan J, Arend KK, Bartell S, Beletsky D, Bosch NS, Brandt SB, Briland RD, Daloğlu I, DePinto J V., et al. 2014. Assessing and addressing the re-eutrophication of Lake Erie: Central basin hypoxia. J Great Lakes Res. 40:226–246.

Schelske CL, Conley DJ, Stoermer EF, Newberry TL, Campbell CD. 1986. Biogenic silica and phosphorus accumulation in sediments as indices of eutrophication in the Laurentian Great Lakes. Hydrobiologia. 143:79–86.

Schelske CL, Stoermer EF, Kenney WF. 2006. Historic low-level phosphorus enrichment in the Great Lakes inferred from biogenic silica accumulation in sediments. Limnol Oceanogr. 51:728–748.

Schindler DW, Hecky RE, Findlay DL, Stainton MP, Parker BR, Paterson MJ, Beaty KG, Lyng M, Kasian SEM. 2008. Eutrophication of lakes cannot be controlled by reducing nitrogen input: Results of a 37-year whole-ecosystem experiment. Proc Natl Acad Sci. 105:11254–11258.

Sgro G V, Reavie ED. 2017. Lake Erie's ecological history reconstructed from the sedimentary record. J Great Lakes Res. 44:54-69.

Smith VH. 1983. Low nitrogen to phosphorus ratios favor dominance by blue-green algae in lake phytoplankton. Science. 221:669–671.

Sokal RR, Rohlf FJ. 1995. Biometry: the principles and practice of statistics in biological research. New York.

Stoermer EF, Emmert G, Julius ML, Schelske CL. 1996. Paleolimnologic evidence of rapid recent change in Lake Erie's trophic status. Can J Fish Aquat Sci. 53:1451–1458.

Stoermer EF, Kociolek JP, Schelske CL, Conley DJ. 1987. Quantitative analysis of siliceous microfossils in the sediments of Lake Erie's central basin. Diatom Res. 2:113–134.

Stumpf RP, Wynne TT, Baker DB, Fahnenstiel GL. 2012. Interannual variability of cyanobacterial blooms in Lake Erie. PLoS One. 7:1–11.

Team RC. 2014. R: A language and environment for statistical computing. Vienna, Austria: R Foundation for Statistical Computing; 2014.

Teubner K, Dokulil MT. 2002. Ecological stoichiometry of TN: TP: SRSi in freshwaters: nutrient ratios and seasonal shifts in phytoplankton assemblages. Arch für Hydrobiol. 154:625–646.

Twiss MR, McKay RML, Bourbonniere RA, Bullerjahn GS, Carrick HJ, Smith REH, Winter JG, D'souza NA, Furey PC, Lashaway AR, et al. 2012. Diatoms abound in ice-covered Lake Erie: An investigation of offshore winter limnology in Lake Erie over the period 2007 to 2010. J Great Lakes Res. 38:18–30.

Walker IR. 1987. Chironomidae (Diptera) in paleoecology. Quat Sci Rev. 6:29–40.

Warwick WF. 1980. Paleolimnology of the Bay of Quinte, Lake Ontario-2800 years of cultural-influence. Can Bull Fish Aquat Sci.:1–118.

Wilhelm SW, Lecleir GR, Bullerjahn GS, Mckay RM, Saxton MA, Twiss MR, Bourbonniere RA. 2014. Seasonal changes in microbial community structure and activity imply winter production is linked to summer hypoxia in a large lake. FEMS Microbiol Ecol. 87:475–485.

Wynne TT, Stumpf RP. 2015. Spatial and temporal patterns in the seasonal distribution of toxic cyanobacteria in western Lake Erie from 2002–2014. Toxins (Basel). 7:1649–1663.

Zhou Y, Michalak AM, Beletsky D, Rao YR, Richards RP. 2015. Record-breaking Lake Erie hypoxia during 2012 drought. Environ Sci Technol. 49:800–807.

Zhou Y, Obenour DR, Scavia D, Johengen TH, Michalak AM. 2013. Spatial and Temporal Trends in Lake Erie Hypoxia, 1987 − 2007. Environ Sci Technol. 47:899–905.

Figures and Tables

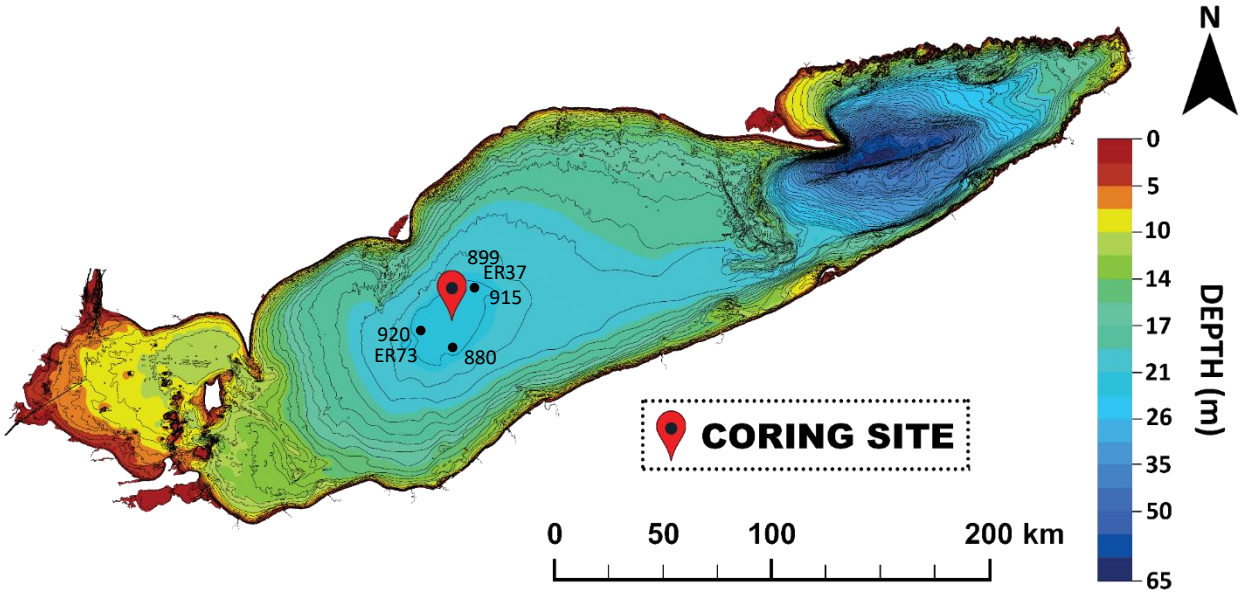

Figure 3.1: Central basin coring site and monitoring stations used. ER sites correspond to Environmental Protection Agency – Great Lakes Environmental Database (EPA-GLENDA) monitoring stations, while numbered sites corespond to Canadian Centre for Inland Waters (CCIW) monitoring stations.

Table 3.1: Explanatory variables included in historical dataset. Variables were grouped into one of three categories: water quality, climate, or land use. N – Number of variables included under variable name; TP – total phosphorus; TIN – total inorganic nitrogen; MSWT – mean surface water temperature; MTA – metric tonnes per annum

Variable Name	N	Record Start	Record End
Water Quality			
Hypolimnetic DO, mg O_2 L^{-1}*	1	1962	2011
TP loads, Apr, ug/L	1	1970	2014
TP loads, Aug, ug/L	1	1970	2014
TIN loads, Apr, ug/L	1	1970	2014
TIN loads, Aug, ug/L	1	1970	2014
TIN:TP, Apr, ug/L	1	1970	2014
TIN:TP, Aug, ug/L	1	1970	2014
Climate			
Mean max temperature, Annual, ^oC	1	1948	2011
Mean max temperature, Seasonal, ^oC	4	1948	2011
Mean max temperature, Monthly, ^oC	12	1948	2011
Mean min temperature, Annual, ^oC	1	1948	2011
Mean min temperature, Seasonal, ^oC	4	1948	2011
Mean min temperature, Monthly, ^oC	12	1948	2011
Mean temperature, Annual, ^oC	1	1948	2011
Mean temperature, Seasonal, ^oC	4	1948	2011
Mean temperature, Monthly, ^oC	12	1948	2011
MSWT, Annual, ^oC	1	1950	2011
MSWT, Seasonal, ^oC	4	1950	2011
MSWT, Monthly, ^oC	12	1950	2011
Precipitation over Lake, Annual, mm	1	1900	2015
Precipitation over Lake, Seasonal, mm	4	1900	2015
Precipitation over Lake, Monthly, mm	12	1900	2015
Precipitation over Land, Annual, mm	1	1882	2015
Precipitation over Land, Seasonal, mm	4	1882	2015
Precipitation over Land, Monthly, mm	12	1882	2015
Gross evaporation, Annual, mm	1	1950	2015
Gross evaporation, Seasonal, mm	4	1950	2015
Gross evaporation, Monthly, mm	12	1950	2015
Runoff, Annual, mm	1	1914	2015
Runoff, Seasonal, mm	4	1914	2015
Runoff, Monthly, mm	12	1914	2015
Net basin supply, m^3 L^{-1}	1	1950	2015
Net basin supply, m^3 L^{-1}	4	1950	2015
Net basin supply, m^3 L^{-1}	12	1950	2015
Maximum ice cover, Annual, %	1	1973	2017
Lake level anomaly, Annual, ft	1	1860	2015
Land Use			
TP loads, MTA	1	1967	2013
Western Lake Erie population	1	1810	2020
Western Lake Erie Agriculture (acres)	1	1850	2020
Western Lake Erie Forest (acres)	1	1788	2020
Lake Erie population	1	1800	2020
Lake Erie Agriculture (acres)	1	1850	2020
Lake Erie Forest (acres)	1	1780	2020

* End-of-summer DO, measured 1m above sediment, standardized to Sept 1st

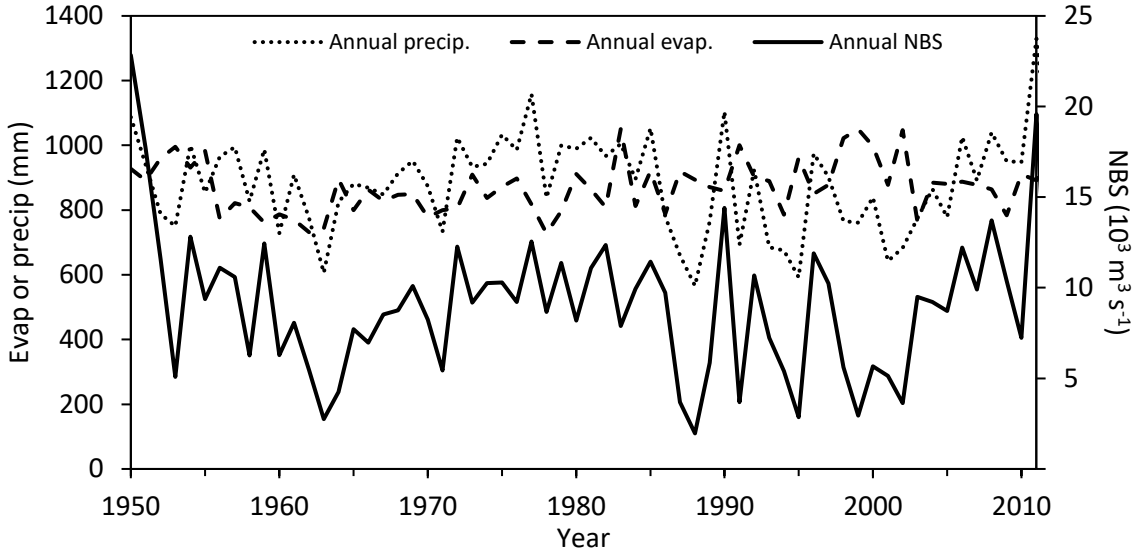

Figure 3.2: Hydrological balance. Total annual precipitation and evaporation (expressed in millimeters over lake); net basin supply (NBS) = precipitation over lake + runoff – evaporation (expressed as cubic meters per second).

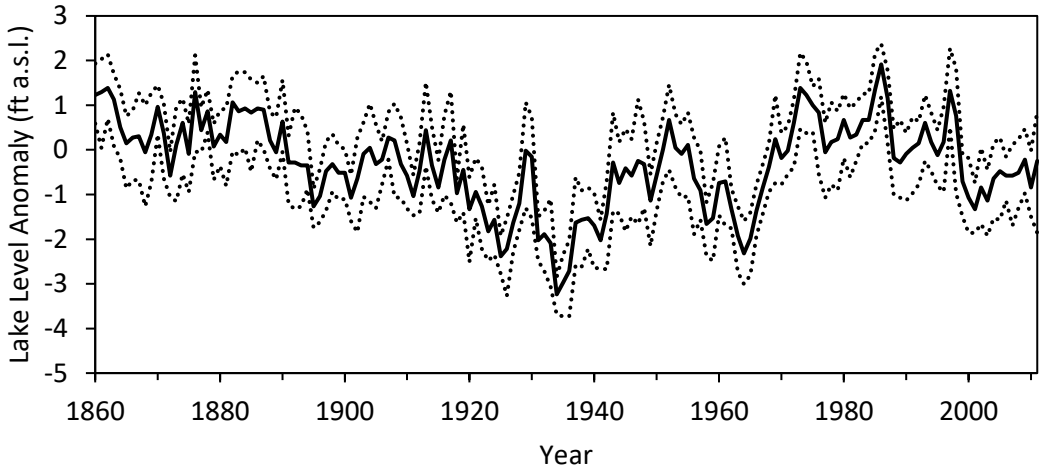

Figure 3.3: Lake Erie water level anomaly referenced to the 1981-2010 average baseline from the International Great Lakes Datum (1985), measured in feet above sea level (ft a.s.l.). Dotted lines represent upper and lower bounds.

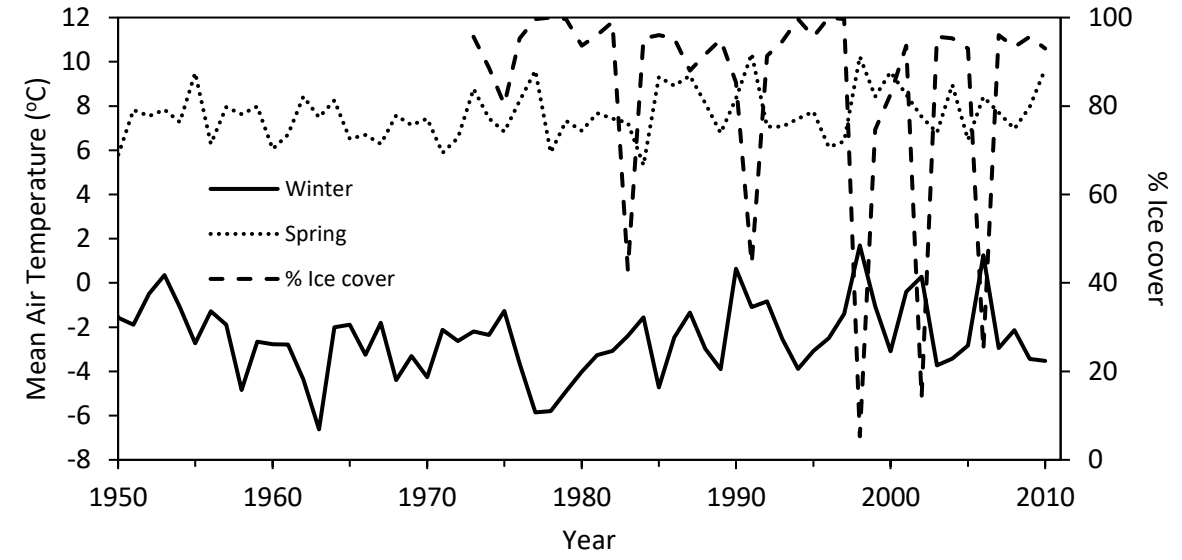

Figure 3.4: Mean spring and winter air temperature (°C) and percent ice cover

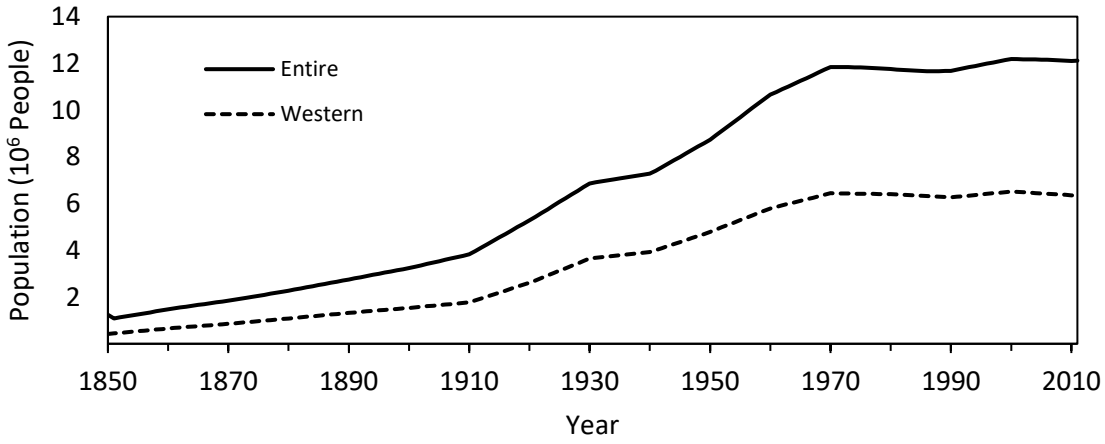

Figure 3.5: Human population in western and entire Lake Erie watersheds (data from Sgro and Reavie (2017)).

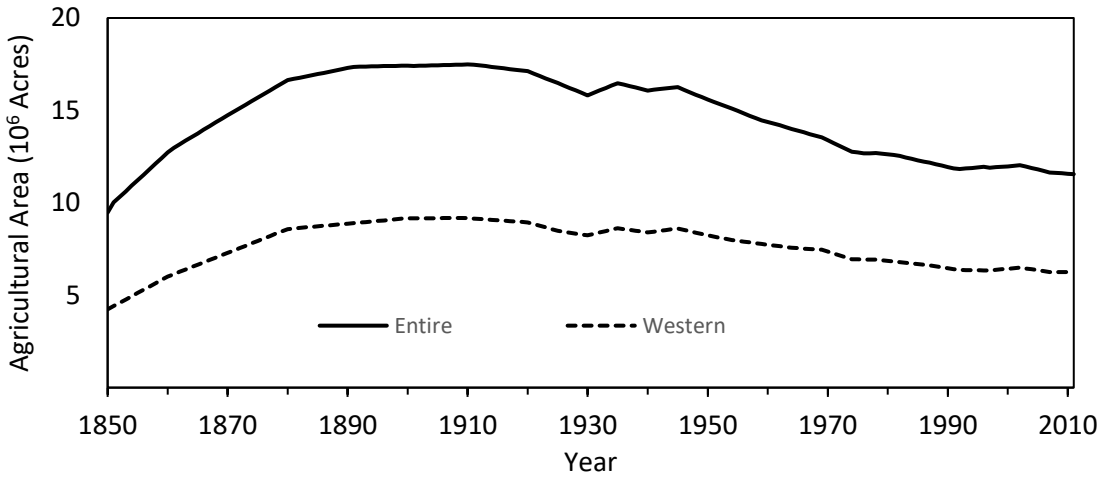

Figure 3.6: Agricultural land cover (acres) in western and entire Lake Erie watersheds (data from Sgro and Reavie (2017)).

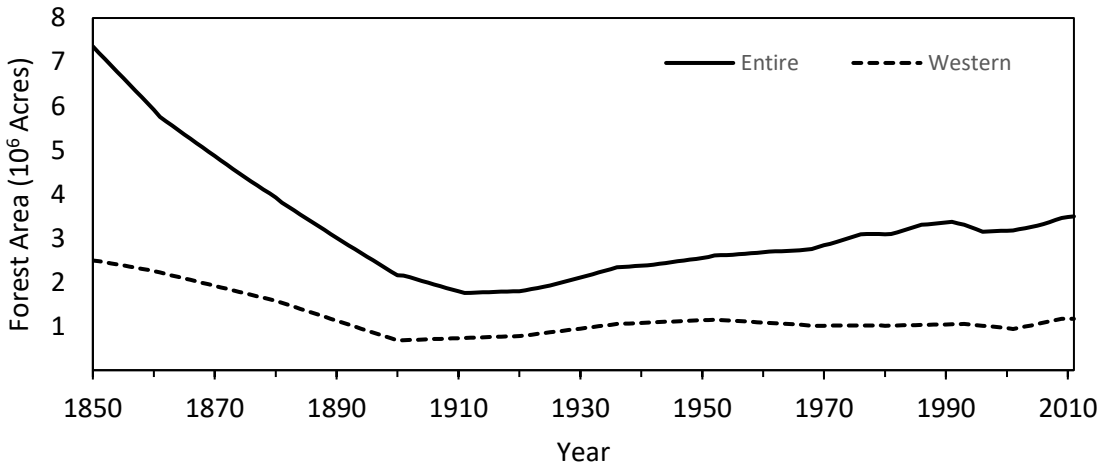

Figure 3.7: Forest land cover (acres) in western and entire Lake Erie watersheds (data from Sgro and Reavie (2017)).

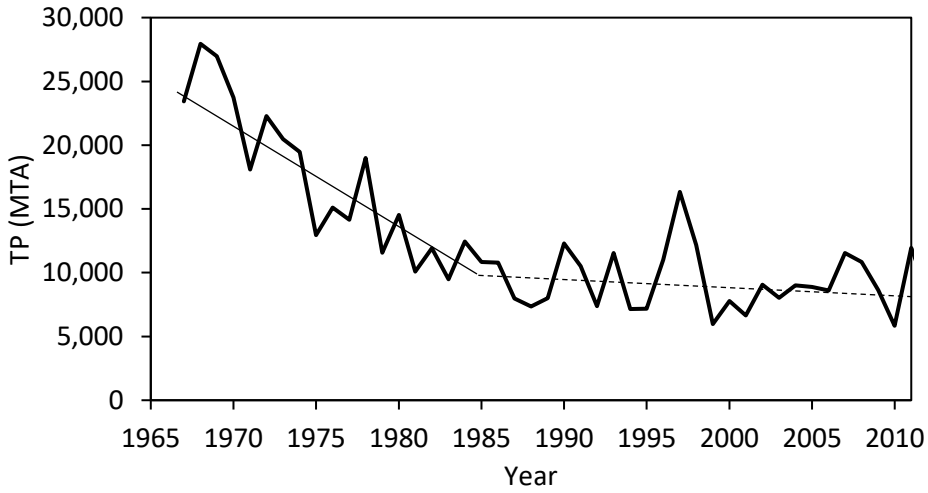

Figure 3.8: Total phosphorus (TP) loads into Lake Erie, measured in metric tonnes per annum (MTA). TP load data, breakpoint date (1987), and two-segment piecewise regression recreated from Maccoux et al. (2016). A significant decline is noted for 1967-1987 period (solid line; $R^2 = 0.814$, $p < 0.001$) rate of 5.3% per year; while during 1988-2011, TP load declined at a non-significant (dashed line; $R^2 = 0.0003$, $p = 0.98$) rate of 0.1% per year.

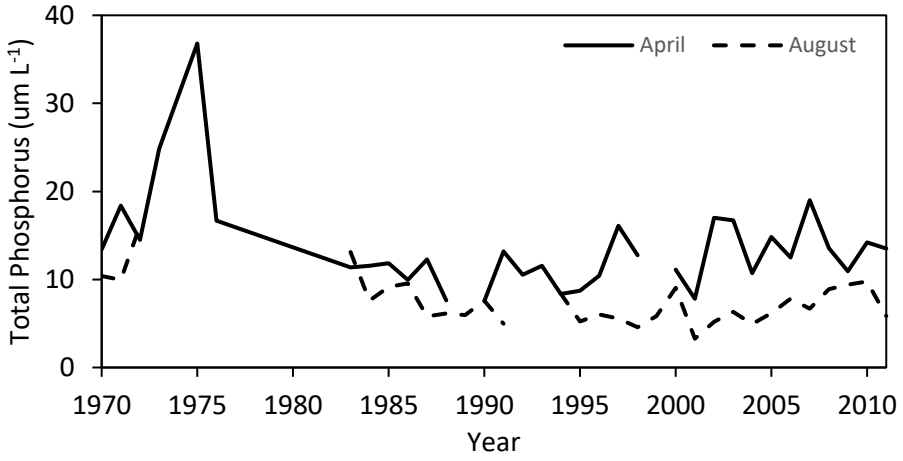

Figure 3.9: Water column total phosphorus (TP, µg L^{-1}) concentrations in the central basin for April and August.

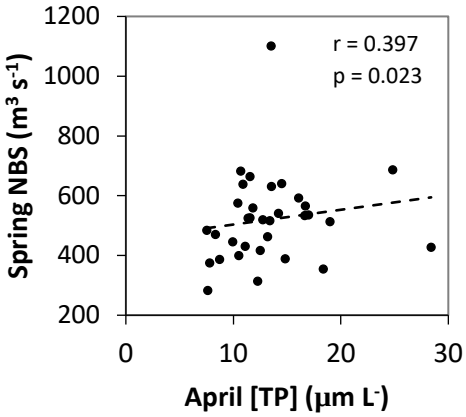

Figure 3.10: Relationship between spring net basin supply (NBS) and April TP concentrations.

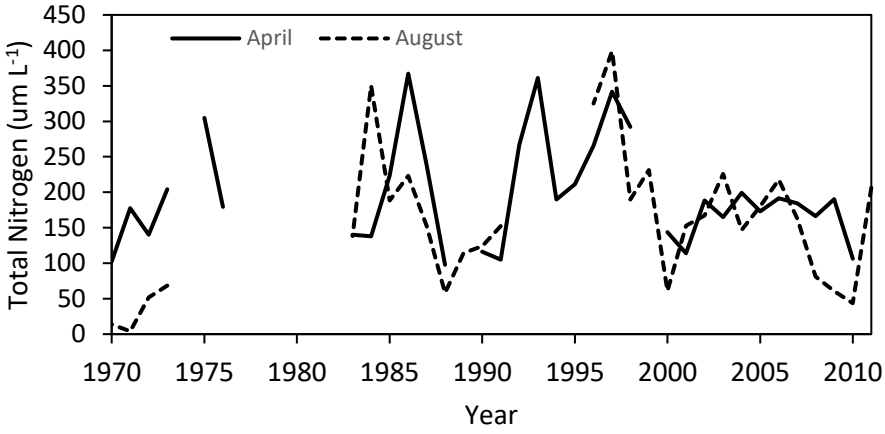

Figure 3.11: Total inorganic nitrogen (TIN, µg L^{-1}) concentrations in the central basin.

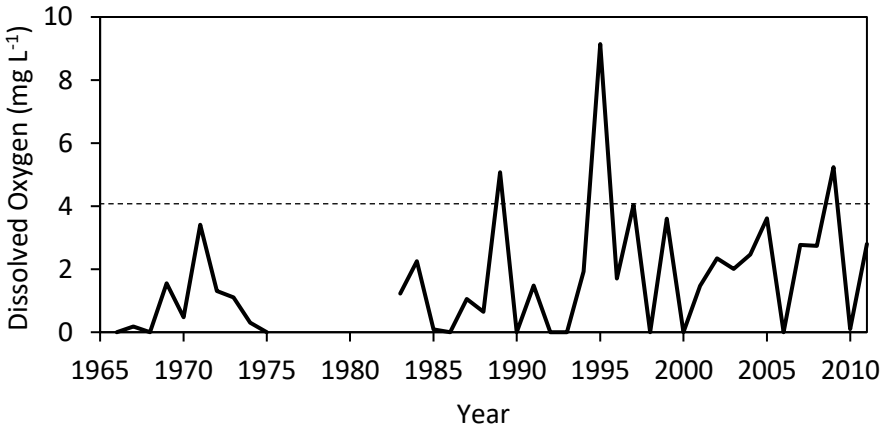

Figure 3.12: Trends in hypolimnetic dissolved oxygen (DO) within the central basin of Lake Erie. DO values represent end-of-summer (Sept 1) estimates 1m above sediment surface. Values below the dashed line represent hypoxic (<4 mg O_2 L^{-1}) to anoxic (<1 mg O_2 L^{-1}) conditions.

Table 3.2: Explanatory variables used in variance partitioning analyses for combination of time periods. Variables are listed according to the variable list categories: water quality, climate, or land use

Variable Category	post-1915	post-1950	post-1970
Water Quality (W)	-	-	None
Climate (C)	Precip over Land in August, Precip over land in the Summer Runoff in June Runoff in July Runoff in August	Mean Temp in March MSWT in April	None
Land Use (L)	Pop. western watershed Agriculture western watershed	Pop. western watershed Agriculture western watershed	None

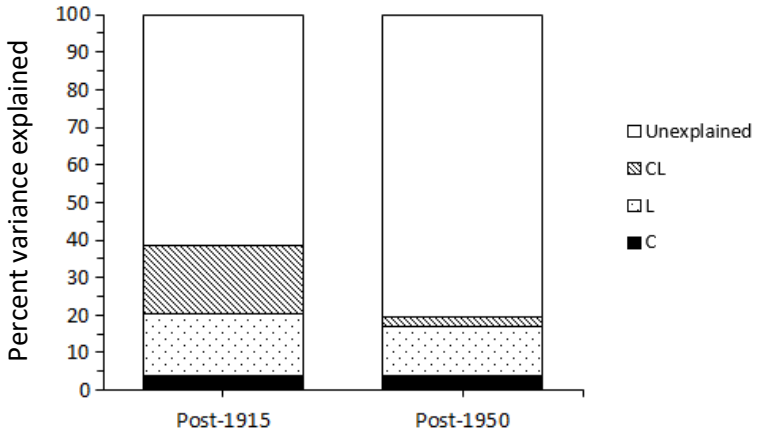

Figure 3.13: The effects of climate (C) and land use (L) on chironomid assemblages from the central basin core of Lake Erie as determined by variance partitioning analyses. Variance partitioning results for ca. 1915-2011 and 1950-2011.

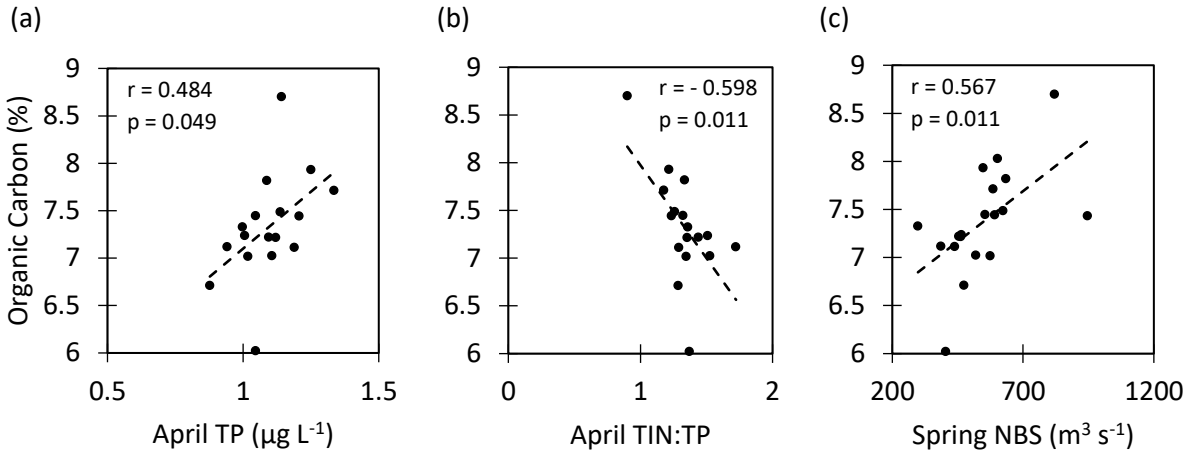

Figure 3.14: Relationship between percent organic C in the central basin core and (a) April TP; (b) April TIN:TP; and (c) spring net basin supply (NBS). Relationships determined by Pearson correlation.

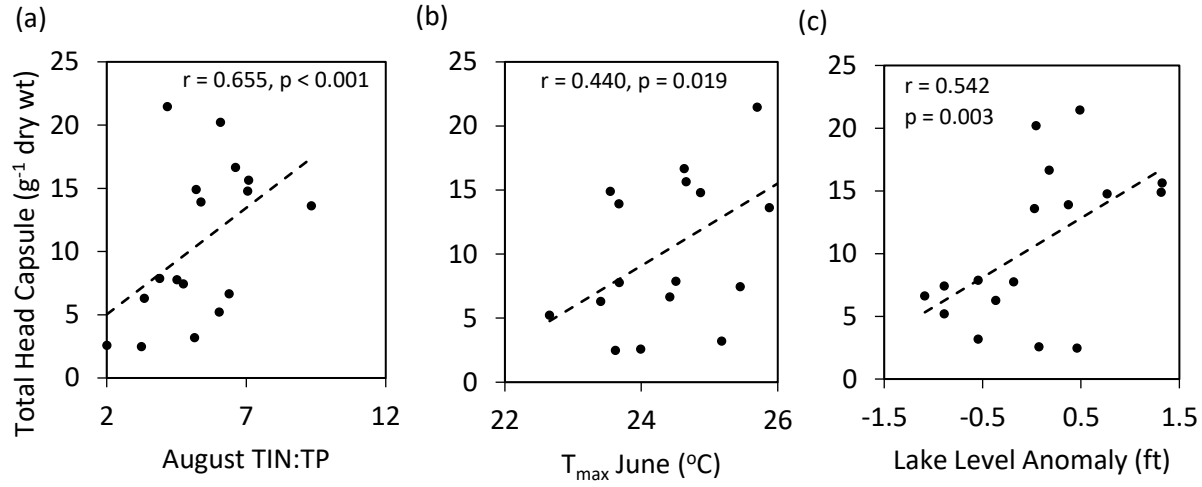

Figure 3.15: Relationship between total head capsule counts in the central basin core and (a) August TIN:TP; (b) June maximum temperature (T_{max}); and (c) lake level anomaly. Relationships determined by Pearson correlation.

Appendix A: Sediment freeze drying standard operating procedure

This SOP describes the procedure for freeze drying sediments and basic troubleshooting using the LABCONCO Triad Freeze Dry System (Model 7400040) in conjunction with the Welch Vacuum Pump (Model 8917).

Introduction

Freeze drying, or lyophilisation, is the first step in preservation and preparation of samples for many analytical procedures (e.g. ^{210}Pb dating, isotope analysis, etc.). In contrast to oven- or air-dried samples, in which heat will degrade the quality of the sample, freeze-dried samples tends to preserve the quality of the sample. Freeze drying is a process whereby water is removed from frozen material by converting the frozen water directly into gas without the intermediate formation of liquid water, this process is called sublimation. This is accomplished by freezing the material and reducing the surrounding pressure in order to allow water to sublimate directly from the solid phase to a gas phase. The efficiency of freeze drying depends on the surface are and thickness of the samples (i.e. greater surface area and lower thickness will result in faster drying).

Table A1**:** Vapour pressure-temperature relationship for ice (Wexler 1977)[1]

°C	≈ mbar	°C	≈ mbar	°C	≈ mbar	°C	≈ mbar
0	6.110	-20	1.030	-40	0.120	-60	0.0110
-1	5.620	-21	0.940	-41	0.110	-61	0.0090
-2	5.170	-22	0.850	-42	0.100	-62	0.0080
-3	4.760	-23	0.770	-43	0.090	-63	0.0070
-4	4.370	-24	0.700	-44	0.080	-64	0.0060
-5	4.020	-25	0.630	-45	0.070	-65	0.0054
-6	3.690	-26	0.570	-46	0.060	-66	0.0047
-7	3.380	-27	0.520	-47	0.055	-67	0.0041
-8	3.010	-28	0.470	-48	0.050	-68	0.0035
-9	2.840	-29	0.420	-49	0.045	-69	0.0030
-10	2.560	-30	0.370	-50	0.040	-70	0.0026
-11	2.380	-31	0.340	-51	0.035	-71	0.0023
-12	2.170	-32	0.310	-52	0.030	-72	0.0019
-13	1.980	-33	0.280	-53	0.025	-73	0.0017
-14	1.810	-34	0.250	-54	0.024	-74	0.0014
-15	1.650	-35	0.220	-55	0.021	-75	0.0012
-16	1.510	-36	0.200	-56	0.018	-76	0.0010
-17	1.370	-37	0.180	-57	0.016		
-18	1.250	-38	0.160	-58	0.014		
-19	1.140	-39	0.140	-59	0.012		

[1] A. Wexler (1977) *J. Res. Nat. Bar. Stds*, 81A, 5–20

Sample preparation

1. Set up a spreadsheet to record your data. An example of how to set up your spreadsheet is given in Figure 1.
2. Weigh all sediment sample bags and record the weight prior to any subsampling (WhirlPak+Sed). *You need the total weight of the sediment interval for gamma ray spectroscopy.*
3. To obtain the net weight of the sediment, you will need to subtract the weight of the WhirlPack; weigh ~10-20 WhirlPaks (ensure that the top portion is ripped off to obtain an accurate weight).
4. Decide what intervals you will be dating, typically you need 12-15 samples for gamma ray analysis, but this can vary. *You can interpolate dates, so you do not need to process all intervals as this will be very expensive.*
5. For freeze drying you will need to use what is available, example plastic scintillation vials or plastic test tubes (ensure that there is a rack available as they will ne to be positioned upright).
6. Label your vials/tubes. Make sure that you label both the tube/vial and its corresponding cap. The information should also be etched into the plastic if they are intended for long-term storage, as the marker may wash off.
7. Weigh each vial/tube with the cap on, record the weight. *You will put the caps back on as soon as the freeze drier cycle is complete and place the caped tubes/vials in the desiccator until they can be weighed*.
8. Mix sediment bag well, then move the sediment towards one side of the bag, then using a metal (or plastic) spatula, scoop the sediment into the labeled vial/tube. The type of analysis to be run will determine the amount of required wet sediment (consult your supervisor if you are unsure).
9. Wash and dry spatula with a paper towel between intervals to ensure that there is no cross contamination.
10. Record the weight of the vial/tube with the sediment and cap on, record weight.
11. Once all sediment intervals are weighted and ready to be freeze dried, remove the cap ad cover the top of the vial/tube with ½ Kimwipe and wrap with an elastic band to ensure it is secured. This will avoid cross-contamination among samples in the freeze drier.
12. Place the samples in the freezer overnight.

Manual with pre-frozen sediment (freezer overnight)

1) Check vacuum pump oil – needs to be clear or slightly cloudy; if light brown requires oil change
2) Turn the freeze drier and vacuum pump power switch ON; make sure the VAC RELEASE valve is in the closed position and the window is locked.
3) DISPLAY set to MANUAL, select the desired temperature (between -55 and -50)
4) Select MAN mode
5) DISPLAY set to SET UP
    a. Select pressure scale (mBar), press ENTER
    b. Select desired pressure, press ENTER; e.g. -40 @ 0.120 mBar (Table 1)
    c. Select °C as temperature units, press ENTER
6) Press RUN/STOP to start the refrigeration system; Press VAC to start the vacuum. *Temperature settings and pressure can be changed at any time during the cycle.*
7) When the shelf temperature reaches -40 (SHLF= -40), press VAC to shut off vacuum pump and set VAC RELEASE in the open position. Allow pressure to equalize.
8) Place the frozen samples on the shelf, close the door, set VAC RELEASE in the close position, press VAC to turn on the vacuum pump. *System will reach -40°C from room temperature in approximately 1.5 hrs, and -55°C in 7hrs.*

Troubleshooting

Target pressure not reached. *Refer to User Manual Chapter 7 (pp. 35-41). Without samples and with refrigeration running, the Freeze Dry System should reach a vacuum of 0.133 mbar within 30 min, and should achieve a vacuum of 0.040 mbar within 3 hrs.*

1) Check vacuum pump tubbing for signs of deterioration (e.g. cracking).
2) Check freeze drier door gasket for indication of deterioration (e.g. cracking). Clean gasket using a soft, moist, lint-free cloth or paper towel.
3) Check the freeze dry system chamber and collector, both must be dry.
4) Check the oil level. Ensure that it is filled to an acceptable range.
   Oil level should fall within the two arrows.

5) Check oil to ensure that it is clean. *Oil should be clear to slightly cloudy, if it has a yellow or brown colour or has any particulates, replace the pump oil. If oil is excessively dirty, it may be necessary to flush the pump with oil several times.* Follow the following steps to change pump oil:
   a. Run the pump for ~10 min to allow the oil to warm up.
   b. Drain oil and refill with clean oil. *Only use certified vacuum pump oil.*
   c. Run the pump for ~10 minutes. *If pump oil becomes very cloudy or has a tint to it, repeat steps b-c.*
6) Check the side valve assembly for air leaks. Ensure that all the valves are in the closed position
   a. Turn on the Freeze drier and run without samples
   b. Turn on the vacuum pump and set it to the desired vacuum pressure using the freeze drier controls
   c. When the vacuum indication is displayed, while the pump is running, wiggle/rotate each valve assembly (the rubber parts) individually and watch the gauge for any fluctuations. The fluctuations will show a potential leak.

d. If the rubber housing seems in good condition (no cracking), apply a thin coat of vacuum grease on the inner stem and outside sealing surface of the valve body, then reinstall the valve. If the issue cannot be resolved, and the source of the problem seems to be the valves, remove them and close the hole with a rubber stopper (apply a thin coat of vacuum grease on the rubber stopper).

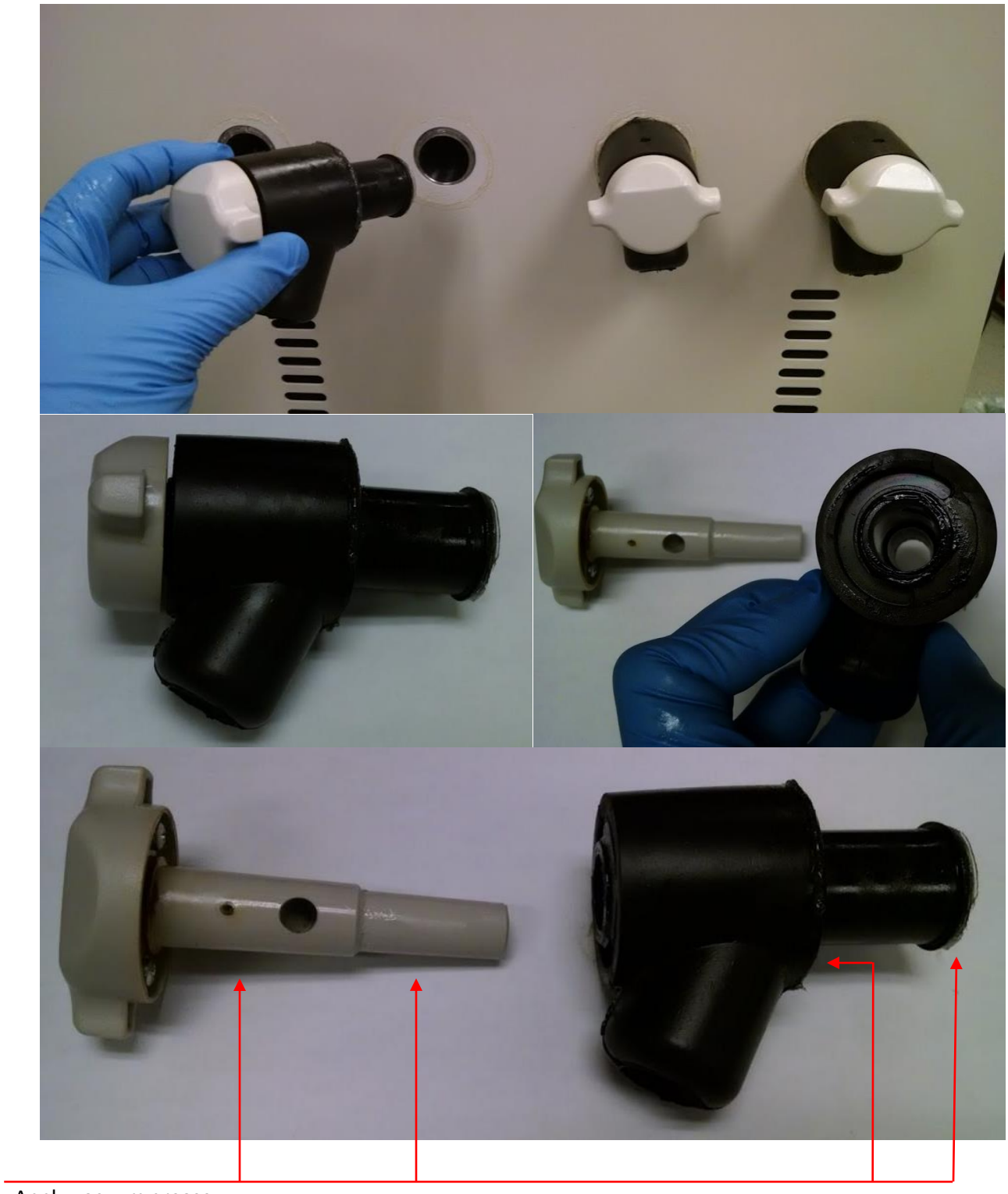

Appendix B: Automated overhead stirrer design

List of parts

- Arduino Uno Rev3
- 400 Tie Point Solderless Breadboard with Self-Adhesive
- Stepper Motor NEMA 14 (200 Steps/Rev, 10V, 500mA, Bipolar)
- Pololu Stepper Motor Driver A4988 Black Edition (8-35V 2A)
- Small Heat Sink (for the A4988 stepper driver)
- Rotary Potentiometer (10k Ohm Linear)
- Black Metal Knob (for the potentiometer)
- On/Off Pushbutton (16mm Illuminated Latching)
- Jumper Wire (40 Pins M/M 20cm)
- L-Bracket for NEMA 14 Stepper Motor (to mount the stepper motor on a stand)
- 100µF 50V 20% Radial Aluminum Capacitor
- 1000 Ohm resistor
- Wall Adapter Power Supply (12VDC 1A – to power the stepper motor)
- DC Barrel Power Connector (Female 5.5mm Breadboard Compatible – not essential, but makes it easy to connect the power supply)
- Enclosure for the device came from a Ferrero Rocher 16-pack box
- 6" x 1.5" x 1.5" piece of wood with a shaft collar pressed in to fit over a lab pole stand
- four rubber bushings to dampen the vibration from the motor
- Modified glass pipette and mount in onto the motor using a piece of air tubing (commonly found in aquarium setups) to serve as stirrer rod

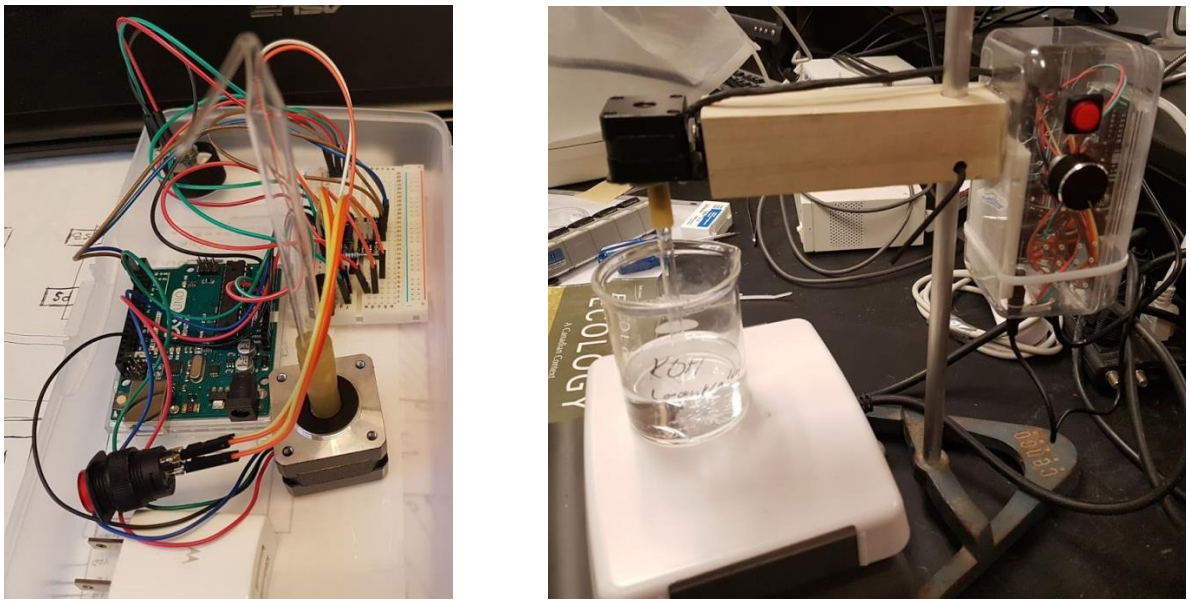

Figure B1: Electrical components and finished product

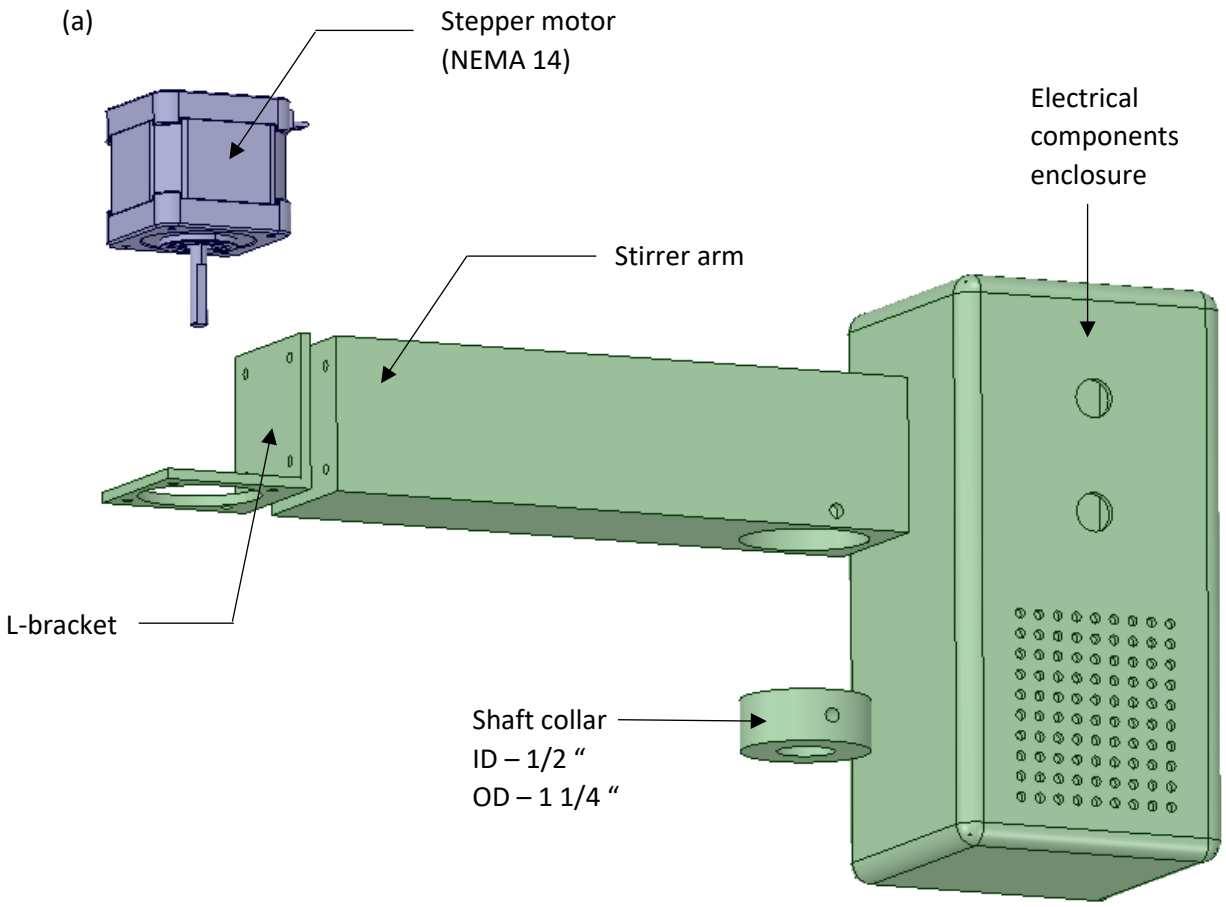
(a)
Stepper motor
(NEMA 14)
Electrical
components
enclosure
Stirrer arm
L-bracket
Shaft collar
ID – 1/2 “
OD – 1 1/4 “

(b)

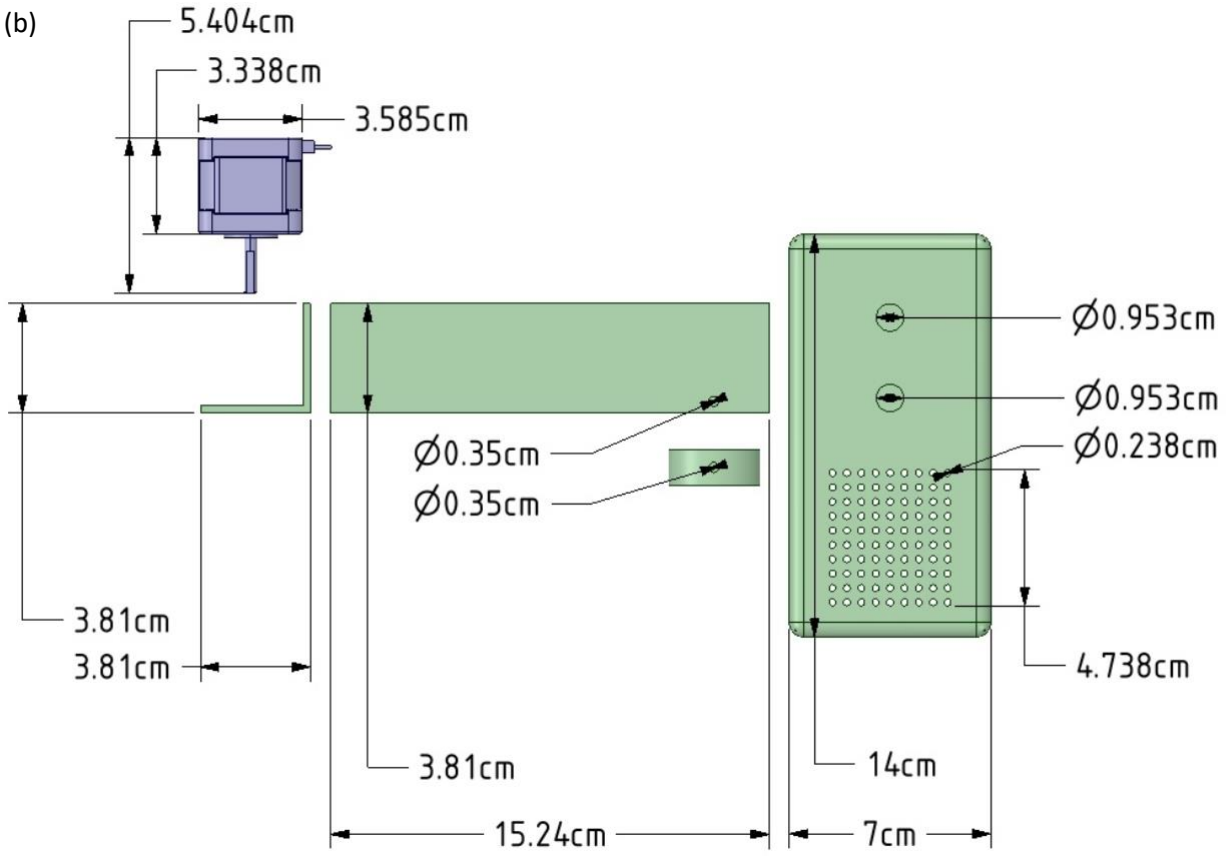
5.404cm
3.338cm
3.585cm
Ø0.953cm
Ø0.953cm
Ø0.238cm
Ø0.35cm
Ø0.35cm
3.81cm
3.81cm
4.738cm
3.81cm
14cm
15.24cm
7cm

(c)

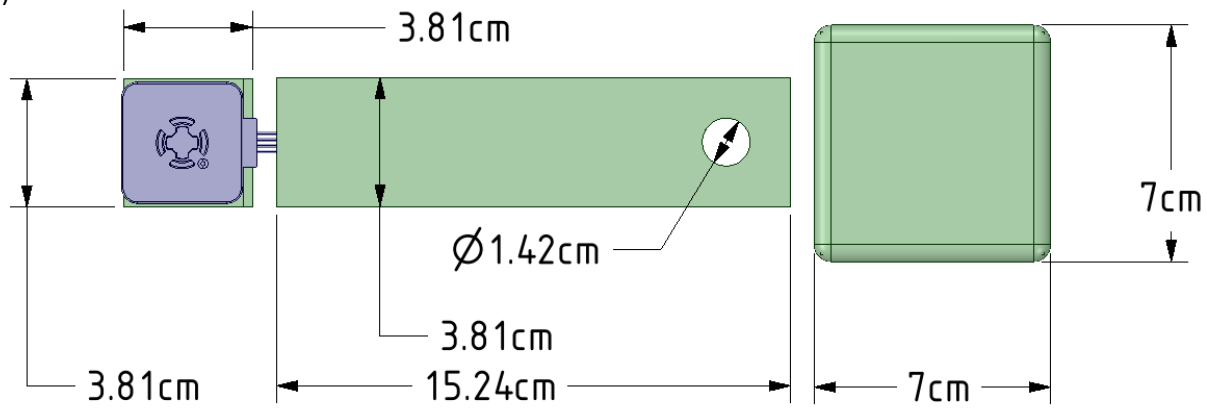
3.81cm
7cm
Ø1.42cm
3.81cm
3.81cm
15.24cm
7cm

(d)

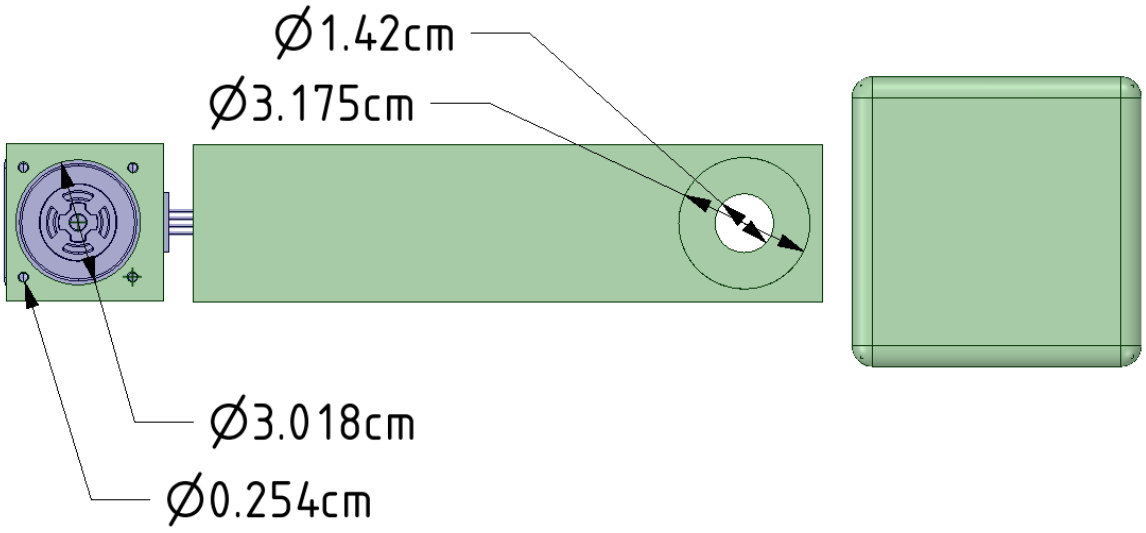

Figure B2: Overhead stirrer stand design showing (a) view of all mechanical components; (b) side view of components and their dimensions; (c) top view of components and their dimensions; (d) bottom view of components and bore dimensions. ID – inner diameter; OD – outer diameter.

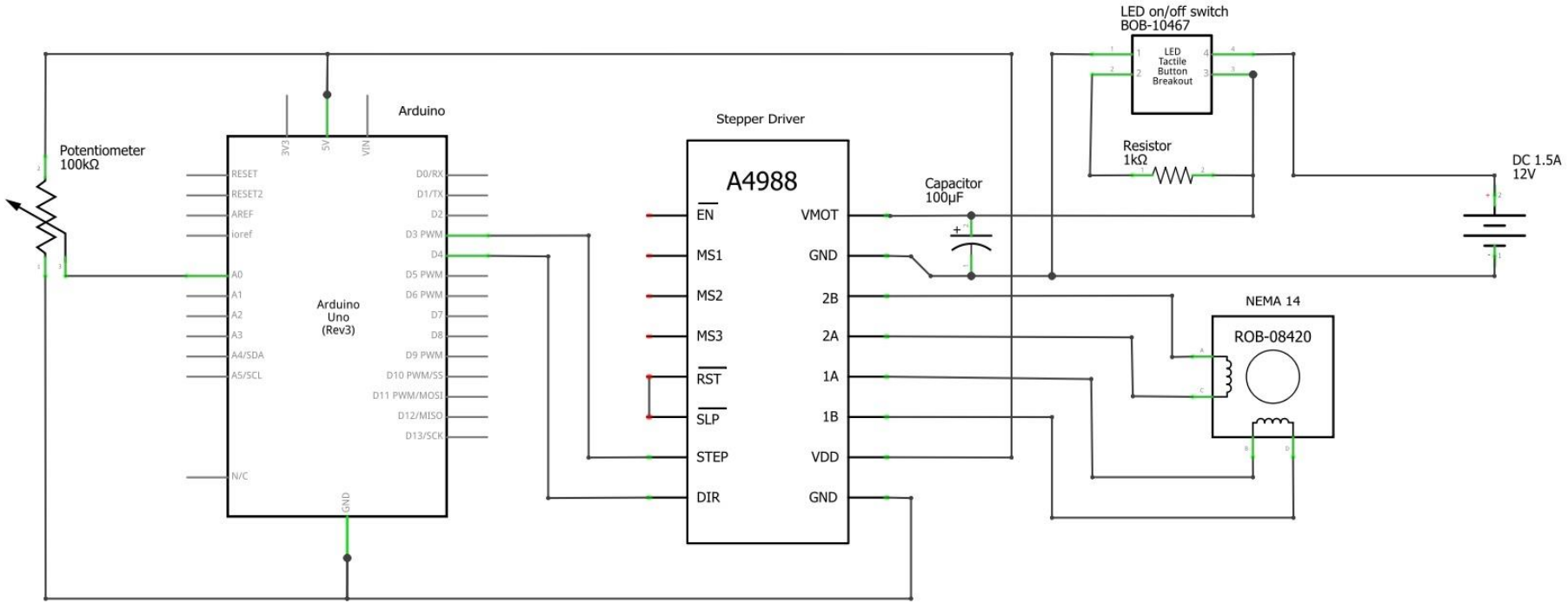

Figure B3: Overhead stirrer circuit diagram

Arduino IDE code

```
/*    Stirrer + Potentiometer
// Defines pins numbers
const int stepPin = 3;
const int dirPin = 4;
int customDelay,customDelayMapped; // Defines variables

void setup() {
  // Sets the two pins as Outputs
  pinMode(stepPin,OUTPUT);
  pinMode(dirPin,OUTPUT);

  digitalWrite(dirPin,HIGH); //Enables the motor to move in a particular direction
}
void loop() {

  customDelayMapped = speedUp(); // Gets custom delay values from the custom speedUp function
  // Makes pules with custom delay, depending on the Potentiometer, from which the speed of the
motor depends
  digitalWrite(stepPin, HIGH);
  delayMicroseconds(customDelayMapped);
  digitalWrite(stepPin, LOW);
  delayMicroseconds(customDelayMapped);
}
// Function for reading the Potentiometer
int speedUp() {
  int customDelay = analogRead(A0); // Reads the potentiometer
  int newCustom = map(customDelay, 0, 1023, 300,4000); // Convrests the read values of the
potentiometer from 0 to 1023 into desired delay values (300 to 4000)
  return newCustom;
}
```

Appendix C: Environmental data – sources, transformations, and ordination analyses results

Table C1: List of environmental variables collected and their sources

Variable Name	Source	Notes
Water Quality		
Hypolimnetic DO, mg O_2 L^{-1} *	EPA-GLENDA	Supplemented with data from CCIW
TP loads, Apr, ug/L	EPA-GLENDA	Supplemented with data from CCIW
TP loads, Aug, ug/L	EPA-GLENDA	Supplemented with data from CCIW
TIN loads, Apr, ug/L	EPA-GLENDA	Supplemented with data from CCIW
TIN loads, Aug, ug/L	EPA-GLENDA	Supplemented with data from CCIW
TIN:TP, Apr, ug/L		Calculated using TP and TIN data
TIN:TP, Aug, ug/L		Calculated using TP and TIN data
Climate		
Mean max temperature, Annual, ^oC	NOAA-GLERL	https://www.glerl.noaa.gov/data/dashboard/data/hydroIO/temps/
Mean max temperature, Seasonal, ^oC	NOAA-GLERL	Calculated using monthly data
Mean max temperature, Monthly, ^oC	NOAA-GLERL	https://www.glerl.noaa.gov/data/dashboard/data/hydroIO/temps/
Mean min temperature, Annual, ^oC	NOAA-GLERL	https://www.glerl.noaa.gov/data/dashboard/data/hydroIO/temps/
Mean min temperature, Seasonal, ^oC	NOAA-GLERL	Calculated using monthly data
Mean min temperature, Monthly, ^oC	NOAA-GLERL	https://www.glerl.noaa.gov/data/dashboard/data/hydroIO/temps/
Mean temperature, Annual, ^oC	NOAA-GLERL	https://www.glerl.noaa.gov/data/dashboard/data/hydroIO/temps/
Mean temperature, Seasonal, ^oC	NOAA-GLERL	Calculated using monthly data
Mean temperature, Monthly, ^oC	NOAA-GLERL	https://www.glerl.noaa.gov/data/dashboard/data/hydroIO/temps/
MSWT, Annual, ^oC	NOAA-GLERL	https://www.glerl.noaa.gov/data/dashboard/data/hydroIO/temps/
MSWT, Seasonal, ^oC	NOAA-GLERL	Calculated using monthly data
MSWT, Monthly, ^oC	NOAA-GLERL	https://www.glerl.noaa.gov/data/dashboard/data/hydroIO/temps/
Precipitation over Lake, Annual, mm	NOAA-GLERL	https://www.glerl.noaa.gov/data/dashboard/data/hydroIO/precip/
Precipitation over Lake, Seasonal, mm	NOAA-GLERL	Calculated using monthly data
Precipitation over Lake, Monthly, mm	NOAA-GLERL	https://www.glerl.noaa.gov/data/dashboard/data/hydroIO/precip/
Precipitation over Land, Annual, mm	NOAA-GLERL	https://www.glerl.noaa.gov/data/dashboard/data/hydroIO/precip/
Precipitation over Land, Seasonal, mm	NOAA-GLERL	Calculated using monthly data
Precipitation over Land, Monthly, mm	NOAA-GLERL	https://www.glerl.noaa.gov/data/dashboard/data/hydroIO/precip/
Gross evaporation, Annual, mm	NOAA-GLERL	https://www.glerl.noaa.gov/data/dashboard/data/hydroIO/evap/
Gross evaporation, Seasonal, mm	NOAA-GLERL	Calculated using monthly data
Gross evaporation, Monthly, mm	NOAA-GLERL	https://www.glerl.noaa.gov/data/dashboard/data/hydroIO/evap/
Runoff, Annual, mm	NOAA-GLERL	https://www.glerl.noaa.gov/data/dashboard/data/hydroIO/runoff/
Runoff, Seasonal, mm	NOAA-GLERL	Calculated using monthly data
Runoff, Monthly, mm	NOAA-GLERL	https://www.glerl.noaa.gov/data/dashboard/data/hydroIO/runoff/
Net basin supply, Annual, m^3 L^{-1}	NOAA-GLERL	https://www.glerl.noaa.gov/data/dashboard/data/hydroIO/nbs/
Net basin supply, Seasonal, m^3 L^{-1}	NOAA-GLERL	Calculated using monthly data
Net basin supply, Monthly, m^3 L^{-1}	NOAA-GLERL	https://www.glerl.noaa.gov/data/dashboard/data/hydroIO/nbs/
Maximum ice cover, Annual, %	NOAA-GLERL	https://www.glerl.noaa.gov/data/ice/#historical
Lake level anomaly, Annual, ft	EPA	https://www.epa.gov/climate-indicators/great-lakes#ref6
Land Use		
TP loads, MTA		Maccoux et al. (2016)[+]
Western Lake Erie population		Sgro and Reavie (2017)[¥]
Western Lake Erie Agriculture (acres)		Sgro and Reavie (2017)[¥]
Western Lake Erie Forest (acres)		Sgro and Reavie (2017)[¥]
Lake Erie population		Sgro and Reavie (2017)[¥]
Lake Erie Agriculture (acres)		Sgro and Reavie (2017)[¥]
Lake Erie Forest (acres)		Sgro and Reavie (2017)[¥]

Table C2: Central basin depths and associated ^{210}Pb dates

Year upper bound	Year lower bound	core mid-point year	Core start depth (cm)	Core end depth (cm)	Core midpoint Depth (cm)
2011	2010	2010.7	0.5	1.5	1
2009	2008	2009.0	1.5	2.5	2
2007	2005	2006.9	2.5	4	3.25
2004	2003	2004.8	4	5	4.5
2002	2001	2002.7	5	6	5.5
2000	1999	2000.3	6	7	6.5
1998	1998	1998.6	7	7.5	7.25
1997	1997	1997.4	7.5	8	7.75
1996	1996	1996.3	8	8.5	8.25
1995	1995	1995.1	8.5	9	8.75
1994	1992	1993.5	9	9.5	9.25
1991	1991	1991.9	9.5	10	9.75
1990	1989	1990.3	10	11	10.5
1988	1987	1988.7	11	12	11.5
1986	1984	1985.9	12	13	12.5
1983	1975	1980.2	13	16	14.5
1974	1966	1971.0	16	19	17.5
1962	1952	1958.1	20	23	21.5
1951	1944	1949.2	23	25	24
1940	1938	1939.9	26	27	26.5
1933	1930	1932.6	28	29	28.5
1929	1923	1927.2	29	31	30
1919	1910	1915.5	32	35	33.5
1909	1903	1906.9	35	37	36
1898	1887	1890.6	38	41	39.5
1881	1868	1875.7	42	45	43.5
1862	1854	1859.3	46	48	47
1853	1849	1852.3	48	49	48.5

Table C3: Variables found to have significant influence on chironomid assemblages within the central basin of Lake Erie as determined by singly constrained RDAs. Annual environmental variables were averaged over each sedimentary interval time period

Variable Name		**Shapiro-Wilk**		**post-1970**	**post-1950**	**post-1915**
	Trans	**W**	**p-value**	**p-value**	**p-value**	**p-value**
Water Quality						
Hypolimnetic DO, mg/L	Log(y+1)	0.957	0.578			
TP loads, Apr, ug/L	Log(y)	0.992	1.000			
TP loads, Aug, ug/L	1/y	0.982	0.976			
TIN loads, Apr, ug/L		0.958	0.592			
TIN loads, Aug, ug/L	SQy	0.970	0.819			
TIN/TP, Apr, ug/L	Log(y)	0.933	0.241			
TIN/TP, Aug, ug/L	SQy	0.984	0.984			
Climate						
TmaxJAN		0.963	0.623			
TmaxFEB		0.907	0.065			
TmaxMAR		0.947	0.348			
TmaxAPR		0.971	0.806			
TmaxMAY		0.923	0.131			
TmaxJUN		0.977	0.901			
TmaxJUL		0.978	0.923			
TmaxAUG		0.977	0.899			
TmaxSEP	y^-3	0.912	0.080			
TmaxOCT	y^2	0.914	0.088			
TmaxNOV	y^2	0.925	0.140			
TmaxDEC		0.945	0.327			
TmaxW		0.949	0.378			
TmaxSP		0.935	0.213			
TmaxSU	y^-2	0.976	0.883			
TmaxF		0.970	0.784			
TmaxAnn	y^-2	0.922	0.124			
TminJAN		0.948	0.368			
TminFEB		0.902	0.054			
TminMAR		0.945	0.326		**0.065**	
TminAPR		0.970	0.773			
TminMAY	log	0.939	0.248			
TminJUN		0.956	0.501			
TminJUL		0.961	0.599			
TminAUG		0.937	0.230			
TminSEP		0.965	0.675			
TminOCT		0.956	0.506			
TminNOV		0.931	0.184			
TminDEC		0.961	0.602			
TminW	y^2	0.966	0.699			
TminSP		0.907	0.065			
TminSU	y^(-2)	0.901	0.051			
TminF		0.925	0.139			
TminAnn	log	0.918	0.104			
TavgJAN		0.945	0.321			
TavgFEB	y^2	0.929	0.168			
TavgMAR		0.957	0.517		0.044	
TavgAPR		0.976	0.887			

Table C3 (con't)

Variable Name		Shapiro-Wilk		post-1970	post-1950	post-1915
	Trans	W	p-value	p-value	p-value	p-value
TavgMAY		0.904	0.057			
TavgJUN		0.964	0.652			
TavgJUL		0.969	0.759			
TavgAUG		0.967	0.713			
TavgSEP		0.956	0.503			
TavgOCT	y^2	0.922	0.123			
TavgNOV		0.907	0.065			
TavgDEC		0.942	0.290			
TavgW		0.901	0.050			
TavgSP		0.903	0.056			
TavgSU		0.934	0.209			
TavgF		0.981	0.952			
TavgAnn	SQRT	0.906	0.064			
MSWT_Jan	SQRT	0.933	0.196			
MSWT_Feb	y^(1/3)	0.779	**0.001**			
MSWT_Mar	y^(1/3)	0.911	0.078			
MSWT_Apr		**0.957**	**0.512**		**0.1**	
MSWT_May		**0.939**	**0.253**		**0.063**	
MSWT_Jun		**0.961**	**0.602**		**0.088**	
MSWT_Jul		0.948	0.358			
MSWT_Aug		0.942	0.289			
MSWT_Sep		0.901	0.051			
MSWT_Oct		0.973	0.841			
MSWT_Nov		0.960	0.563			
MSWT_Dec		0.927	0.150			
MSWT_W	y^(-2)	0.948	0.364			
MSWT_SP		0.910	0.075			
MSWT_SU		0.916	0.097			
MSWT_F		0.968	0.735			
MSWT_Annual		0.917	0.098			
PLk_Jan		0.982	0.929			
PLk_Feb		0.967	0.591			
PLk_MAR		0.970	0.670			
PLk_APR		0.976	0.821			
PLk_MAY		0.963	0.500			
PLk_JUN		0.960	0.440			
PLk_JUL		0.966	0.570			
PLk_AUG		0.955	0.353			
PLk_SEP	log	0.930	0.096			
PLk_OCT		0.970	0.661			
PLk_NOV		0.939	0.154			
PLk_DEC		0.987	0.981			
PLk_W		0.926	0.081			
PLk_SP		0.963	0.503			
PLk_SU	y^2	0.927	0.086			
PLk_F	SQRT	0.926	0.081			
PLk_Annual		0.973	0.744			
PLd_JAN		0.950	0.276			
PLd_FEB		0.949	0.262			
PLd_Mar		0.971	0.683			
PLd_APR		0.984	0.960			
PLd_MAY		0.925	0.074			

Table C3 (con't)

Variable Name		Shapiro-Wilk		post-1970	post-1950	post-1915
	Trans	W	p-value	p-value	p-value	p-value
PLd_JUN		0.934	0.119			
PLd_JUL		0.936	0.134			
PLd_AUG		0.968	0.628		0.046	0.018
PLd_SEP		0.938	0.151			
PLd_OCT		0.944	0.196			
PLd_NOV		0.975	0.780			
PLd_DEC		0.972	0.716			
PLd_W		0.930	0.096			
PLd_SP		0.921	0.063			
PLd_SU	y^2	0.942	0.185			0.018
PLd_F		0.975	0.778			
PLd_Ann		0.966	0.569			
EvapJan		0.966	0.686			
EvapFeb		0.963	0.623			
EvapMarch		0.945	0.329			
EvapApr		0.920	0.115			
EvapMay		0.906	0.062			
EvapJun		0.955	0.472			
EvapJul		0.932	0.192			
EvapAug		0.961	0.590			
EvapSep		0.954	0.467			
EvapOct		0.977	0.903			
EvapNov		0.967	0.708			
EvapDec		0.968	0.738			
EvapW		0.976	0.891			
EvapSP	y^(-1/2)	0.953	0.450			
EvapSU	y^(-1)	0.905	0.061			
EvapF		0.968	0.736			
EvapAnn	y^(-1)	0.898	**0.046**			
RunJan		0.950	0.298			
RunFeb		0.960	0.456			
RunMar		0.964	0.557			
RanApr		0.985	0.970			
RunMay	log	0.972	0.733			
RunJun	SQRT	0.958	0.428			0.041
RunJul		0.967	0.617			0.069
RunAug	SQRT	0.971	0.721			0.04
RunSep		0.957	0.397			
RunOct		0.958	0.419			
RunNov		0.962	0.511			
RunDec		0.961	0.494			
RunW		0.967	0.617			
RunSP		0.977	0.850			
RunSU		0.981	0.915			0.021
RunF		0.960	0.464			
RunAnn		0.941	0.187			
NBS_Jan	SQRT	0.765	**0.000**			
NBS_Feb		0.902	0.053			
NBS_Mar		0.915	0.090			
NBS_Apr		0.911	0.079		0.023	
NBS_May		0.939	0.252			
NBS_Jun		0.961	0.589			

Table C3 (con't)

Variable Name		Shapiro-Wilk		post-1970	post-1950	post-1915
	Trans	W	p-value	p-value	p-value	p-value
NBS_Jul	SQRT	0.879	**0.021**			
NBS_Aug		0.979	0.932			
NBS_Sep		0.945	0.321			
NBS_Oct		0.990	0.999			
NBS_Nov		0.979	0.930			
NBS_Dec		0.988	0.996			
NBS_W	SQRT	0.768	**0.000**			
NBS_SP		0.917	0.098		0.048	
NBS_SU		0.916	0.094			
NBS_F		0.971	0.792			
NBS_Ann		0.914	0.089			
LvlAnomal		0.972	0.679			
MaxIce%	y^3	0.829	**0.005**			
Land Use						
MTA	log	0.913	0.113			
WE_pop	log	0.677	**< 0.0001**		0.023	0.075
WE_Ag (acres)	SQRT	0.889	**0.006**		0.023	0.018
WE_Forest acres	SQRT	0.725	**< 0.0001**			
AE_pop	log	0.689	**< 0.0001**		0.023	0.075
AE_Ag (acres)	SQRT	0.821	**0.000**		0.023	0.018
AE_Forest acres	SQRT	0.882	**0.004**		0.023	0.043

Table C4: Untransformed environmental variables used in a series of singly constrained RDAs to determine variable significance on variation in chironomid assemblages. Annual environmental variables were averaged over each sedimentary interval time period. ^{210}Pb Year showing the interval midpoint year, see Table C2 for rear range per interval. DO – dissolved oxygen; TP – total phosphorus; TIN – total inorganic nitrogen; Tmin – minimum temp (°C); Tmax – maximum temp (°C); Tavg – mean temp (°C); MSWT – mean surface water temp (°C); PLk -precip over lake (mm); PLd – precip over land (mm); Run – Runoff (mm)

^{210}Pb Year	Interval Depth (cm)	DO (mg L^{-1})	TP_Apr (mg L^{-1})	TP_Aug (mg L^{-1})	TIN_Apr (mg L^{-1})	TIN_Aug (mg L^{-1})	TIN/TP_Apr (mg L^{-1})	TIN/TP_Aug (mg L^{-1})
2011	0.5-1.5	1.45	13.87	7.81	106.20	125.00	7.66	16.00
2009	1.5-2.5	3.99	12.23	9.15	178.45	71.13	14.59	7.77
2007	2.5-4	2.13	15.45	6.90	183.06	186.81	11.85	27.06
2005	4-5	2.24	13.70	5.63	182.01	186.41	13.28	33.13
2003	5-6	1.91	12.42	4.23	151.17	160.04	12.17	37.85
2000	6-7	1.80	11.13	7.45	143.71	146.14	12.91	19.61
1999	7-7.5	0.00	12.76	4.58	292.14	190.00	22.90	41.48
1997	7.5-8	4.04	16.08	5.54	341.75	399.00	21.25	72.03
1996	8-8.5	1.70	10.42	6.04	265.40	325.00	25.48	53.83
1995	8.5-9	9.14	8.73	5.24	211.33	253.36	24.20	48.32
1994	9-9.5	0.64	10.15	8.38	272.56	326.76	26.86	38.98
1992	9.5-10	1.48	13.20	4.96	105.00	152.50	7.95	30.75
1990	10-11	2.54	7.54	6.76	116.25	119.25	15.42	17.64
1989	11-12	0.85	9.96	5.98	167.54	105.00	16.83	17.57
1986	12-13	0.78	11.12	8.77	242.83	254.07	21.84	28.97
1980	13-16	0.62	21.61	13.10	208.13	138.33	9.63	10.56
1971	16-19	0.93	17.79	12.15	156.16	33.58	8.78	2.76

Table C4 (con't)

^{210}Pb Year	Interval Depth (cm)	Tmin JAN (°C)	Tmin FEB (°C)	Tmin MAR (°C)	Tmin APR (°C)	Tmin MAY (°C)	Tmin JUN (°C)	Tmin JUL (°C)	Tmin AUG (°C)	Tmin SEP (°C)	Tmin OCT (°C)	Tmin NOV (°C)	Tmin DEC (°C)	Tmin Annual Avg (°C)
2011	0.5-1.5	-6.67	-6.37	-0.87	5.04	10.83	16.03	18.70	18.71	13.61	8.02	1.71	-5.50	6.10
2009	1.5-2.5	-8.09	-6.88	-3.29	3.70	7.91	14.61	16.42	16.50	13.69	6.21	2.80	-4.71	4.90
2007	2.5-4	-4.30	-7.25	-2.84	3.09	8.68	15.40	17.70	17.94	13.91	8.69	2.30	-2.77	5.88
2005	4-5	-10.12	-8.07	-2.16	2.87	9.16	13.89	17.01	16.61	13.87	7.10	3.23	-3.25	5.01
2003	5-6	-3.83	-3.71	-2.57	4.04	8.86	15.03	17.45	17.77	13.42	7.37	3.21	-2.32	6.23
2000	6-7	-7.91	-4.14	-1.60	3.37	10.26	15.36	17.36	15.73	12.50	6.95	2.14	-5.99	5.33
1999	7-7.5	-2.51	-1.36	0.07	4.10	12.58	14.89	17.06	17.31	14.00	7.66	2.97	-1.36	7.12
1997	7.5-8	-8.58	-4.47	-2.09	1.23	5.87	14.75	16.38	15.11	12.28	6.60	0.56	-2.00	4.64
1996	8-8.5	-8.86	-7.81	-5.76	1.54	8.26	15.47	16.08	16.54	13.04	7.26	-1.18	-2.20	4.37
1995	8.5-9	-4.69	-8.64	-1.95	1.40	9.16	15.76	18.16	19.03	11.12	8.44	-0.69	-6.35	5.06
1994	9-9.5	-7.39	-8.03	-3.50	2.91	7.78	13.72	17.44	15.73	12.11	5.86	2.39	-2.58	4.70
1992	9.5-10	-6.69	-4.11	-1.03	5.59	12.62	15.53	17.35	16.95	11.69	7.91	0.30	-3.07	6.09
1990	10-11	-3.06	-6.06	-2.22	2.78	8.35	14.60	16.95	15.98	12.32	6.66	1.36	-6.79	5.07
1989	11-12	-6.82	-7.47	-2.25	3.53	9.83	14.43	18.30	17.35	12.93	4.49	2.73	-2.90	5.35
1986	12-13	-9.23	-6.40	-3.44	3.54	8.97	13.60	16.54	16.11	12.98	8.15	1.68	-3.77	4.89
1980	13-16	-9.48	-8.35	-2.79	2.18	8.76	13.69	16.83	16.29	12.42	6.22	1.69	-5.03	4.37
1971	16-19	-7.95	-8.13	-2.91	2.71	7.53	14.17	16.71	16.24	12.76	7.34	1.65	-3.65	4.71
1958	20-23	-7.10	-6.05	-3.11	3.23	8.37	14.02	16.70	16.37	12.78	7.01	1.48	-4.31	4.95
1949	23-25	-5.86	-6.65	-3.36	2.35	8.12	14.41	17.22	15.75	12.06	7.66	0.67	-4.38	4.83

Table C4 (con't)

^{210}Pb Year	Interval Depth (cm)	Tmax JAN (°C)	Tmax FEB (°C)	Tmax MAR (°C)	Tmax APR (°C)	Tmax MAY (°C)	Tmax JUN (°C)	Tmax JUL (°C)	Tmax AUG (°C)	Tmax SEP (°C)	Tmax OCT (°C)	Tmax NOV (°C)	Tmax DEC (°C)	Tmax Ann (°C)
2011	0.5-1.5	-1.21	-0.71	7.50	15.82	19.72	24.51	28.07	27.14	22.31	16.21	10.14	-0.64	14.07
2009	1.5-2.5	-0.55	1.08	5.10	13.72	17.64	23.41	25.03	25.33	22.40	14.38	9.42	2.45	13.28
2007	2.5-4	2.49	-0.12	5.24	12.60	18.43	25.18	26.77	26.35	22.64	16.33	9.86	2.91	14.06
2005	4-5	-3.22	-0.12	6.62	12.30	18.50	22.66	25.22	25.08	22.35	15.25	10.55	3.32	13.21
2003	5-6	1.98	3.81	5.31	14.06	18.40	24.42	27.14	27.30	23.35	15.33	10.34	3.76	14.60
2000	6-7	0.36	4.12	7.70	13.09	21.07	25.45	27.38	25.51	23.03	16.62	9.86	1.15	14.61
1999	7-7.5	3.63	5.17	7.72	14.15	22.82	24.87	27.20	27.21	24.88	17.17	10.60	6.62	16.00
1997	7.5-8	-0.13	3.69	6.65	11.41	15.33	24.66	26.28	24.06	21.70	16.28	6.66	3.12	13.31
1996	8-8.5	-0.64	0.51	3.40	11.58	17.87	24.63	25.91	26.91	21.75	16.19	5.35	4.03	13.12
1995	8.5-9	1.63	-0.48	8.02	10.91	18.97	25.88	27.82	28.47	21.73	17.37	6.07	0.04	13.87
1994	9-9.5	-0.36	0.32	4.36	12.86	18.70	23.67	26.34	25.20	21.34	15.24	9.28	3.56	13.38
1992	9.5-10	0.08	3.11	7.84	14.43	22.75	26.19	27.73	26.74	22.29	16.99	7.56	4.13	14.99
1990	10-11	4.05	1.36	6.74	12.14	17.58	23.68	26.33	25.33	21.53	16.36	9.58	0.75	13.78
1989	11-12	0.13	0.78	7.19	13.16	21.01	25.70	28.40	26.72	22.00	12.72	10.03	3.35	14.26
1986	12-13	-1.91	1.24	5.44	13.84	18.74	23.55	26.18	25.51	22.23	16.61	8.75	2.57	13.56
1980	13-16	-2.04	-0.04	5.98	11.57	19.07	23.62	26.70	25.72	21.94	14.80	9.10	2.12	13.21
1971	16-19	-0.27	-0.19	5.46	12.35	17.40	24.00	26.36	26.01	22.30	16.22	8.19	2.65	13.37
1958	20-23	0.02	1.67	4.93	13.09	18.87	24.53	27.00	26.41	22.94	16.74	9.23	2.38	13.98
1949	23-25	1.99	2.08	5.58	11.99	19.32	24.91	27.02	26.40	21.90	17.46	7.90	3.01	14.13

Table C4 (con't)

^{210}Pb Year	Interval Depth (cm)	Tavg JAN (°C)	Tavg FEB (°C)	Tavg MAR (°C)	Tavg APR (°C)	Tavg MAY (°C)	Tavg JUN (°C)	Tavg JUL (°C)	Tavg AUG (°C)	Tavg SEP (°C)	Tavg OCT (°C)	Tavg NOV (°C)	Tavg DEC (°C)	Tavg Ann (°C)
2011	0.5-1.5	-3.94	-3.54	3.32	10.43	15.28	20.27	23.39	22.93	17.96	12.12	5.93	-3.07	10.09
2009	1.5-2.5	-4.32	-2.90	0.90	8.71	12.78	19.01	20.72	20.91	18.04	10.30	6.11	-1.13	9.09
2007	2.5-4	-0.91	-3.69	1.20	7.84	13.56	20.29	22.23	22.14	18.28	12.51	6.08	0.07	9.97
2005	4-5	-6.67	-4.09	2.23	7.59	13.83	18.27	21.12	20.84	18.11	11.17	6.89	0.04	9.11
2003	5-6	-0.93	0.05	1.37	9.05	13.63	19.73	22.29	22.53	18.38	11.35	6.78	0.72	10.41
2000	6-7	-3.78	-0.01	3.05	8.23	15.66	20.41	22.37	20.62	17.76	11.78	6.00	-2.42	9.97
1999	7-7.5	0.56	1.91	3.90	9.13	17.70	19.88	22.13	22.26	19.44	12.42	6.79	2.63	11.56
1997	7.5-8	-4.36	-0.39	2.28	6.32	10.60	19.71	21.33	19.59	16.99	11.44	3.61	0.56	8.97
1996	8-8.5	-4.75	-3.65	-1.18	6.56	13.07	20.05	21.00	21.73	17.40	11.73	2.09	0.92	8.74
1995	8.5-9	-1.53	-4.56	3.04	6.16	14.07	20.82	22.99	23.75	16.43	12.91	2.69	-3.16	9.47
1994	9-9.5	-3.88	-3.86	0.43	7.89	13.24	18.70	21.89	20.47	16.73	10.55	5.83	0.49	9.04
1992	9.5-10	-3.31	-0.50	3.41	10.01	17.69	20.86	22.54	21.85	16.99	12.45	3.93	0.53	10.54
1990	10-11	0.50	-2.35	2.26	7.46	12.96	19.14	21.64	20.65	16.92	11.51	5.47	-3.02	9.43
1989	11-12	-3.35	-3.35	2.47	8.34	15.42	20.07	23.35	22.03	17.46	8.61	6.38	0.23	9.80
1986	12-13	-5.57	-2.58	1.00	8.69	13.86	18.58	21.36	20.81	17.60	12.38	5.22	-0.60	9.23
1980	13-16	-5.76	-4.19	1.60	6.87	13.91	18.66	21.77	21.00	17.18	10.51	5.39	-1.45	8.79
1971	16-19	-4.11	-4.16	1.28	7.53	12.46	19.08	21.53	21.12	17.53	11.78	4.92	-0.50	9.04
1958	20-23	-3.54	-2.19	0.91	8.16	13.62	19.27	21.85	21.39	17.86	11.87	5.36	-0.97	9.47
1949	23-25	-1.93	-2.29	1.11	7.17	13.72	19.66	22.12	21.08	16.98	12.56	4.29	-0.69	9.48

Table C4 (con't)

^{210}Pb Year	Interval Depth (cm)	TminW (°C)	TminSP (°C)	TminSU (°C)	TminF (°C)	TmaxW (°C)	TmaxSP (°C)	TmaxSU (°C)	TmaxF (°C)	TavgW (°C)	TavgSP (°C)	TavgSU (°C)	TavgF (°C)
2011	0.5-1.5	-6.18	5.00	17.81	7.78	-0.85	14.35	26.57	16.22	-3.52	9.67	22.19	12.00
2009	1.5-2.5	-6.56	2.77	15.84	7.56	0.99	12.15	24.59	15.40	-2.78	7.46	20.21	11.48
2007	2.5-4	-4.77	2.98	17.01	8.30	1.76	12.09	26.10	16.28	-1.51	7.53	21.55	12.29
2005	4-5	-7.14	3.29	15.84	8.07	0.00	12.47	24.32	16.05	-3.57	7.88	20.08	12.06
2003	5-6	-3.29	3.44	16.75	8.00	3.18	12.59	26.28	16.34	-0.05	8.01	21.52	12.17
2000	6-7	-6.01	4.01	16.15	7.19	1.87	13.95	26.11	16.50	-2.07	8.98	21.13	11.85
1999	7-7.5	-1.74	5.58	16.42	8.21	5.14	14.90	26.43	17.55	1.70	10.24	21.42	12.88
1997	7.5-8	-5.02	1.67	15.41	6.48	2.23	11.13	25.00	14.88	-1.40	6.40	20.21	10.68
1996	8-8.5	-6.29	1.35	16.03	6.37	1.30	10.95	25.82	14.43	-2.50	6.15	20.92	10.40
1995	8.5-9	-6.56	2.87	17.65	6.29	0.40	12.63	27.39	15.06	-3.08	7.75	22.52	10.67
1994	9-9.5	-6.00	2.40	15.63	6.79	1.17	11.97	25.07	15.29	-2.41	7.19	20.35	11.04
1992	9.5-10	-4.62	5.73	16.61	6.63	2.44	15.01	26.89	15.61	-1.09	10.37	21.75	11.12
1990	10-11	-5.30	2.97	15.84	6.78	2.05	12.15	25.11	15.82	-1.63	7.56	20.48	11.30
1989	11-12	-5.73	3.70	16.69	6.72	1.42	13.78	26.94	14.92	-2.16	8.74	21.82	10.82
1986	12-13	-6.47	3.02	15.42	7.60	0.63	12.67	25.08	15.86	-2.92	7.85	20.25	11.73
1980	13-16	-7.62	2.71	15.60	6.77	0.02	12.21	25.35	15.28	-3.80	7.46	20.47	11.03
1971	16-19	-6.58	2.44	15.71	7.25	0.73	11.74	25.45	15.57	-2.92	7.09	20.58	11.41
1958	20-23	-5.82	2.83	15.70	7.09	1.36	12.30	25.98	16.30	-2.23	7.56	20.84	11.70
1949	23-25	-5.63	2.37	15.79	6.80	2.36	12.30	26.11	15.75	-1.63	7.33	20.95	11.28

Table C4 (con't)

^{210}Pb date	Interval Depth (cm)	MSWT Jan (°C)	MSWT Feb (°C)	MSWT Mar (°C)	MSWT Apr (°C)	MSWT May (°C)	MSWT Jun (°C)	MSWT Jul (°C)	MSWT Aug (°C)	MSWT Sep (°C)	MSWT Oct (°C)	MSWT Nov (°C)	MSWT Dec (°C)
2011	0.5-1.5	0.10	0.00	0.00	2.34	10.00	18.29	23.11	23.60	21.21	16.94	11.27	5.33
2009	1.5-2.5	0.39	0.00	0.00	1.19	8.84	16.83	21.24	22.75	21.20	15.95	10.66	3.95
2007	2.5-4	1.76	0.23	0.19	2.91	10.59	18.60	22.97	24.22	21.97	17.80	11.29	4.55
2005	4-5	0.53	0.00	0.02	2.00	9.85	17.70	22.60	24.08	21.44	15.63	11.37	5.75
2003	5-6	1.60	1.12	1.11	3.56	10.76	18.32	23.53	25.09	23.18	18.33	11.94	6.23
2000	6-7	0.68	0.00	0.54	4.63	12.66	19.09	23.69	24.22	22.49	17.03	11.65	4.76
1999	7-7.5	1.64	1.76	2.04	6.52	14.22	18.88	24.07	25.13	23.40	18.69	12.09	7.92
1997	7.5-8	0.54	0.00	0.00	1.87	8.41	16.46	21.98	22.37	21.04	17.35	9.90	4.98
1996	8-8.5	0.00	0.00	0.00	0.27	5.48	15.88	21.43	24.10	22.34	17.21	10.26	4.51
1995	8.5-9	1.78	0.03	0.15	2.63	9.98	18.36	23.29	26.41	22.53	18.05	10.08	2.39
1994	9-9.5	0.69	0.00	0.08	1.49	8.71	16.52	21.78	22.88	21.52	16.36	10.81	5.45
1992	9.5-10	1.15	0.00	0.98	5.10	12.88	20.44	24.09	24.11	22.68	16.74	10.15	4.80
1990	10-11	0.32	0.06	0.00	2.16	9.22	16.81	21.86	23.22	21.76	16.35	10.74	4.12
1989	11-12	0.65	0.00	0.00	1.61	9.48	17.42	22.60	24.42	21.21	15.80	9.87	4.75
1986	12-13	0.58	0.00	0.13	2.75	10.44	17.40	22.25	23.83	21.45	17.83	12.29	5.23
1980	13-16	0.58	0.07	0.28	1.82	8.68	16.92	22.31	23.42	21.55	16.55	10.96	4.54
1971	16-19	0.52	0.01	0.07	1.57	8.08	16.39	21.37	22.91	21.47	17.13	11.40	5.14
1958	20-23	0.80	0.17	0.35	2.84	10.10	17.43	22.30	23.57	22.11	17.76	11.69	5.12
1949	23-25	1.15	0.44	0.06	2.24	9.90	17.81	21.71	22.80	21.44	17.91	11.15	3.70

Table C4 (con't)

^{210}Pb date	Interval Depth (cm)	Evap Jan (°C)	Evap Feb (°C)	Evap Mar (°C)	Evap Apr (°C)	Evap May (°C)	Evap Jun (°C)	Evap Jul (°C)	Evap Aug (°C)	Evap Sep (°C)	Evap Oct (°C)	Evap Nov (°C)	Evap Dec (°C)
2011	0.5-1.5	39.0	20.8	10.5	7.8	16.6	49.9	77.8	120.0	153.6	182.0	132.6	90.3
2009	1.5-2.5	46.4	20.5	13.8	1.9	14.1	22.6	60.9	106.1	129.2	183.3	117.0	108.1
2007	2.5-4	40.5	30.3	16.6	7.0	14.0	30.1	68.0	114.1	146.3	183.4	134.9	96.6
2005	4-5	35.3	11.3	8.0	4.8	7.9	35.2	66.5	106.1	170.7	165.2	113.3	100.5
2003	5-6	33.4	31.7	26.5	11.9	26.0	24.9	91.9	119.0	161.1	208.8	120.3	106.8
2000	6-7	50.3	17.9	18.8	15.2	27.1	43.2	79.1	135.0	193.9	179.2	157.4	106.6
1999	7-7.5	32.6	18.3	31.2	20.2	17.5	46.1	101.6	111.4	162.4	207.5	152.8	120.2
1997	7.5-8	55.1	14.6	18.6	10.1	19.3	10.3	76.2	112.8	153.3	191.4	143.1	72.7
1996	8-8.5	35.1	12.6	19.4	1.6	6.4	11.9	80.9	91.1	175.5	178.3	161.8	75.2
1995	8.5-9	63.8	39.3	8.5	11.0	8.5	15.6	58.8	107.7	190.0	200.3	171.1	87.9
1994	9-9.5	42.3	23.1	19.5	3.1	11.2	26.2	56.8	98.8	165.2	183.5	140.3	89.3
1992	9.5-10	54.9	22.8	15.1	6.7	13.6	47.4	99.5	110.9	216.6	169.4	154.9	88.3
1990	10-11	23.8	29.5	17.5	7.0	12.4	24.5	61.4	97.5	170.4	179.7	149.0	92.3
1989	11-12	49.6	28.9	19.6	5.4	8.9	42.4	49.9	132.7	138.5	223.9	114.4	92.1
1986	12-13	41.3	15.7	15.1	3.1	10.8	31.5	58.4	112.5	131.9	156.3	157.3	106.4
1980	13-16	41.4	17.8	15.9	8.8	8.4	25.4	61.1	104.0	157.3	191.5	134.1	95.2
1971	16-19	43.9	24.9	15.4	5.4	13.4	26.3	65.0	101.0	142.4	161.6	142.1	93.8
1958	20-23	34.8	17.4	17.3	6.0	16.7	34.6	73.6	108.2	149.3	166.8	138.1	84.7
1949	23-25	34.9	27.7	23.1	8.7	11.3	42.0	76.5	118.9	165.5	147.7	176.6	76.5

Table C4 (con't)

^{210}Pb date	Interval Depth (cm)	MSWT W (°C)	MSWT SP (°C)	MSWT SU(°C)	MSWT SP (°C)	MSWT Ann (°C)	Evap W (mm)	Evap SP (mm)	Evap SU (mm)	Evap F (mm)	Evap Ann (mm)
2011	0.5-1.5	1.81	4.11	21.66	16.47	11.01	150.0	34.9	247.6	468.3	900.8
2009	1.5-2.5	1.44	3.34	20.27	15.93	10.25	175.0	29.8	189.6	429.6	823.9
2007	2.5-4	2.18	4.56	21.93	17.02	11.42	167.5	37.6	212.3	464.6	882.0
2005	4-5	2.09	3.95	21.46	16.14	10.91	147.2	20.7	207.8	449.2	824.8
2003	5-6	2.98	5.14	22.31	17.82	12.06	171.8	64.3	235.8	490.2	962.1
2000	6-7	1.81	5.94	22.33	17.05	11.78	174.9	61.1	257.3	530.5	1023.8
1999	7-7.5	3.77	7.59	22.69	18.06	13.03	171.1	68.9	259.2	522.8	1021.9
1997	7.5-8	1.84	3.43	20.27	16.10	10.41	142.4	48.1	199.2	487.8	877.4
1996	8-8.5	1.50	1.92	20.47	16.60	10.12	122.9	27.4	183.9	515.6	849.8
1995	8.5-9	1.40	4.25	22.69	16.89	11.31	191.0	27.9	182.1	561.4	962.3
1994	9-9.5	2.05	3.42	20.39	16.23	10.52	154.7	33.7	181.8	489.0	859.3
1992	9.5-10	1.98	6.32	22.88	16.52	11.93	165.9	35.3	257.9	540.9	1000.0
1990	10-11	1.50	3.79	20.63	16.28	10.55	145.6	36.8	183.4	499.1	865.0
1989	11-12	1.80	3.70	21.48	15.63	10.65	170.6	34.0	225.0	476.9	906.3
1986	12-13	1.94	4.44	21.16	17.19	11.18	163.4	28.9	202.5	445.5	840.4
1980	13-16	1.73	3.59	20.88	16.36	10.64	154.4	33.1	190.4	482.8	860.7
1971	16-19	1.89	3.24	20.22	16.66	10.50	162.7	34.3	192.4	446.0	835.4
1958	20-23	2.03	4.43	21.10	17.19	11.19	136.9	40.0	216.4	454.3	847.5
1949	23-25	1.76	4.06	20.77	16.83	10.86	139.0	43.1	237.4	489.8	909.3

Table C4 (con't)

^{210}Pb date	Interval Depth (cm)	PLk Jan (mm)	PLk Feb (mm)	PLk MAR (mm)	PLk APR (mm)	PLk MAY (mm)	PLk JUN (mm)	PLk JUL (mm)	PLk AUG (mm)	PLk SEP (mm)	PLk OCT (mm)	PLk NOV (mm)	PLk DEC (mm)	PLk Ann (mm)
2011	0.5-1.5	52.5	69.4	73.9	108.6	134.5	91.6	95.8	83.9	118.1	118.6	110.7	81.3	1139.1
2009	1.5-2.5	58.3	83.2	98.2	70.9	68.6	107.3	96.3	81.4	80.9	87.3	71.3	91.6	995.3
2007	2.5-4	82.5	38.8	44.4	68.3	56.8	61.1	101.6	102.8	105.1	80.6	80.2	76.6	898.9
2005	4-5	40.9	27.6	63.6	59.4	128.3	59.3	96.5	59.3	86.3	56.2	72.1	69.9	819.4
2003	5-6	37.3	41.0	43.8	71.9	83.1	45.6	36.4	42.3	72.4	73.5	60.5	54.5	662.3
2000	6-7	65.5	38.8	40.5	99.4	76.4	93.0	74.7	77.6	67.1	55.8	59.2	52.3	800.2
1999	7-7.5	92.0	46.7	86.8	110.3	45.0	59.1	80.5	83.1	37.1	41.3	40.8	43.7	766.2
1997	7.5-8	55.9	79.0	95.4	45.4	119.5	110.7	58.4	89.8	78.0	51.2	61.6	57.9	902.8
1996	8-8.5	47.6	26.3	34.3	88.2	57.3	110.2	102.2	33.1	218.3	94.8	81.4	81.6	975.2
1995	8.5-9	74.8	21.4	27.1	55.7	57.6	35.4	54.1	53.8	29.1	85.9	70.5	26.6	592.1
1994	9-9.5	58.0	36.3	54.9	75.6	35.3	77.9	80.5	79.0	85.1	52.0	79.1	47.8	761.4
1992	9.5-10	52.3	33.0	66.6	90.6	63.4	24.8	43.5	74.7	42.6	84.3	67.2	49.9	692.8
1990	10-11	44.8	64.1	42.6	58.6	112.1	79.7	73.5	83.3	115.0	83.4	73.3	104.3	934.6
1989	11-12	30.7	25.7	41.4	44.3	32.3	48.6	59.3	90.0	54.7	77.8	57.8	50.6	613.3
1986	12-13	42.3	67.4	74.7	54.1	89.3	88.6	68.1	80.7	84.4	73.8	113.2	73.2	909.9
1980	13-16	63.1	50.2	78.4	85.6	74.9	97.0	89.4	106.1	112.6	75.5	81.4	85.6	999.9
1971	16-19	53.1	44.0	66.6	78.0	88.3	95.9	80.0	64.0	78.0	64.0	99.9	87.2	898.9
1958	20-23	67.2	59.2	65.4	93.2	73.4	75.1	73.9	87.1	74.0	74.7	69.0	58.9	870.9
1949	23-25	69.0	63.4	86.1	83.2	94.1	92.6	71.2	69.1	80.5	67.3	84.8	67.8	929.0
1940	26-27	43.3	89.6	76.5	74.6	78.3	91.0	70.9	77.7	84.2	51.1	61.2	60.7	859.2
1933	28-29	81.6	43.8	60.8	63.4	72.3	56.5	62.9	51.5	75.1	61.1	62.3	56.4	747.6
1927	29-31	62.2	51.4	61.6	74.0	63.9	80.8	79.3	61.7	93.2	69.0	81.2	74.9	853.0
1915	32-35	80.7	54.5	70.5	76.1	91.8	72.3	70.7	92.5	73.4	90.5	58.1	59.0	890.1
1907	35-37	72.6	64.7	69.2	69.4	79.1	74.8	88.5	80.3	60.6	71.0	50.0	66.0	846.4

Table C4 (con't)

^{210}Pb date	Interval Depth (cm)	PLd Jan (mm)	PLd Feb (mm)	PLd MAR (mm)	PLd APR (mm)	PLd MAY (mm)	PLd JUN (mm)	PLd JUL (mm)	PLd AUG (mm)	PLd SEP (mm)	PLd OCT (mm)	PLd NOV (mm)	PLd DEC (mm)	PLd Ann (mm)
2011	0.5-1.5	40.1	72.6	75.8	113.1	152.4	103.5	91.6	84.0	110.3	84.8	117.1	70.8	1115.9
2009	1.5-2.5	63.2	96.7	105.6	82.7	87.2	111.4	93.6	76.2	79.8	84.6	57.0	97.0	1034.9
2007	2.5-4	106.5	51.3	55.5	81.0	70.3	64.8	112.0	115.9	88.3	80.6	85.1	89.9	1001.2
2005	4-5	47.6	32.6	67.6	57.1	157.2	88.8	124.8	90.2	95.5	64.4	85.4	76.7	987.8
2003	5-6	43.0	57.3	52.7	89.5	110.7	65.2	61.4	65.2	89.0	99.5	69.2	60.6	863.3
2000	6-7	72.3	47.5	42.2	97.8	98.4	117.9	88.5	82.0	86.8	59.1	57.1	70.4	920.1
1999	7-7.5	87.8	54.1	89.3	99.9	49.2	100.9	88.6	121.7	34.7	50.5	40.1	36.9	853.8
1997	7.5-8	63.1	88.2	90.7	41.1	139.2	104.6	86.6	105.3	89.9	49.9	59.5	54.2	972.4
1996	8-8.5	66.4	40.3	53.2	116.7	103.3	117.1	95.2	41.8	140.5	73.2	81.6	89.6	1018.8
1995	8.5-9	91.8	28.5	43.7	95.3	89.6	77.6	75.8	87.6	33.4	111.2	93.3	36.5	864.3
1994	9-9.5	73.4	39.2	61.9	98.3	54.4	100.2	115.4	84.9	96.3	55.7	101.0	59.3	939.9
1992	9.5-10	48.4	36.1	68.0	97.8	89.0	33.6	77.5	84.2	50.2	105.6	63.9	50.3	804.7
1990	10-11	49.4	74.6	51.3	71.7	130.9	106.9	95.6	84.2	100.4	84.9	73.6	100.9	1024.4
1989	11-12	39.1	33.4	51.7	54.7	50.2	66.5	93.2	105.9	67.0	79.4	80.8	69.0	790.9
1986	12-13	38.5	65.3	77.9	68.7	94.2	87.6	90.2	93.8	94.1	79.2	102.7	67.5	959.7
1980	13-16	58.1	47.9	75.2	85.1	81.9	101.5	86.9	99.6	92.6	66.2	75.7	77.8	948.6
1971	16-19	51.8	41.7	67.1	79.2	95.4	96.8	89.1	66.2	81.4	60.1	90.9	85.8	905.6
1958	20-23	62.0	58.1	66.6	90.6	79.7	81.8	87.6	83.7	68.4	70.7	65.7	52.1	866.9
1949	23-25	68.4	60.5	83.9	86.0	99.2	105.5	75.5	66.7	80.9	68.4	74.2	68.4	937.6
1940	26-27	45.9	80.3	80.2	84.8	76.4	115.5	77.6	80.8	66.1	50.3	52.8	55.2	865.8
1933	28-29	78.4	41.4	66.7	66.6	82.3	69.0	62.2	58.8	87.8	59.8	61.6	60.7	795.2
1927	29-31	61.6	48.8	65.0	71.8	75.6	86.9	86.8	67.8	96.1	67.1	79.7	71.6	878.8
1915	32-35	73.3	47.4	67.0	77.6	92.2	74.9	74.4	87.7	77.9	84.8	56.2	53.4	866.6
1907	35-37	70.7	65.9	72.6	74.9	88.9	87.8	96.0	83.2	63.9	65.4	55.5	67.6	892.2

Table C4 (con't)

^{210}Pb date	Interval Depth (cm)	Run Jan (mm)	Run Feb (mm)	Run Mar (mm)	Ran Apr (mm)	Run May (mm)	Run Jun (mm)	Run Jul (mm)	Run Aug (mm)	Run Sep (mm)	Run Oct (mm)	Run Nov (mm)	Run Dec (mm)	RunAnn (mm)
2011	0.5-1.5	56	67	224	138	176	74	33	24	36	66	90	148	1133
2009	1.5-2.5	91	196	231	128	67	58	46	26	23	29	41	115	1051
2007	2.5-4	228	96	137	107	64	34	35	42	29	55	70	140	1036
2005	4-5	61	45	154	91	147	89	59	43	50	34	72	120	967
2003	5-6	42	140	95	131	95	38	13	12	13	49	30	79	736
2000	6-7	76	66	73	115	61	74	29	28	24	24	33	55	660
1999	7-7.5	165	112	156	132	58	41	38	68	12	12	13	16	824
1997	7.5-8	84	164	196	67	117	128	45	31	34	20	41	84	1010
1996	8-8.5	132	81	115	144	164	97	28	18	41	47	77	149	1092
1995	8.5-9	111	34	108	112	54	41	30	28	8	22	80	36	664
1994	9-9.5	113	70	147	146	40	43	60	33	45	29	100	65	890
1992	9.5-10	140	103	115	121	41	34	13	13	9	23	28	39	680
1990	10-11	102	121	84	107	107	85	49	25	42	56	55	126	961
1989	11-12	47	64	92	92	30	24	35	18	19	28	53	78	580
1986	12-13	63	155	184	118	64	54	34	21	32	54	100	102	981
1980	13-16	64	103	183	129	68	54	32	29	39	34	55	105	897
1971	16-19	85	90	144	118	87	45	36	17	19	23	66	108	839
1958	20-23	108	113	178	153	80	41	29	27	20	39	43	61	892
1949	23-25	155	152	208	163	100	67	32	18	21	29	49	97	1092
1940	26-27	20	98	162	148	25	37	16	10	7	6	11	34	573
1933	28-29	152	60	91	83	58	12	7	3	6	7	16	48	543
1927	29-31	87	102	145	98	56	37	24	10	31	35	49	96	770
1915	32-35	66	63	148	87	56	34	20	20	21	25	29	39	609

Table C4 (con't)

Pb date	Interval Depth (cm)	Western watershed population	Western Agricul (acres)	Western Forest (acres)	Entire watershed population	Entire Watershed Agricul (acres)	Entire Watershed Forest (acres)
2011	0.5-1.5	6356825	6255367	1169305	12111519	11566018	3484417
2009	1.5-2.5	6380897	6255330	1154201	12125799	11605347	3435536
2007	2.5-4	6420145	6303330	1078573	12155973	11721895	3322664
2005	4-5	6459677	6423711	1004623	12169435	11923859	3241427
2003	5-6	6491331	6480067	951255.1	12177787	12019600	3186242
2000	6-7	6502447	6416360	961438.4	12161656	11960020	3166943
1999	7-7.5	6464731	6368476	985013.3	12086626	11923841	3161538
1997	7.5-8	6439979	6336241	997538.1	12036923	11899036	3154679
1996	8-8.5	6414969	6341806	1010079	11987073	11939520	3147899
1995	8.5-9	6389684	6347627	1022845	11937137	11911024	3200518
1994	9-9.5	6339928	6358959	1043018	11838110	11853774	3298286
1992	9.5-10	6290022	6415975	1042667	11738725	11857561	3367040
1990	10-11	6271720	6492725	1038287	11676388	11972065	3348779
1989	11-12	6298619	6595787	1032511	11667814	12125940	3322128
1986	12-13	6332311	6690609	1025215	11676724	12297369	3259306
1980	13-16	6397711	6873320	1016045	11767999	12626425	3099496
1971	16-19	6364801	7305231	1015274	11709896	13342098	2843711
1958	20-23	5482301	7864131	1106783	10060795	14734479	2647655
1949	23-25	4571123	8413662	1119787	8371390	15900956	2502242
1940	26-27	3892763	8443963	1067753	7235414	16155071	2365325
1933	28-29	3688177	8351961	970933.2	6927976	16012420	2160892
1927	29-31	3232389	8453021	876356.4	6228719	16342586	1961780
1915	32-35	2148441	9068800	749256.3	4478107	17334251	1775417
1907	35-37	1676492	9169802	706002	3591244	17449695	1948294
1891	38-41	1374670	8945163	1012816	2874875	17319818	2795471
1876	42-45	957863.4	7863447	1762160	2035582	15580924	4433908
1859	46-48	607406.9	5634108	2300735	1385488	12096177	6203337
1852	48-49	454486.6	4497560	2462879	1154163	10107876	6788516

Table C4 (con't)

Pb date	Interval Depth (cm)	Western watershed population	Western Agricul (acres)	Western Forest (acres)	Entire watershed population	Entire Watershed Agricul (acres)	Entire Watershed Forest (acres)
2011	0.5-1.5	6356825	6255367	1169305	12111519	11566018	3484417
2009	1.5-2.5	6380897	6255330	1154201	12125799	11605347	3435536
2007	2.5-4	6420145	6303330	1078573	12155973	11721895	3322664
2005	4-5	6459677	6423711	1004623	12169435	11923859	3241427
2003	5-6	6491331	6480067	951255.1	12177787	12019600	3186242
2000	6-7	6502447	6416360	961438.4	12161656	11960020	3166943
1999	7-7.5	6464731	6368476	985013.3	12086626	11923841	3161538
1997	7.5-8	6439979	6336241	997538.1	12036923	11899036	3154679
1996	8-8.5	6414969	6341806	1010079	11987073	11939520	3147899
1995	8.5-9	6389684	6347627	1022845	11937137	11911024	3200518
1994	9-9.5	6339928	6358959	1043018	11838110	11853774	3298286
1992	9.5-10	6290022	6415975	1042667	11738725	11857561	3367040
1990	10-11	6271720	6492725	1038287	11676388	11972065	3348779
1989	11-12	6298619	6595787	1032511	11667814	12125940	3322128
1986	12-13	6332311	6690609	1025215	11676724	12297369	3259306
1980	13-16	6397711	6873320	1016045	11767999	12626425	3099496
1971	16-19	6364801	7305231	1015274	11709896	13342098	2843711
1958	20-23	5482301	7864131	1106783	10060795	14734479	2647655
1949	23-25	4571123	8413662	1119787	8371390	15900956	2502242
1940	26-27	3892763	8443963	1067753	7235414	16155071	2365325
1933	28-29	3688177	8351961	970933.2	6927976	16012420	2160892
1927	29-31	3232389	8453021	876356.4	6228719	16342586	1961780
1915	32-35	2148441	9068800	749256.3	4478107	17334251	1775417
1907	35-37	1676492	9169802	706002	3591244	17449695	1948294
1891	38-41	1374670	8945163	1012816	2874875	17319818	2795471
1876	42-45	957863.4	7863447	1762160	2035582	15580924	4433908

Appendix D: Sediment core chironomid head capsule count data

Table D1: Chironomid head capsule counts from the central basin core

Year	**2011**	**2010**	**2009**	**2009**	**2008**	**2007**	**2006**	**2005**	**2004**	**2003**
Interval depth (cm)	**0.5-1**	**1-1.5**	**1.5-2**	**2-2.5**	**2.5-3**	**3-3.5**	**3.5-4**	**4-4.5**	**4.5-5**	**5-5.5**
Sed Analyzed (g dry weight)	1.041	4.938	3.073	6.960	3.183	1.922	5.263	3.017	3.514	3.086
Chironomini larvula			2					1		
Chironomus			1							
Chironomus anthracinus	1	1	2	7	8	1	6	4	3	2
Chironomus plumosus		6	4	2	2		1	3	2	1
Cricotopus cylindraceus										
Harnischia/Paracladopelma										
Heterotrissocladius grp										
Micropsectra insignilobus										
Paracladius										
Paracladopelma										
Paracricotopus										
Paratanytarsus										
Procladius					1			1		
Tanytarsus lugens	1	35	15	29	10	2	2	3	16	18
Tanytarsus mendax		2	1							
Tanytarsus-undif		1						1		
Total	**2**	**45**	**25**	**38**	**21**	**3**	**9**	**13**	**21**	**21**

Table D1 (con't)

Year	**2002**	**2001**	**2000**	**1999**	**1997**	**1996**	**1995**	**1994**	**1992**	**1990**
Interval depth (cm)	**5.5-6**	**6-6.5**	**6.5-7**	**7-7.5**	**7.5-8**	**8-8.5**	**8.5-9**	**9-9.5**	**9.5-10**	**10-11**
Sed Analyzed (g dry weight)	4.759	2.264	4.340	2.708	4.481	1.442	4.339	3.093	2.771	5.287
Chironomini larvula		1		1			1			
Chironomus										
Chironomus anthracinus	6	4	10	6	15		11	5	14	8
Chironomus plumosus	6	4	2	4	11	7	6	4	4	5
Cricotopus cylindraceus										
Harnischia/Paracladopelma										
Heterotrissocladius grp										
Micropsectra insignilobus										
Paracladius										
Paracladopelma										
Paracricotopus										
Paratanytarsus										
Procladius	1					1	2	2		
Tanytarsus lugens	18	9	17	28	44	16	39	31	38	28
Tanytarsus mendax				1						
Tanytarsus-undif			2					1		
Total	**31**	**18**	**31**	**40**	**70**	**24**	**59**	**43**	**56**	**41**

Table D1 (con't)

Year	**1989**	**1986**	**1983**	**1980**	**1977**	**1974**	**1971**	**1968**	**1961**	**1958**
Interval depth (cm)	**11-12**	**12-13**	**13-14**	**14-15**	**15-16**	**16-17**	**17-18**	**18-19**	**20-21**	**21-22**
Sed Analyzed (g dry weight)	2.472	5.173	3.911	5.393	4.116	5.239	2.286	5.339	5.385	3.807
Chironomini larvula										
Chironomus										
Chironomus anthracinus	1	2	5	2	1	2		6	1	1
Chironomus plumosus	3	2		2	2			4	1	
Cricotopus cylindraceus										
Harnischia/Paracladopelma								1		
Heterotrissocladius grp		1								
Micropsectra insignilobus										
Paracladius										
Paracladopelma										
Paracricotopus										
Paratanytarsus										
Procladius	1					1	1	1	3	
Tanytarsus lugens	48	72	11	5	4	5	7	5	3	6
Tanytarsus mendax										
Tanytarsus-undif			1							1
Total	**53**	**77**	**17**	**9**	**7**	**8**	**8**	**17**	**8**	**8**

Table D1 (con't)

Year	**1955**	**1951**	**1947**	**1940**	**1933**	**1929**	**1926**	**1919**	**1912**	**1909**
Interval depth (cm)	**22-23**	**23-24**	**24-25**	**26-27**	**28-29**	**29-30**	**30-31**	**32-33**	**34-35**	**35-36**
Sed Analyzed (g dry weight)	5.522	3.403	5.299	5.168	5.384	3.501	5.124	5.362	5.393	3.859
Chironomini larvula										
Chironomus										
Chironomus anthracinus	3		1	6		3				2
Chironomus plumosus	4	4	2	1	1	2	8	1	2	
Cricotopus cylindraceus										
Harnischia/Paracladopelma										
Heterotrissocladius grp						1			2	
Micropsectra insignilobus	1	1	4	4	4		4	1		2
Paracladius										
Paracladopelma										
Paracricotopus										
Paratanytarsus					1					
Procladius	1	2	1	5	10	3	5	1	3	1
Tanytarsus lugens	12	8	10	7	9	9	10	22	9	14
Tanytarsus mendax				1						
Tanytarsus-undif				1	1					1
Total	**21**	**15**	**18**	**25**	**26**	**18**	**27**	**25**	**16**	**20**

Table D1 (con't)

Year	**1905**	**1898**	**1889**	**1885**	**1880**	**1871**	**1862**	**1857**	**1852**
Interval depth (cm)	**36-37**	**38-39**	**40-41**	**41-42**	**42-43**	**44-45**	**46-47**	**47-48**	**48-49**
Sed Analyzed (g dry weight)	5.342	5.105	5.503	4.638	5.571	5.284	5.527	3.199	5.343
Chironomini larvula									
Chironomus									
Chironomus anthracinus	1				1		2	1	3
Chironomus plumosus	1		1	3	3	1	3	9	14
Cricotopus cylindraceus									1
Harnischia/Paracladopelma					2				1
Heterotrissocladius grp					3				
Micropsectra insignilobus	2	1		1		3	3		4
Paracladius								1	
Paracladopelma								1	
Paracricotopus				1					
Paratanytarsus			1						
Procladius	1	1	8		3	3	4	2	6
Tanytarsus lugens	26	12	2	1	16	13	6	7	13
Tanytarsus mendax	1								1
Tanytarsus-undif					1				
Total	**32**	**14**	**12**	**6**	**29**	**20**	**18**	**21**	**43**

Table D2: Chironomid head capsule counts from the central basin core, adjacent intervals with low counts combined

Year	**2011**	**2009**	**2007**	**2005**	**2003**	**2000**	**1999**	**1997**	**1996**	**1995**
Interval depth (cm)	**0.5-1.5**	**1.5-2.5**	**2.5-4**	**4-5**	**5-6**	**6-7**	**7-7.5**	**7.5-8**	**8-8.5**	**8.5-9**
Sed Analyzed (g dry weight)	2.989	5.016	3.456	3.266	3.923	3.923	2.708	4.481	1.442	4.339
Chironomini larvula		2		1		1	1			1
Chironomus		1								
Chironomus anthracinus	2	9	15	7	8	14	6	15		11
Chironomus plumosus	6	6	3	5	7	6	4	11	7	6
Cricotopus cylindraceus										
Harnischia/Paracladopelma										
Heterotrissocladius grp										
Micropsectra insignilobus										
Paracladius										
Paracladopelma										
Paracricotopus										
Paratanytarsus										
Procladius			1	1	1				1	2
Tanytarsus lugens	36	44	14	19	36	26	28	44	16	39
Tanytarsus mendax	2	1					1			
Tanytarsus-undif	1			1		2				
Total	**47**	**63**	**33**	**34**	**52**	**49**	**40**	**70**	**24**	**59**

Table D2 (con't)

Year	**1994**	**1992**	**1990**	**1989**	**1986**	**1980**	**1971**	**1958**	**1949**	**1940**
Interval depth (cm)	**9-9.5**	**9.5-10**	**10-11**	**11-12**	**12-13**	**13-16**	**16-19**	**20-23**	**23-25**	**26-27**
Sed Analyzed (g dry weight)	3.093	2.771	5.287	2.472	5.173	4.473	4.288	4.904	4.351	5.168
Chironomini larvula										
Chironomus										
Chironomus anthracinus	5	14	8	1	2	8	8	5	1	6
Chironomus plumosus	4	4	5	3	2	4	4	5	6	1
Cricotopus cylindraceus										
Harnischia/Paracladopelma							1			
Heterotrissocladius grp					1					
Micropsectra insignilobus								1	5	4
Paracladius										
Paracladopelma										
Paracricotopus										
Paratanytarsus										
Procladius	2			1			3	4	3	5
Tanytarsus lugens	31	38	28	48	72	20	17	21	18	7
Tanytarsus mendax										1
Tanytarsus-undif	1					1		1		1
Total	**43**	**56**	**41**	**53**	**77**	**33**	**33**	**37**	**33**	**25**

Table D2 (con't)

Year	**1933**	**1927**	**1915**	**1907**	**1891**	**1876**	**1859**	**1852**
Interval depth (cm)	**28-29**	**29-31**	**32-35**	**35-37**	**38-41**	**42-45**	**46-48**	**48-49**
Sed Analyzed (g dry weight)	5.384	4.312	5.377	4.600	5.082	5.427	4.363	5.343
Chironomini larvula								
Chironomus								
Chironomus anthracinus		3		3		1	3	3
Chironomus plumosus	1	10	3	1	4	4	12	14
Cricotopus cylindraceus								1
Harnischia/Paracladopelma						2		1
Heterotrissocladius grp		1	2			3		
Micropsectra insignilobus	4	4	1	4	2	3	3	4
Paracladius							1	
Paracladopelma							1	
Paracricotopus					1			
Paratanytarsus	1				1			
Procladius	10	8	4	2	9	6	6	6
Tanytarsus lugens	9	19	31	40	15	29	13	13
Tanytarsus mendax				1				1
Tanytarsus-undif	1			1		1		
Total	**26**	**45**	**41**	**52**	**32**	**49**	**39**	**43**

Table D3: Chironomid head capsule counts from the western basin core

Year	**2011.1**	**2010.5**	**2009.9**	**2009.3**	**2008.8**	**2008.2**	**2007**	**2005.2**	**2003.3**
Interval depth (cm)	**0.5-1**	**1-1.5**	**1.5-2**	**2-2.5**	**2.5-3**	**3-3.5**	**4-4.5**	**5-5.5**	**5.5-6.5**
Sed Analyzed (g dry weight)	3.126	3.208	12.256	9.101	8.725	2.895	4.301	4.845	3.567
Chironomus anthracinus	14	15	32	18	11.5	18	12.5	18	8
Chironomus plumosus	8	4	12	3.5	10	10	21.5	15.5	7
Cladotanytarsus mancus					0.5			0.5	
Constempellina-Thienemanniola									
Cricotopus cylindraceus								1	
Cryptochironomus		1	1	1.5	1	1.5		4	1
Demicryptochironomus									
Glyptotendipes pallens									
Harnischia									
Heterotrissocladius grimshawi									
Microchironomus				1					
Paramerina							1		
Paratanytarsus									
Polypedilum nubeculosum						3	1		
Procladius	2	1	4	1.5	4	11	4	5	2
Tanytarsus lactescens					1				
Tanytarsus lugens				1					
Tanytarsus nospur									
Grand Total	24	21	49	26.5	28	43.5	40	44	18

Table D3 (con't)

Year	**2000.4**	**1999.4**	**1997.3**	**1992.4**	**1990**	**1987.7**	**1982.8**	**1972.7**	**1970.2**
Interval depth (cm)	**7.5-8**	**8-8.5**	**9-9.5**	**11-12**	**12-13**	**13-14**	**15-16**	**19-20**	**20-21**
Sed Analyzed (g dry weight)	5.949	2.241	2.297	7.086	6.599	6.719	5.972	6.093	5.972
Chironomus anthracinus	11.5	7	6	7	8.5	16	22	27.5	23
Chironomus plumosus	2	3	3	5	12	17.5	25	33.5	39
Cladotanytarsus mancus							1.5		
Constempellina-Thienemanniola									1
Cricotopus cylindraceus									
Cryptochironomus	1	1	1	0.5			1.5	2	0.5
Demicryptochironomus							1		
Glyptotendipes pallens	1							2	
Harnischia				1					
Heterotrissocladius grimshawi					0.5				
Microchironomus				1					1
Paramerina									
Paratanytarsus							1		
Polypedilum nubeculosum			1						1
Procladius	2	1	1	4.5	3	9.5	10.5	11.5	9.5
Tanytarsus lactescens									
Tanytarsus lugens								2	4
Tanytarsus nospur	1	1							1
Grand Total	18.5	13	12	19	24	43	62.5	78.5	80

Table D4: Chironomid head capsule counts from the eastern basin core

Year	**2017**	**2014**	**2012**	**2009**	**2007**	**2005**	**2001**	**1999**	**1996**	**1994**
Interval depth (cm)	**1-1.5**	**3-3.5**	**5-5.5**	**7-7.5**	**9-9.5**	**10-11**	**13-14**	**15-16**	**17-18**	**19-20**
Sed Analyzed (g wet weight)	10.502	10.134	10.432	10.721	10.816	10.122	10.323	10.292	10.232	10.913
Chironomus anthracinus		3	1							
Chironomus plumosus		1		1						
Cladopelma										
Corynoneura coronata										
Cryptochironomus						1				
Harnischia				1						
Micropsectra										
Procladius	1			1						
Stictochironomus										1
Tanytarsus lugens		1					1			
Tanytarsus no spur										
Grand Total	**1**	**5**	**1**	**3**	**0**	**1**	**1**	**0**	**0**	**1**

Table D3 (con't)

Year	**1993**	**1990**	**1987**	**1980**	**1974**	**1968**
Depth end (cm)	**20-21**	**22-23**	**25-26**	**30-31**	**35-36**	**40-41**
Sed Analyzed (g wet weight)	10.747	10.797	10.761	10.055	10.320	10.242
Chironomus anthracinus				2	1	
Chironomus plumosus				1	1	
Cladopelma			1			
Corynoneura coronata					1	
Cryptochironomus						
Harnischia				1		
Micropsectra						2
Procladius				1	2	
Stictochironomus						
Tanytarsus lugens				1		
Tanytarsus no spur				3		
Grand Total	**0**	**0**	**1**	**9**	**5**	**2**

Table D5: Central basin core PCA axes scores, inferred avgVWHO, and geochemical data

^{210}Pb Year	Interval midpoint depth (cm)	PCA1	PCA2	Inferred avgVWHO (mg O_2 L^{-1})	Sed Accum (g cm^{-2} yr^{-1})	Organics (%)	Carbonates (%)
2010.681	1	-0.4529	-0.478	4.37116	0.175713	8.699962	7.120546
2009.006	2	-0.7115	-0.1294	3.67962	0.173738	7.818417	6.462783
2006.913	3.25	-0.6047	0.7932	2.35944	0.171269	7.112934	6.132819
2004.819	4.5	-0.4148	0.3104	3.10958	0.168209	7.486321	4.972452
2002.656	5.5	-0.4259	-0.0245	3.70237	0.1621	7.219107	5.592278
2000.331	6.5	-0.7963	0.3973	2.99816	0.1554	6.021635	6.113197
1998.588	7.25	-0.7116	-0.1035	3.75429	0.150375	7.023411	6.084281
1997.425	7.9	-0.7253	0.1071	3.34296	0.147025	7.443366	5.151456
1996.263	8.25	0.2115	-0.704	3.61173	0.143675	7.017544	6.383158
1995.1	8.75	-0.4231	0.1021	3.51739	0.14037	7.118644	6.937627
1993.5	9.25	-0.2344	-0.0892	4.01672	0.13711	7.236842	4.488158
1991.9	9.75	-0.8104	0.0888	3.59778	0.13385	7.216495	5.470103
1990.3	10.5	-0.7279	-0.0011	3.62	0.12896	6.711409	6.104698
1988.7	11.5	-0.2086	-0.7649	4.79522	0.1228	7.326007	4.997802
1985.85	12.5	-0.4765	-0.8904	5.07304	0.117	7.446809	4.838298
1980.15	14.5	-0.7437	0.2193	3.38265	0.105758	7.711787	5.177378
1970.983	17.5	-0.1721	0.4424	3.10243	0.094758	7.931008	4.739989
1958.083	21.5	0.227	0.2723	3.67953	0.084363	8.028675	5.183077
1949.225	24	0.7302	-0.0325	4.79314	0.0798	7.434688	5.917268
1939.925	26.5	0.7302	0.982	4.17416	0.090463	5.574913	7.13101
1932.575	28.5	1.6472	-0.0591	4.71064	0.097613	5.723906	5.359596
1927.225	30	0.805	0.2431	3.91421	0.103325	6.156023	5.443976
1915.45	33.5	0.5822	-0.8303	5.04832	0.111156	5.376241	5.182659
1906.875	36	0.1914	-0.2583	5.18839	0.10325	5.816576	4.045706
1890.567	39.5	1.2528	-0.3168	3.99849	0.084988	5.694702	4.324397
1875.65	43.5	0.7058	-0.2689	5.1709	0.082125	6.225608	3.723136
1859.288	47	0.7529	0.4744	3.25398	0.082125	5.400155	4.614726
1852.275	48.5	0.8033	0.5184	3.33595	0.082125	5.369128	4.578523

Table D6: Western basin core sample PCA axes scores and geochemical data

^{210}Pb Year	Interval midpoint depth (cm)	PCA1	PCA2	Sed Accum (g cm^{-2} yr $^{-1}$)	Organics (%)	Carbonates (%)
2011.106	1	-0.0955	-0.4906	0.2725	8.83	10.76
2010.519	1.5	0.7662	-0.2445	0.2675	7.75	10.94
2009.931	2	0.3924	-0.2816	0.2625	7.31	11.28
2009.344	2.5	0.9294	-0.1013	0.2575	5.20	14.55
2008.756	3	-0.1823	-0.047	0.2526	4.58	14.86
2008.169	3.5	-0.0626	0.8895	0.2476	5.54	12.60
2006.994	4.5	-0.9228	0.0766	0.2376	6.61	11.28
2005.238	5.5	0.0556	0.0958	0.2352	5.57	12.67
2003.288	6.5	-0.0466	-0.0518	0.2352	6.13	13.34
2000.363	8	1.1087	-0.1409	0.2353	5.88	11.55
1999.388	8.5	0.7256	-0.1122	0.2354	6.37	10.25
1997.31	9.5	0.3467	0.8185	0.2343	5.66	10.52
1992.413	12	-0.1304	0.2588	0.2273	5.31	11.53
1990.038	13	-0.7765	-0.4005	0.2184	5.62	11.68
1987.663	14	-0.6652	-0.2044	0.2094	5.90	11.08
1982.838	16	-0.4454	-0.0394	0.1984	6.06	9.76
1972.725	20	-0.3486	-0.126	0.2148	5.65	10.70
1970.175	21	-0.6488	0.1011	0.2137	5.39	10.65

Table D7: A goodness-of-fit diagnostic of the avgVWHO model with passively projected Lake Erie central basin core chironomid assemblages (samples 55-82) onto an RDA containing training set chironomid data (samples 1-54) constrained to the training set avgVWHO. Values represent squared residual lengths for untransformed and square root transformed species data

Sample#	Sample	Untrans	Tran.
1	12	2.4148	1.0922
2	BH	0.9267	1.2128
3	BG	0.6859	0.8714
4	BC	0.4297	0.7429
5	BO	1.0702	0.9532
6	BU	0.5461	1.1104
7	CA	1.2295	0.8274
8	CL	1.8587	0.9945
9	CR C2	0.6289	0.9962
10	DI C1	0.3726	0.6632
11	EA	0.4345	1.0163
12	FI	0.2088	0.3248
13	HL	0.3655	0.639
14	HS	0.6609	0.6596
15	HM	0.4574	0.4342
16	HB	1.1683	1.2849
17	HP	0.4873	0.7753
18	KA-S	1.3133	1.0304
19	KE	0.1654	0.4929
20	KN	0.9852	0.6508
21	KU-S	1.6826	0.9414
22	LC	0.7744	1.2215
23	LH	0.3278	0.4755
24	LE	0.5237	0.6094
25	MC	0.6794	1.1467
26	PL	1.3494	0.8195
27	RC-E	0.5064	1.0656
28	RC-M	0.8598	1.0961
29	RS	0.7729	0.628
30	RH	0.8144	0.5792
31	SG	0.8403	0.7131
32	ST	1.3021	1.3354
33	WA	1.2048	0.848
34	BE	1.0179	1.0836
35	BB	0.348	0.7162
36	HO	0.7694	1.0573
37	LI	0.823	0.7514
38	MG	1.0813	0.5202
39	MS	0.7079	0.7328
40	MT	2.5339	0.8074
41	NU	0.2287	0.5408
42	PI	1.2861	1.2944
43	POM	0.4372	0.9938
44	POE	0.4727	0.9006
45	AR	0.3494	0.6536
46	BL	0.4178	0.5963
47	DA	0.3713	0.8154
48	ES	0.3594	0.5975
49	GM	0.972	1.1724
50	GO	0.7823	1.2383
51	HU	1.6324	0.8737
52	LO	0.3533	0.8015
53	MF	0.6411	0.4951
54	WI	0.498	1.0349
55	1.25	8.4413	2.6959
56	2.25	6.4587	2.6307
57	3.5	5.6738	2.7354
58	4.75	5.0997	2.4849
59	5.75	6.2725	2.5689
60	6.75	5.5142	2.7269
61	7.5	6.6368	2.6346
62	8	5.9806	2.7765
63	8.5	5.812	2.5127
64	9	5.6831	2.4522
65	9.5	6.7157	2.474
66	10	6.3402	2.7466
67	11	6.3789	2.7443
68	12	10.0138	2.5559
69	13	10.804	2.5625
70	15	6.0257	2.7715
71	18	4.225	2.5031
72	22	4.4727	2.206
73	24.5	3.4768	1.9464
74	27	2.3864	2.022
75	29	3.0801	1.9586
76	30.5	2.7408	1.8709
77	34	6.5559	1.8701
78	36.5	7.5852	2.0805
79	40.67	2.8985	1.966
80	44	4.0378	1.6836
81	47.5	2.8852	2.1677
82	49	2.9251	2.1064